UNIVERSITÀ DEGLI STUDI DI UDINE
hic sunt futura
www.uniud.it

PhD Course in:
"Food and Human Health"

31° Cycle

Thesis title

Alteration of the Mechanotransduction Properties of Human Cardiac Progenitor Cells Isolated from Ischemic Hearts

PhD STUDENT
Andrea Zanello

SUPERVISOR
Dr. Antonio Paolo Beltrami

Year 2019

ABSTRACT

Background

Ischemic cardiomyopathy is characterized by loss of a large number of cardiomyocytes and pervasive fibrosis that lead to heart failure. Effective therapies are far from being approved in clinical practice, compelling heart transplantation as the unique care. Resettle lost cardiomyocytes, boosting the function of cardiac progenitor cells (CPC), is under investigation as a promising therapy, but clinically meaningful results are hampered by the pathological traits of the tissue in which CPC reside. Since cells are able to sense the external environment through the mechanotransduction process, physical and biological alterations characterizing the extracellular matrix (ECM) of the pathologic heart, might lead to an improper function of CPC.

Aim

To investigate if CPC isolated from ischemic hearts presents defects in mechanotransduction.

Methods and Results

CPC were obtained from healthy donors (healthy CPC) and from heart failure patients (ischemic CPC). The transcription profile of healthy and ischemic CPC was analyzed and compared identifying an imbalance in genes involved in "Focal adhesion" and "Regulation of actin cytoskeleton" that, interestingly, are very closed to mechanotransduction. To test the involvement of these pathways, cells were stained with paxillin and phalloidin, a marker respectively of focal adhesion and F-actin. Consistently, ischemic CPC displayed differences in cytoskeleton morphology and high number of focal adhesions. Given the link between mechanotransduction, stiffness and ECM, we evaluated the responses of CPC plated on a soft (16kPa), intermediate (231kPa) and very hard (in order to GPa) substrates coated with two different fibronectin (FN) concentrations (1 and 25μg/mL). Data showed that ischemic CPC resulted more spread, less polarized and with less branching, displaying moreover a partial indifference to stiffness and FN. Interestingly, atomic force microscopy measure of cell stiffness, evidenced that ischemic CPC display the same indifference to substrate rigidity. Since all these data demonstrated that ischemic CPC behave differently with respect to healthy CPC when exposed to mechanical stimuli, we decided to study, in the same conditions, the nuclear shuttling of YAP and MRTF-A, two of the best-

known transducers of these stimuli into biochemical responses. Consistently with previous results, ischemic CPC are indifferent to applied stimuli since no differences in YAP and MRTF-A shuttling emerged. Moreover, in healthy CPC, but not ischemic CPC, the shuttling of YAP and MRTF-A is correlated. Finally, acting on pathways controlling YAP and MRTF-A, we found that healthy and ischemic CPC differ in pathways involved in signal transduction and in the degree of responses.

Conclusion

This study demonstrated that CPC isolated from ischemic hearts are characterized by altered mechanotransduction properties. The lost link between YAP and MRTF-A shuttling with physical cues and the aberrant response to treatment, suggest that restoring those pathways could result in improved CPC function.

TABLE OF CONTENTS

1. INTRODUCTION

1.1.HEART FAILURE

1.1.1. *The burden of heart failure*

Heart failure (HF) is a syndrome characterized by the altered ability of the heart to either contract (systolic heart failure or heart failure with reduced ejection fraction) to meet the metabolic needs of the body or to relax (diastolic heart failure or heart failure with preserved ejection fraction) (Komajda & Lam, 2014). The prevalence (number of people affected on total population) of HF is age-dependent, ranging from less than 1% of people younger than 60 years to almost 10% of those older than 75 years, as reported by the Rochester Epidemiologic Project (Redfield et al., 2003) and by the Rotterdam study (Mosterd et al., 1999). From these data, it is possible to extrapolate that about 26 million adults worldwide are living with heart failure (Bui, Anh, Horwish, Tamara, & Fonarow, Gregg, 2012) making it one of the most widespread illnesses after cancer (Torre et al., 2015) and HIV infections (Piot & Quinn, 2013). Across the globe, 17-45% of patients admitted to the hospital with a diagnosis of HF die within 1-year of admission, while most patients die within 5 years of admission (Bui, Anh et al., 2012). In North America, the incidence (newly affected patients per year) ranges from 2 to 5 per 1,000 person-year. In the Framingham Heart Study (Levy et al., 2002), the mean incidence of HF is 4.45 per 1,000 person-year, whereas in Olmsted cohort (Roger, Weston, Redfield, & al, 2004) the rate is 3.33 per 1,000 person-year. A very recent Italian study reported that the overall HF prevalence rate in our country in 2013 was 1.25% with estimates increasing with age, achieving 13.36% in people older than 90 years. The overall incidence was 1.99 per 1,000 person-year. Similarly, the incidence rate increases with age, especially in people older than 65 years (Piccinni et al., 2017).

The contribution of improved measures in treating heart attacks, which increase the proportion of survivors, and the ageing of general population, will lead to an alarming increase in heart failure burden (Heidenreich et al., 2013).

1.1.2. *Etiology*

A wide range of factors are known that may lead to HF, as reported by The Global Burden of Disease Study which determined 17 primary etiologies (Hawkins et al., 2009). Nonetheless, more than two-thirds of all cases of HF can be attributed to four conditions: ischemic heart disease, chronic obstructive pulmonary disease, hypertensive heart disease, and rheumatic heart disease. In the developed world, ischemic heart disease remains the leading cause.

Ischemic heart disease or Ischemic Cardiopathy (IC) is a pathologic condition caused by coronary atherosclerosis, leading, in the worst cases, to myocardial infarction (MI). In the 10 years after an MI, more than one-third of patients will develop HF (Hellermann et al., 2003).

1.1.3. *Pathology and classification*

The American College of Cardiology (ACC) and American Heart Association (AHA) define HF as "a complex clinical syndrome that results from any structural or functional impairment of ventricular filling or ejection of blood" (Yancy et al., 2013).

Historically, cardiac dysfunction has been assessed with reference to left ventricular ejection fraction (LVEF), accepted as normal over 50-60% values. However, it is now well documented that even patients which have a normal range LVEF, but a substantial impairment of diastolic relaxation or filling, may show HF syndrome symptoms. This led to classify, clinically, two main types of HF, based on the functional status of the heart: heart failure with preserved ejection fraction (HFpEF) and heart failure with reduced ejection fraction (HFrEF). Despite a LVEF that range over than 50% and a maintained left-ventricular (LV) cavity volume, heart in HFpEF subjects suffers of thickened and stiffened LV wall, hence, the ratio of LV mass/end-diastolic volume is high. In contrast, in patients with HFrEF, the LV cavity is typically dilatated and muscle fibers are stretched (Ohtani et al., 2012). Recently, a further sub-class has been created including patients with an LVEF in the range of 40–49% representing a 'grey area', defined as heart failure with mid-range ejection fraction (HFmrEF) (Andronic, Mihaila, & Cinteza, 2016). Howsoever, the end result of either HFrEF, HFpEF and HFmrEF is a fall in cardiac output.

Other clinical classifications have been employed for heart failure:

The New York Heart Association (NYHA) functional classification (Ponikowski et al., 2016) defines four functional classes as:

Class I: HF does not cause limitations to physical activity (ordinary physical activity does not cause symptoms);

Class II: HF causes slight limitations to physical activity (the patients are comfortable at rest, but ordinary physical activity results in HF symptoms);

Class III: HF causes marked limitations of physical activity (the patients are comfortable at rest, but less than ordinary activity causes symptoms of HF);

Class IV: HF patients are unable to carry on any physical activity without HF symptoms or have symptoms when at rest.

The American College of Cardiology/American Heart Association (ACC/AHA) staging system (Yancy et al., 2013) is defined by the following four stages:

Stage A: High risk of heart failure, but no structural heart disease or symptoms of heart failure;

Stage B: Structural heart disease, but no symptoms of heart failure;

Stage C: Structural heart disease and symptoms of heart failure;

Stage D: Refractory heart failure requiring specialized interventions.

1.1.4. *Adverse cardiac remodeling*

The development of the HF phenotype arises from a group of molecular, cellular and interstitial changes that manifest clinically as changes is size, mass, geometry and function of the heart after injury, called cardiac remodeling (Cohn, Ferrari, & Sharpe, 2000). Extensive myocardial remodeling is a process that occurs in both the infarcted and non-infarcted myocardium, leading to: altered tissue structure, increase tissue stiffness and ventricular dysfunction. This process involves abnormalities in energy metabolism (Azevedo, Minicucci, Santos, Paiva, & Zornoff, 2013), oxidative stress (Münzel, Gori, Keaney, Maack, & Daiber, 2015), inflammation (Epelman, Liu, & Mann, 2015), altered expression or function of contractile proteins (Maytin & S. Colucci, 2002), calcium transport (Min & Mark, 2014), neurohormonal activation (Florea & Cohn, 2014) and fibrosis (Leask, 2015).

Remodeling can begin with an acute infarction, leading to myocardial injury and cell death but involves a progressive group of changes, that affect the whole organ and were arbitrarily divided into an early phase (within 72 hours) and a late phase (beyond 72 hours) (Figure 1.1).

Early remodeling. In the 3-4 days after the MI and after the massive myocardial necrosis, an influx of inflammatory cells leads to the destruction of the collagen scaffolding that helps to maintain ventricular shape (Cleutjens, Kandala, Guarda, Guntaka, & Weber, 1995). Infarct expansion results in wall thinning and ventricular dilatation, causing diastolic and systolic wall stress, that stimulates the release of angiotensin II, which initiates the increases the synthesis of collagen (Sadoshima, Jahn, Takahashi, Kulik, & Izumo, 1992) and promotes cardiomyocyte hypertrophy and apoptosis (Watkins, Borthwick, Oakenfull, Robson, & Arthur, 2011)(Goldenberg, Grossman, Jacobson, Shneyvays, & Shainberg, 2001). The activation of the renin-angiotensin-aldosterone system (RAAS) stimulates the production of atrial and brain natriuretic peptides (ANP and BNP) to normalize ventricular filling and pump function. In this period, cardiac fibroblasts are recruited to the infarcted site and begin to deposit new collagen matrix that contribute to scar formation.

Late remodeling. Over the months, the main changes involve the viable myocardium. To compensate the loss of dead myocardium and preserve cardiac output, the increasing load on the non-infarcted myocardium leads to eccentric hypertrophy and LV cavity dilatation. Over the time, these initial compensatory mechanism switch to an adverse effect increasing LV size, which causes increasing wall stress and further dilatation (SMG Sutton & Sharpe, 2009).

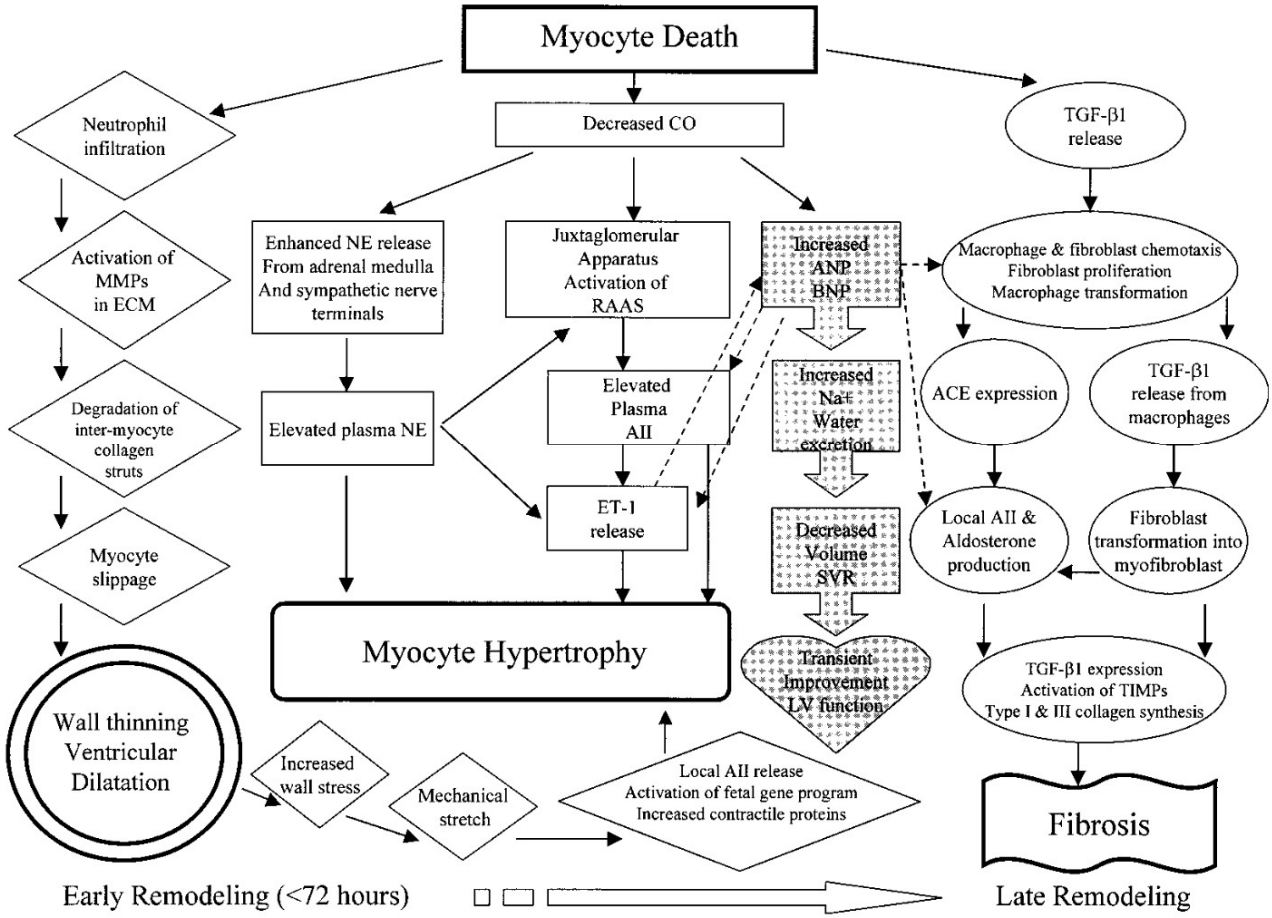

Figure 1.1 **Schematic representation of factors involved in the progression of ventricular remodeling**. ECM, extracellular matrix; RAAS, renin-angiotensin-aldosterone system; CO, cardiac output; SVR, systemic vascular resistance; LV, left ventricular; and AII, angiotensin II. The figure has been extracted from Martin G. St. John Sutton and Norman Sharpe, Left Ventricular Remodeling After Myocardial Infarction: Pathophysiology and Therapy, Circulation. 2000; 101:2981-2988.

1.2.THERAPY

Evidence from rodent and human studies challenges the view of the heart as a terminally differentiated organ (Bergmann et al., 2009). The heart seems to possess some regenerative capacities, that have been attributed to endogenous progenitor cell populations recently identified in the adult myocardium by several independent laboratories (Barile, Gherghiceanu, Popescu, Moccetti, & Vassalli, 2013; Uchida et al., 2013). Intrinsically, this regenerative capacity is insufficient to prevent the progression towards heart failure following various insults. To address this limitation, a common strategy has been to deliver stem/progenitor cells to the diseased heart through local implantation or promoting systemic migration (Segers & Lee, 2008). Since the beginning of this century, scientists have thus experimented the possibility to stimulate cardiac regeneration mainly through stem or progenitor cell administration (Schneider, 2016) with the primary objective to replace damaged myocardium and restore cardiac function (Witman & Sahara, 2018).

Skeletal myoblast was the first cellular type to be used for this purpose, since their ability to differentiate in muscle cells. However, clinical relevance was limited due to their reduced ability to commit to the cardiomyocyte fate (Menasché et al., 2008). The recognized differentiation plasticity of bone marrow derived stem cells led clinicians to test their potential use in cardiac regeneration. Although the implant of these cells produced an improvement in cardiac function, the results obtained were considered modest and, partially, contradictory (Fisher, Doree, Mathur, & Martin-Rendon, 2015). The reasons of these conclusion were attributed to the mechanism of action of implanted cells (release of extracellular factors) (Gnecchi, Zhang, Ni, & Dzau, 2008) rather than their differentiation towards the cardiomyocyte phenotype (Wu et al., 2015).

Recently, embryonic stem cells have been tested for their ability to promote cardiac regeneration. Such cells can be induced to differentiate easily in cardiac progenitors and cardiomyocytes and might ensure an almost unlimited source of cells to implant in the infarcted heart. However, ethical as well as biological issues (teratoma formation and rejection) have limited the use of these cells in clinical practice (Sanganalmath & Bolli, 2013).

A step to overcome these problems arrived thanks at the generation of induced Pluripotent Stem Cells (Takahashi & Yamanaka, 2006). Nevertheless, although unconstrained from ethical and rejection issues, iPSC efficiency in differentiation in mature cardiomyocytes was considered to be low (Takahashi & Yamanaka, 2006).

A promising set of cell population suitable for cardiac regeneration was found in the pool of stem/progenitor cells that resides in heart tissue. Beltrami et al. were the first who discovered self-renewing c-Kit+ cells in the adult heart, able to differentiate into cardiomyocytes, endothelial cells and smooth muscle cells and to support the regeneration of heart tissue (Beltrami et al., 2003). These cells

harbor the classical markers of stemness (self-renewal, clonogenicity and multipotency) and are able to differentiate in myocytes, smooth muscle and endothelial cells (Leri, Kajstura, & Anversa, 2011).

SCIPIO and CADUCEUS were the first two phase I clinical trials performed to study the safety and the potential efficacy of heart stem/progenitor cell for the treatment of patients suffering from ischemic heart disease. In 2011, data from the SCIPIO trial demonstrated no mortality or adverse events following the intracoronary infusion of autologous c-Kit+ CSC (cardiac stem cell) and improvement in heart functions (Bolli et al., 2011; Chugh et al., 2012). However, an important controversy has followed this trial. Indeed, the Lancet wrote a letter of concern about the integrity of some data contained in the paper (Editors, 2014). Nonetheless, the benefits of CSC were further confirmed by the CADUCEUS trial. In this case, cells were initially grown from endomyocardial biopsies as floating cell aggregates (named cardiospheres) that are enriched in primitive cells. Subsequently, cardiosphere-derived cells or CDC were obtained as cells outgrowing from the cardiospheres when these were attached to adhesive culture dishes. Finally, CDC were delivered into the heart of patients with severe LV dysfunction, reducing infarct size (Makkar et al., 2012; Malliaras et al., 2014). In the first randomized controlled phase II clinical trial PERSEUS the absolute changes in LV function were significantly greater in CDC-treated patients than in controls (Ishigami et al., 2017). Therefore, it was demonstrated that the administration of stem cells in ischemic hearts is a feasible procedure, devoid of risks in short and midterm nevertheless, there are several open questions on using CSC such as the mechanism of action, the dose and the best way of administration (Sanganalmath & Bolli, 2013).

A further approach aims to stimulate endogenously the cardiac stem cells pool (Castaldi et al., 2016; Zhang et al., 2016). However, our group and others have observed that, when stem cells are subjected to a stressful condition (i.e. any condition other than normal), peculiar stem cell features, such as telomerase activity and self-renewal, are lost, while increased apoptotic and cellular senescence rates are observed (Cesselli et al., 2011; Lewis-McDougall et al., 2018; Nguyen & Sussman, 2015). Unfortunately, there are several factors limiting the success of cardiac regeneration, that often do not (only) rely on the intrinsic cells features listed above, but also to the complex environment in which such cell resides.

1.3. EXTRACELLULAR MATRIX

1.3.1. *Cardiac ecm components*

Stem cells and their daughter progenitor cells reside within the stem cell niche, a specific environment arranged to maintain their proper function during life-cycle (Ferraro, Celso, & Scadden, 2010).
The extracellular matrix (ECM) is a key component of the stem cell niche. Its components embed the stem cells residing within, providing the right mechanical scaffold and the right anchor. Stem cell niche is intimately connected to the surrounding cardiac tissue, allowing stem cells to respond to signals from the outside, as in the case of myocardial injury.
The cardiac ECM is composed of different proteins, proteoglycans, and glycosaminoglycans that form a fibrillar mechanical support in which cells are embedded. These structural components include collagen types I, III, and V, as well as elastin. In addition to structural components, the ECM is composed of nonstructural elements that regulate important cellular functions, such as adhesion, proliferation, and differentiation. These are primarily type IV collagen, laminins, and fibronectin (Jourdan-Lesaux, Zhang, & Lindsey, 2010; Matsui, Morimoto, & Uede, 2010).

1.3.2. *Effects of ecm in stem/progenitor cell function*

The adhesion of cells to the extracellular matrix (ECM) regulates many cellular functions including spreading, migration, proliferation and differentiation, thus playing a major role in embryonic development, adult tissue homeostasis and disease pathogenesis (Discher, Mooney, & Zandstra, 2009; Jaalouk & Lammerding, 2009; Wozniak & Chen, 2009).
Additionally, as anticipated, environmental factors other than the chemical ones regulate the activity of stem cell/progenitor. Indeed, relatively recent works have demonstrated that the differentiation potential of MSCs is regulated by both substrate composition (Tan et al., 2010) and stiffness (Engler, Sen, Sweeney, & Discher, 2006). Following these pioneering studies, the impact that the substrate stiffness exerts on stem cell fate has become a major topic of investigation. Stiffness is defined by the Young's elastic modulus (E, measured in Pascals) which is the force needed to stretch a given material. Of peculiar importance for our work, studies conducted employing cardiogenic cells isolated from chick embryos, showed an increase by 60% of the myofibril orientation and by 3-fold the Troponin T levels when cells were cultured onto support with tunable stiffness compared to those with static stiffness (Young & Engler, 2011).Furthermore, embryonic stem cells grown on sections of decellularized cardiac ECM differentiate more promptly into cardiomyocytes (Higuchi et al., 2013). In line, it was shown that, when MSCs were cultured on ECM substrates coated with different collagen subtypes, Collagen V promoted cardiomyogenic differentiation whereas Collagen I and III demonstrated no effect (Tan et al., 2010).

One of the first studies that evaluated the effects of ECM composition on human c-kit+ CPC was conducted by Castaldo, Di Meglio and collaborators, who showed that human c-kit+ cells were more abundant in the epicardial/subepicardial regions of the heart. Importantly, epicardial cells could be grown as epithelial monolayers only in the presence of either subepicardial fibroblasts or the extracellular matrix produced in vitro by cardiac fibroblasts but underwent epithelial to mesenchymal transition and expressed c-kit after TGFβ stimulation (Di Meglio et al., 2010).

Additionally, French at al. analyzed the behavior of rat c-kit+ CPC cultured on decellularized porcine ventricular ECM or standard collagen type I (Matsui et al., 2010). They showed that early cardiac genes for GATA-binding protein-4 (GATA-4), Nkx2.5, α-myosin heavy chain, and troponin C and T were increased when CPCs were cultured for 2 days on cardiac ECM compared to collagen. Moreover, independent laboratories cultured c-kit+ cells isolated from pediatric patients onto 3D structures of rat ECM plus fibrin whose stiffness ranged from 2 to 32kPa, showing that the stiffness of the substrate influenced their differentiation status, as assessed by evaluating the expression of cardiomyocytes, endothelial and smooth muscle cell genes (Williams et al., 2015).

Altogether these results suggest that, since the commitment of stem cells to mature cell types is mediated by heart-specific ECM cues (that include its peculiar structure, elasticity and composition) and the heart remodeling process that follows cardiac ischemia leads to dramatic alterations in both stiffness and composition of cardiac ECM, cardiac pathology could possibly alter stem/progenitor cell functions by altering their niches.

1.3.3. *Ecm and cardiac fibrosis*

In the healthy heart, fibroblasts maintain ECM homeostasis by preserving tissue organization and structure, allowing a uniform excitation of the heart. The myocardial ECM contains a wide range of proteins including mainly: fibrillar type I and III collagen, fibronectin, elastin, laminin as well as proteoglycans and glycoproteins (McCulloch Christopher A. and Coelho, 2015). The fine balance between all these elements is massively disturbed in conditions of heart fibrosis and remodeling. For this last concept, it is worth to note that two thirds of heart volume are composed by cardiac fibroblasts (Camelliti, Borg, & Kohl, 2005). Being the most abundant cell type in the heart, is reasonable to think that after cardiac injury, propelled by the release of ANG II, TGF-β1, IGF-1, and TNF-α, fibroblasts, now turned into ECM-producing myofibroblasts, produce a massive deposition of new ECM, leading to fibrosis (D. Fan, Takawale, Lee, & Kassiri, 2012; Leask, 2015)(Figure 1.2).

The fibrosis process is associated with a remodeling of the ECM that, in chronic ischemia, consists of increased expression of collagen type I and III plus an abnormal fibril cross-linking. Besides collagen, expression of many other ECM components, including elastin, fibrillin, fibronectin, and proteoglycans,

are also changed (D. Fan et al., 2012). Fibrosis can be distinct in two patterns, *the reparative fibrosis,* aimed at replacing dead cardiomyocytes and *the reactive fibrosis* that occurs in the perivascular and interstitial space, in the absence of cell loss (Weber, Pick, Jalil, Janicki, & Carroll, 1989).

Reactive fibrosis is triggered by post-MI mechanical stress and induces the expansion of connective tissue in areas that are remote from the infarction, leading to enhanced stiffness of the myocardium and to the impairment of heart diastolic and systolic functions, thus compromising cardiac output (Diez et al., 2002). Heart muscle stiffness is largely determined by the composition of the muscle itself hence, in pathological conditions with increased ECM deposition, the muscle is stiffer. Specifically, in normal conditions, the heart muscle has a Young's modulus of about 10-15 kPa whereas fibrotic tissue typically ranges from 20 kPa to over 100 kPa (K. Herum, Lunde, McCulloch, & Christensen, 2017) (Figure 1.3).

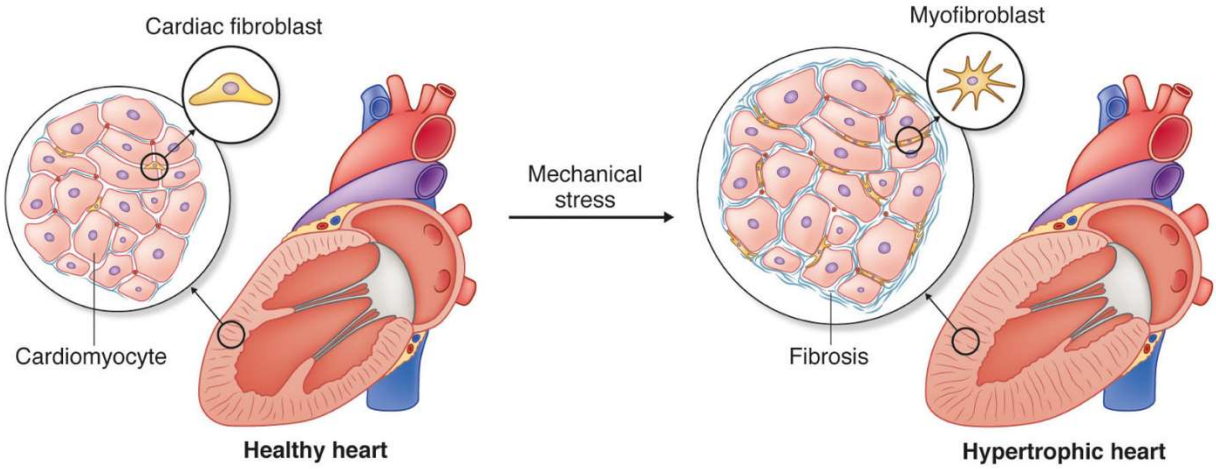

Figure 1.2. **The linkage between fibroblasts and cardiac fibrosis**. Cardiac fibroblasts are widely distributed within heart tissue surrounded by cardiomyocytes where they ensure the physiological amount and composition of extracellular matrix in the healthy heart. Mechanical stress promotes the transition of fibroblasts to the active myofibroblast phenotype, leading to fibrosis, causing cardiac remodeling and compromising cardiac function. The figure has been extracted from Herum et al. *The Soft- and Hard-Heartedness of Cardiac Fibroblasts: Mechanotransduction Signaling Pathways in Fibrosis of the Heart,* Journal of Clinical Medicine 2017

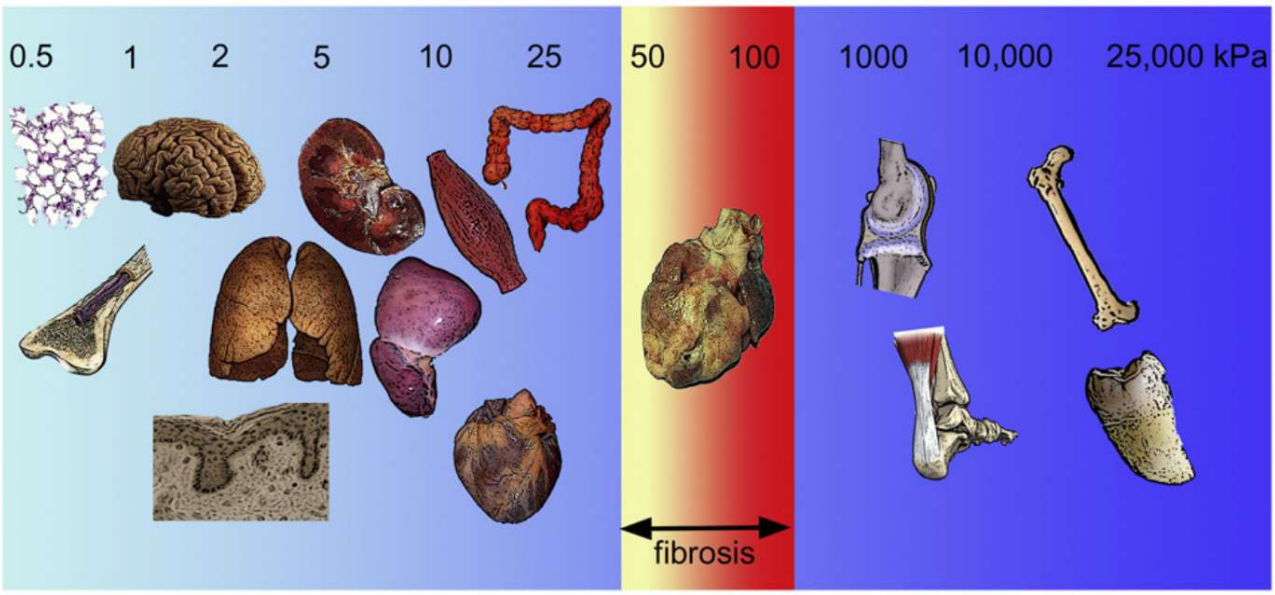

Figure 1.3. **Representation of the stiffness of organs and fibrotic scars**. Stiffness, represented as Young's elastic modulus (E), is a key component to preserve the physiological function of different organs. As clearly depicted by the figure, according to E it can be possible to categorize two groups, the parenchymal tissue and the bone-like tissue. Fibrosis cause an increasing of E creating a pathological category in which fibrotic heart belongs. The figure has been extracted from B. Hinz, *Matrix mechanics and regulation of the fibroblast phenotype*, Periodontol. (2013) 14–28.

1.4.MECHANOBIOLOGY

Aside from circulating cells in the blood, that are freely to move within the blood vessels, most of the body cells are anchored to the extracellular matrix and to other cells. As stated in previous paragraphs, the extracellular matrix is an active protagonist in driving the fate of cells in physiologic conditions, as well as during disease onset and progression. However, the comprehension of the mechanisms by which pathology-related modifications can change the response of cells has been obscure for long time.

The belief that cells rely to other types of stimuli beyond the classical soluble factors (cytokines or growth factors) has arisen from the discovery that the RGD (Arg-Gly-Asp) peptide of fibronectin interacts with a cell surface receptor identified, later, as the first integrin (Tamkun et al., 1986). In 1993 it was published the first evidence that integrins and focal adhesions cooperate to transmit mechanical forces (N Wang, Butler, & Ingber, 1993). Few years later, scientists demonstrated that cells can sense and respond to applied forces (N Wang & Ingber, 1994; Zhelev & Hochmuth, 1995). In the 90s, thus, the concept that cells are not inert to physical forces but instead, interact with them, generating biochemical responses, led to the bloom of the new field of mechanobiology.

Thus, those pioneering studies have demonstrated that cells are not only able to sense biochemical stimuli but also physical factors such as force and matrix elasticity and composition. To respond to various mechanical stresses, cells must have sensor molecules (mechanosensors) to translate mechanical forces into biochemical signals (mechanotransduction).

1.4.1. *Contributors to cellular mechanosensing*

A central element in mechanobiology is the cellular "mechanosensing" or the process by which cells sense the mechanical signals from the outside. The ability to probe the mechanical properties of the extracellular space is mainly based on the actin cytoskeleton and on the adhesion complexes that physically connect the cytoskeleton to the ECM. Extracellular forces travel through the ECM via collagen, fibronectin and laminin and are sensed actively via mechanosensory proteins such as integrins (Hynes, 2002), paxillin (Pasapera, Schneider, Rericha, Schlaepfer, & Waterman, 2010), vinculin (Carisey et al., 2013), p130Cas (Sawada et al., 2006), cytoskeleton (Burridge & Wittchen, 2013; Hayakawa, Tatsumi, & Sokabe, 2012) and stretch-activated ion channels (Kobayashi & Sokabe, 2010). Beyond these relevant examples, the list of mechanosensory proteins is more remarkable (Martino, Perestrelo, Vinarský, Pagliari, & Forte, 2018) leading the understanding of this process very arduous.

The mechanosensing is just a half of the process that allows the cell to adapt to external stimuli. To be effective, mechanical cues are transformed in biological signals such as post-translational modifications (Lachowski et al., 2018), intracellular shuttling (Dupont et al., 2011), protein unfolding (del Rio et al.,

2009) and novel interactions (Humphries et al., 2007) between a large number of molecules displaying a status change in response to mechanical stimulation.
Thus, the molecular mechanisms by which cells respond to mechanical stimuli are referred to as mechanotransduction. The cellular response to mechanical signals involves reorganization of the cytoskeleton, affecting cellular shape, orientation, polarity, migration and gene expression.

1.4.2. *Cytoskeleton*

The cytoskeleton is a dynamic structure that provides mechanical support to the cells, controlling their shape and tension homeostasis (Fletcher & Mullins, 2010). The propagation of extracellular and cell-generated forces is ensured by the regulation of cytoskeleton tension (Discher, Janmey, & Wang, 2005) and its disruption can lead to changes in gene expression and the consequent alterations of cell biological responses (Tamada, Sheetz, & Sawada, 2004).
The actin cytoskeleton consists of filamentous actin (F-actin), a helical polymer of globular (G) actin molecules, and a large number of actin-binding proteins. Cytoskeleton contractility is ensured by F-actin and myosin II held together in complex structures called stress fibers (SF), that are clearly visible in 2D substrates (Burridge & Wittchen, 2013). As anticipated, mechanical stress-mediated alterations of the actin filaments dynamics can modulate gene expression: when cells adhere to a stiff substrate, the F-actin to G-actin ratio increases and stress fibers are formed, causing nuclear translocation and activation of the transcriptional co-activator YAP. On the other hand, when cells adhere to a soft substrate or stress fibers are inhibited by drug treatment, YAP is retained in the cytoplasm (Halder, Dupont, & Piccolo, 2012). Thus, actin cytoskeletal remodeling has the potential to mediate mechanical stress-induced modulation of gene expression, playing crucial roles in mechanical force-induced cell proliferation, differentiation as well as in distinct pathophysiological processes, including embryogenesis, organogenesis, tissue homeostasis, organ size control and cancer progression.

1.4.3. *Focal adhesions*

The cell surface interface for mechanotransduction processes are Focal Adhesions (FA), specialized plasma membrane protein complexes composed of: adhesion receptors, signaling molecules and cytoskeletal proteins. The mechanosensing activity of FA consists in perceiving and transducing the mechanical cues arising from the extracellular milieu or the extracellular cytoskeleton into biochemical signals. Focal adhesion kinase (FAK) is one of the first molecules recruited to the developing FA in response to mechanical stimuli. FAK is a 125 kDa tyrosine kinase that exerts its function only when localized on FA (Shen & Schaller, 1999). The activation of FAK is accomplished when the clustering into focal adhesions enhances its autophosphorylation at Y397 (Schaller et al., 1994). Phosphorylation of FAK

at Y397 create a docking site for the SH2 domain of Src family kinases which, in turn, together with FAK, phosphorylates components of focal adhesion including FAK, paxillin and p130Cas, resulting in recruitment of additional signaling intermediates and activation of downstream signaling pathways. The main adhesion complexes that are involved in mechanosensing are the integrin-based focal adhesions (Winograd-Katz, Fässler, Geiger, & Legate, 2014). Integrins directly and rapidly activate nonreceptor protein tyrosine kinases, such as focal adhesion kinase (FAK), Src and Fyn in response to tension and stiffness (Carraher & Schwarzbauer, 2013; K. M. Herum, Choppe, Kumar, Engler, & McCulloch, 2017; Seong et al., 2013). FAK induces a cascade of signaling events involving ERK1/2 and MAPKs (Hynes, 2002) and with Src and Fyn facilitates the activation of Rho GTPases through activating guanine nucleotide exchange factors (GEFs) and GTPases-activating proteins (GAPs) in response to increased tension (Guilluy et al., 2011; Rossman, Der, & Sondek, 2005).

Extracellular matrix composition drives the expression of precise integrin subsets, that activate different signaling cascades and thus, different cellular response (Seetharaman & Etienne-Manneville, 2018). During the mechanotransduction process, stress fibers (SF) and FA cooperate and stabilize each other: the relocation of FA crosslinker proteins upon mechanical loading fosters SF reinforcement and cytoskeletal tension; on the other hand, SF contractility prompt vinculin recruitment to the FA (Fabry, Klemm, Kienle, Schäffer, & Goldmann, 2011; Yamashita et al., 2014). SF link to FA at-cell substrate contact and are well known to play critical roles in both sensing mechanical forces as well as generating mechanical forces (Pollard & Borisy, 2003).

1.4.4. *Rho*

The mammalian Rho-family contains approximately 20 members of small GTPases that are key molecules in regulating and remodeling the actin cytoskeleton under stress conditions. The family is divided in three groups in which RhoA, Rac1 and Cdc42 are the representative molecules for each family, and the best studied.

Rho/Rac1/Cdc42 activity is under the control of the opposing actions of Rho-Guanine nucleotide Exchange Factors (GEF) and Rho-GTPase Activating Proteins (GAP) (Bos, Rehmann, & Wittinghofer, 2007) regulating migration and cytoskeletal shaping by affecting the activities of downstream proteins (Ridley, 2015).

Rho-GEF and Rho-GAP are, in turn controlled by physical extracellular stimuli that regulate actin cytoskeleton are extremely different and include soluble factors or physical interactions with neighboring cells or matricellular proteins. These signals are sensed by various receptor proteins including G protein-coupled receptors (GPCRs) (Chiariello, Vaqué, Crespo, & Gutkind, 2010), receptors for integrins and transforming growth factor-β (TGF- β) (Ji et al., 2014) (REF) and Receptor Tyrosine Kinases (RTKs) (Schiller, 2006).

Rac1 and Cdc42 mediated the extension of lamellipodia and filipodia, respectively, contributing predominantly to cell migration whereas Rho is required to cell adhesion (C D Nobes & Hall, 1999; Catherine D. Nobes & Hall, 1995). In general, they act as promoters of both actin nucleation and branching, even if, among them, only Rho, through its downstream effector ROCK, is able to promotes stress fiber assembly (Watanabe et al., 1997) and FA formation (Riveline et al., 2001).

1.4.5. *Yap*

The Hippo signaling pathway is a complex network of proteins that control organ size via regulation of cellular proliferation, survival and differentiation. First discovered in *Drosophila*, the core of the Hippo pathway consists of a pair of highly conserved transcriptional coactivators that in mammals are known as YAP and TAZ. Briefly, in mammals, Mst1 and Mst2 activate other kinases (Lats1 and Lats2) that phosphorylate the transcriptional activator YAP and TAZ, causing it to be excluded from the nucleus and retained in the cytoplasm (Zhu, Li, & Zhao, 2014). YAP and its homologue TAZ are potent transcriptional coactivators that associate with various DNA-binding proteins, for example TEAD factors, to drive gene transcription (Zhu et al., 2014). YAP cannot bind to DNA directly and it is brought to certain gene promoters by partner transcription factors. The TEAD family transcription factors were identified as potent DNA-binding partner of YAP. Indeed, a point mutation of YAP (S94A) that eliminates its ability to interact with TEADs strongly abolishes YAP-induced gene expression as well as YAP induced cellular transformation (Zhao, Ye, et al., 2008).

In recent years, a plethora molecules and pathways acting upstream of the core Hippo pathway, that either activate or inhibit YAP/TAZ, have been discovered. These include different kinases (Yu & Guan, 2013), Wnt pathway (Varelas et al., 2010) and receptor tyrosine kinases (Reddy & Irvine, 2013), metabolic pathways (deRan et al., 2014; Liang et al., 2014; Sorrentino et al., 2014), cell adhesion and cell junction proteins, cell polarity proteins, and the state of the actin cytoskeleton (Boggiano & Fehon, 2012).

The latter is a central signaling system that the cell uses to make essential decisions, such as the decision to proliferate, differentiate and maintain stem cell proprieties (Mammoto & Ingber, 2009). Strikingly, these mechanical and cytoskeletal inputs represent a central mechanism to control YAP/TAZ activity (Figure 1.4)

The investigation of cell morphology on the regulation of Hippo has shown that when cells are grown on confined spaces, YAP is mostly cytoplasmic, whereas when cells are free to spread on the substrate YAP is localized to the nucleus (Nardone et al., 2017; Wada, Itoga, Okano, Yonemura, & Sasaki, 2011).

ECM stiffness is another potent controller of YAP/TAZ translocation. On hard substrates YAP and TAZ are predominantly nuclear and become cytoplasmic on softer substrates (Dupont et al., 2011). When distinct cell types (including epithelial cells and mesenchymal stem cells) adhere to a stiff substrate or are subjected to tensile force, the ratio of F- actin to G-actin increases and actin stress fibers are

formed, causing nuclear translocation and activation of the transcriptional co-activator YAP. In contrast, when these cells adhere to a soft substrates or stress fiber formation is inhibited by ROCK or myosin II inhibitors, YAP is phosphorylated by the upstream kinase, LATS, resulting in its inactivation via cytoplasmic retention or degradation (Dupont et al., 2011; Halder et al., 2012). In sparsely crowded cell cultures, YAP is predominantly localized to the nucleus and in its active un-phosphorylated form. On the other hand, in high density cultures Yap is phosphorylated and localized to the cytoplasm (Zhao et al., 2007).

Published works provide compelling evidence for a critical role of actin dynamics in the regulation of YAP through mechanical cues. Particularly, by correlating the activity of YAP with actin stress fiber formation and showing YAP inactivation by the use of F-actin or Rho inhibitors, but not by inhibiting microtubules or Rac1-GEFs (Dupont et al., 2011; Halder et al., 2012; Zhao et al., 2012).

YAP can also be regulated through G-protein coupled receptors (GPCRs) and serum starvation inhibits YAP activity via reduced GPCR signaling. GPCR receptor agonists (e.g., Lysophosphatidic acid (LPA), sphingosine-1- phosphate (S1P)) activate YAP/TAZ while epinephrine and glucagon inhibit YAP/TAZ via Gs-coupled GPCR signaling (Yu et al., 2012) (Figure 1.5).

Those studies point the importance of mechanical stress and cytoskeletal organization as dominant regulator of YAP and TAZ.

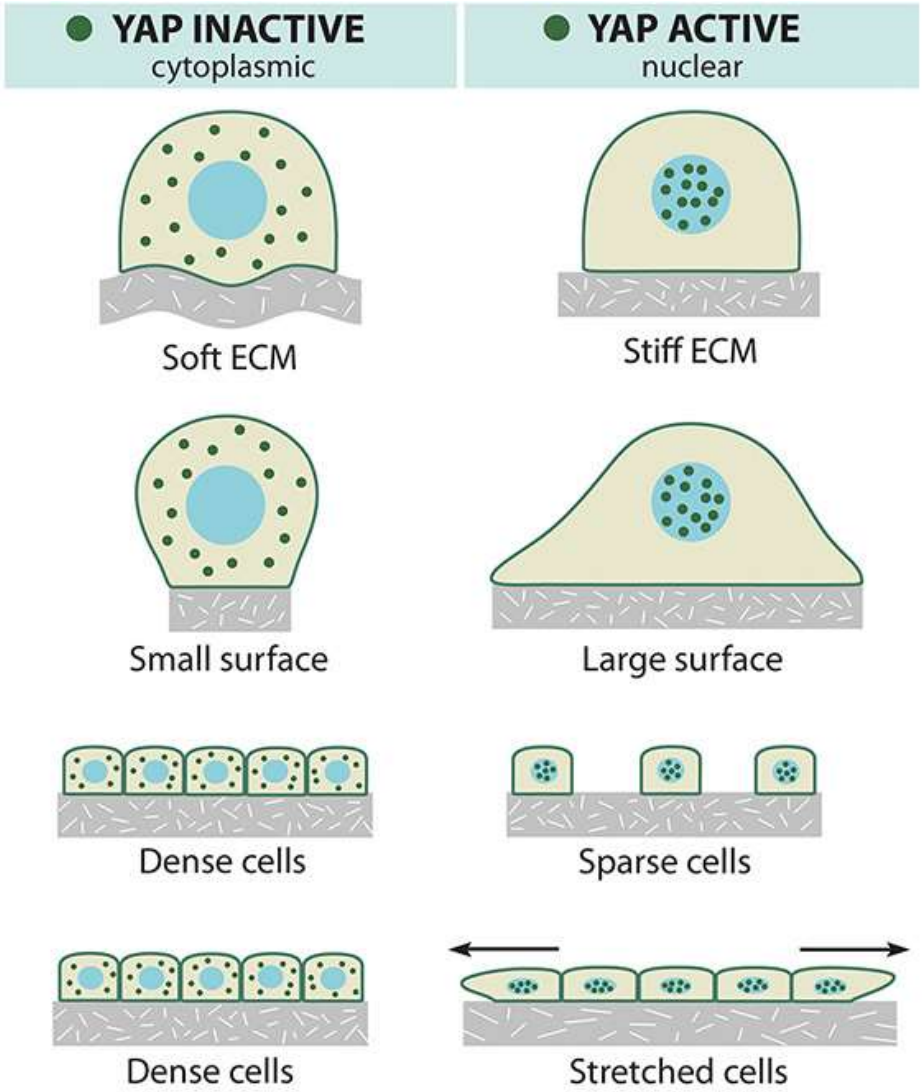

Figure 1.4 **Physical control of transcription factors shuttling**. The nuclear translocation of transcription factors is finely tuned by physical patterns following an on/off scheme. Yap was the first identified to rely to this principle. Picture downloaded from https://www.mechanobio.info

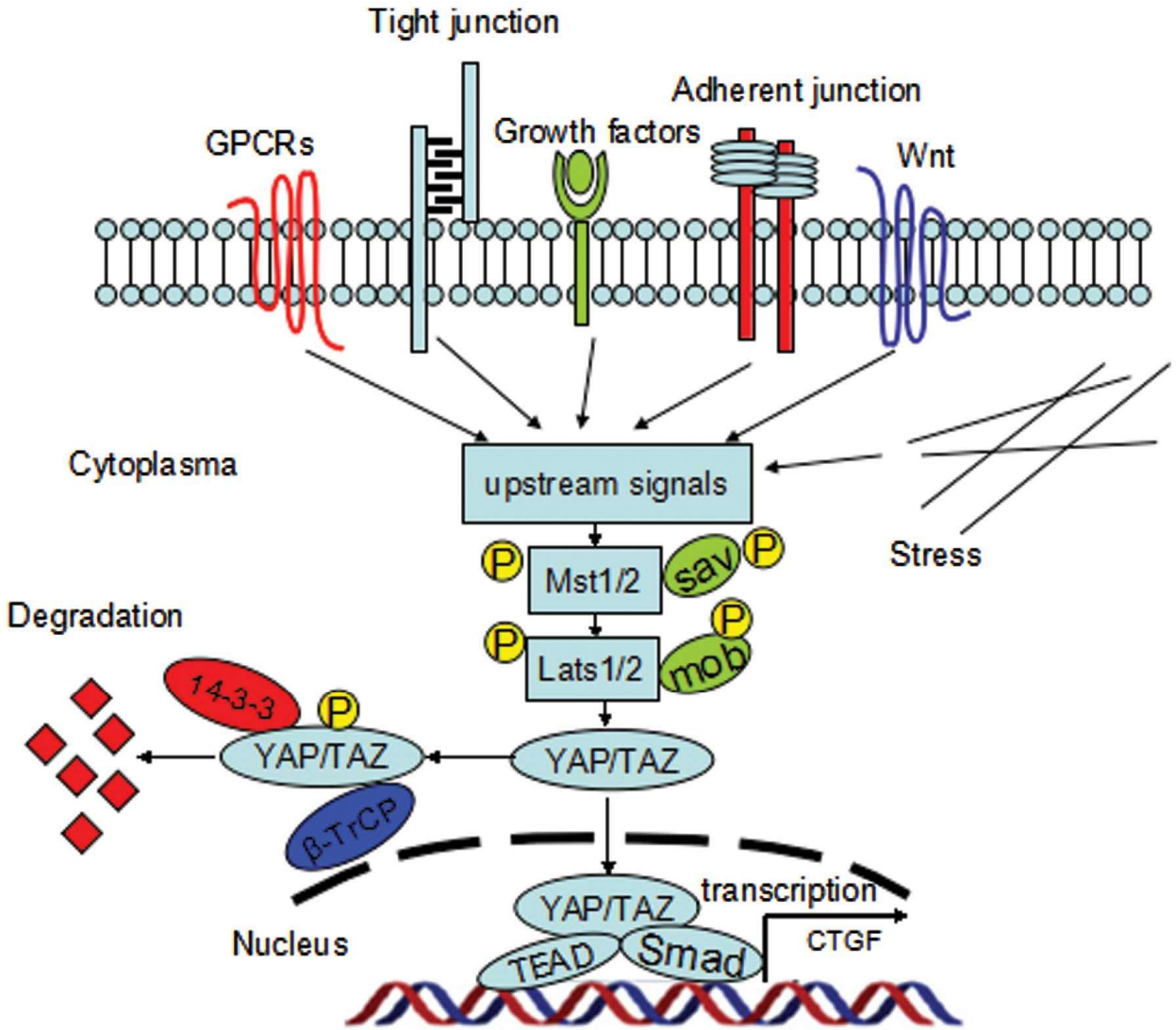

Figure 1.5. **Mechanisms of YAP regulation**. Mechanical cues controlling yap translocation act in synergy with a plethora of different receptors. Picture from Guo et al, *YAP/TAZ for cancer therapy: Opportunities and challenges (Review),* Int. J. Oncol. 2015

1.4.5.1. Yap biological significance

The Hippo-Yap pathway has been recently identified as a crucial axis in the regulation of organ size and shape during organogenesis, as well as a possible modulator of cancer growth (Zhao, Lei, & Guan, 2008). It is not surprising, therefore, that mechanical signaling has been linked to the regulation of YAP activity in a variety of biological contexts, such as cellular differentiation, fibrosis and cancer.

The Hippo-YAP pathway plays a critical role in the multipotency and differentiation of embryonic stem cells, neuronal progenitors, and intestinal stem cells (Barry et al., 2013; Cao, Pfaff, & Gage, 2008; Lian et al., 2010). In vitro, YAP/TAZ activity has been associated with mesenchymal stem cell (MSC) fate decision as well as a central regulator of human embryonic stem cell self-renewal through the control of SMAD complex shuttling to the nucleus (Mo, Park, & Guan, 2014). More recently, Panciera et al demonstrated that transient expression of exogenous YAP or TAZ, converts several differentiated mouse cell types to tissue-specific stem/progenitor cells (Panciera et al., 2016). Chromatin immunoprecipitation (ChIP) experiments indicated that YAP– TEAD binds to promoters of many stemness-promoting genes such as Oct4 (Bora-Singhal et al., 2015). Furthermore, although it seems to be dispensable for self-renewal it is claimed to be essential for ES differentiation Yap1 is dispensable for self-renewal but required for proper differentiation of mouse embryonic stem (ES) cells (Chung et al., 2016).

Given the functions of YAP in proliferation and stem/progenitor cell expansion a role of YAP in tissue regeneration has been postulated. In mouse, postnatal hearts have regeneration ability, which is quickly lost after day P7. Interestingly, knockout of Yap impairs regeneration of hearts infarcted on P2, while its over-expression improves regeneration of hearts infarcted at P28 (Xin et al., 2013).

1.4.6. *Mrtf*

Additional transcription factors whose activity is regulated by actin dynamics are already known.

The Myocardin-Related Transcription Factor A (MRTF-A/MKL-1) is another important mechanoresponsive signaling pathway. MRTF-A plays a critical role in transducing Rho/actin signaling from the cytoplasm to the nucleus by activating SRF-dependent transcription. In fact, RhoA signaling promotes actin polymerization (thus decreasing the concentration of free G-actin), resulting in the translocation of MRTF-A from the cytoplasm to the nucleus (Esnault et al., 2014). In line, MRTF-A is localized in the cytoplasm and translocate to the nucleus in response to either serum stimulation or other signals that promote actin polymerization. Specifically, MRTF is normally sequestered by G-actin in the cytoplasm but both mechanical and serum stimuli increase actin polymerization, resulting in the nuclear accumulation of MRTF, where it, together with serum-response factor (SRF), activates numerous cytoskeletal genes (Vartiainen, Guettler, Larijani, & Treisman, 2007). As shown in figure 1.6, Rho GTPase regulates actin cytoskeleton dynamics, promoting the assembly of G-actin in F-actin filaments (see rho chapter). Consistently, the nuclear accumulation of MRTF-A can be inhibited by forced expression of non-polymerizing actin mutants (Miralles, Posern, Zaromytidou, & Treisman, 2003). Last, Rho/ actin-induced nuclear import of MRTFs is also regulated by STARS (striated muscle activator of Rho signaling) protein, which binds to F-actin, facilitating translocation of MRTF-A to the nucleus (Kuwahara, Barrientos, Pipes, Li, & Olson, 2005).

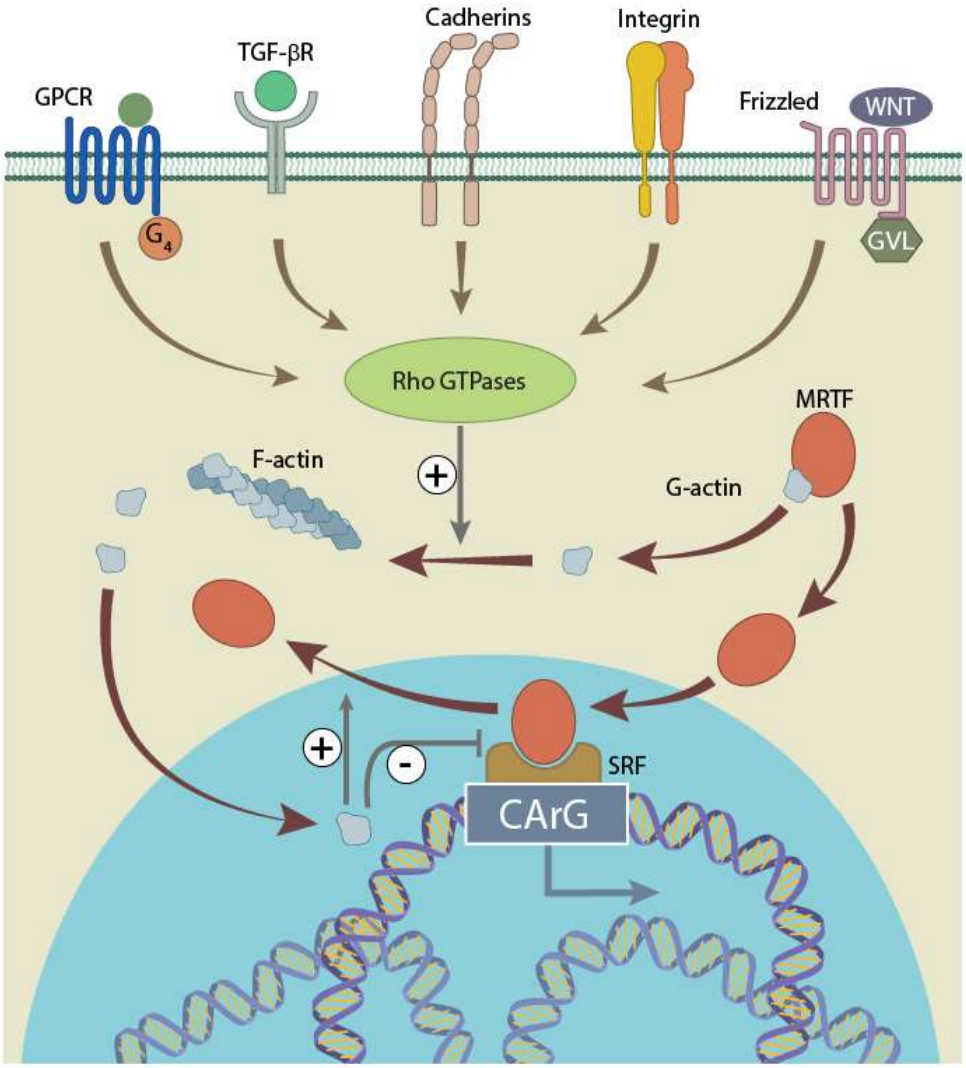

Figure 1.6 **MRTF-A nuclear translocation**. MRTF-A shuttling is closely related to the intracellular balance of glomerular actin (G-actin) and filamentous actin (F-actin). MRTF-A translocation is inhibited when high concentrations of G-actin are present in the cytosol. An increase in the actin bundles, make MRTF-A free to enter the nucleus and to bind to SRF, promoting gene transcription.

1.4.6.1. Mrtf biological significance

The SRF (serum response factor) transcription factor is an important regulator of cytoskeletal and muscle-specific gene expression and MRTF-A is essential for SRF function and, therefore, for SRF function (Olson & Nordheim, 2010).

SRF binds with high affinity and specificity to the palindromic CC(A/T)6GG DNA sequence, called the CArG-box (Pellegrini, Tan, & Richmond, 1995) and nearly all smooth muscle-specific genes and many cardiac and skeletal muscle genes are controlled by CArG-boxes. Given the plethora of genes encoding contractile proteins that are regulated by SRF and members of the myocardin family, it is not surprising that mis-regulation of the MRTF/SRF pathway is implicated in many diseases affecting mechanically-stressed tissues, such as the heart (Ho, Jaalouk, Vartiainen, & Lammerding, 2013; Parlakian et al., 2004). MRTF-A/SRF driven gene expression is observed in multiple cell lineages including undifferentiated ES cells. Moreover MRTF-A is co-expressed with myocardin in the human heart and aortic fibroblasts (Du et al., 2004; D.-Z. Wang et al., 2002). MRTF-A is central in promoting the myofibroblast phenotype, as stated in a study in which cardiac fibrosis was determined when MRTF-A-deficient animals were subjected to myocardial infarction; MRTF-A-null animals had reduced scar formation after MI (Small et al., 2010). Last, the MRTF/SRF axis has implications for the regulation of genes that provide a boost in CPC proliferation and gene transcription (Castaldi et al., 2016).

2. RATIONALE AND AIMS

Heart failure (HF) is the term used to describe a clinical condition characterized by the inability of the heart to sustain its workload reducing the delivery of a proper blood flow to the body. Population aging and improved survival of patient with acute myocardial infarction are leading to a yearly growing prevalence and incidence of HF, making it a global pandemic, affecting at least 26 million people worldwide.

So far, the only resolutive care for end stage HF patients is the heart transplantation. Of course, there is a manifest imbalance between the number of available donor hearts and patients in the waiting list for an organ. Moreover, life expectancy after transplantation is low, compelling the individuation of new therapies.

Advances in stem cell biology has highlighted that the heart is not a terminally differentiated organ, as previously thought. In fact, cells with a regenerative potential reside into cardiac tissue. From this promising discover, it was suggested that the heart tissue could be regenerated. Thus, new therapies have been experimented with the intent to regenerate lost tissue by either administering stem/progenitor cell with the potential to differentiated into cardiomyocyte or activating the residents Cardiac Progenitors Cell (CPC) pool.

In last years, many studies, including clinical trials, have been performed to investigate the best source of stem cells that needed to be used to achieve the aim. Despite promising results, an evidence of strong efficacy is still lacking. Since the experimental use of different stem cell types failed to produce considerable amelioration of patient outcome, it was suggested that this partial unsuccess was not due to the cells itself, but rather to the milieu in which the cells have to exploit their function.

Ischemic heart disease, the leading cause of HF, is in fact characterized by a severe loss of cardiomyocytes that are replaced by pervasive fibrosis leading to modifications of the extracellular matrix composition and stiffness, attributes considered critical for stem cell function (Ahmed & Ffrench-Constant, 2016). In this context, mechanotransduction pathways, used by cells to adapt to physical changes, have been progressively more investigated. This as a consequence of an increasing body of literature (Ning Wang, 2017), that shed light on the principal modifications of cell behavior in response to physical stimuli. It was demonstrated that physical stimuli mainly act on cytoskeleton dynamics and cell shape that, in turn, control the nuclear translocation of proteins known to be a master regulator of cell-ECM interaction (i.e. YAP and MRTF-A) (Finch-Edmondson & Sudol, 2016).

Since dramatic biomechanical changes dominate the ischemic heart, it is essential to understand if such extended changes impair the mechanotransductional apparatus of CPC. Aim of this study is, therefore, to find pieces of evidence of impaired mechanotransduction pathways in CPC isolated from ischemic hearts, comparing them with CPC isolated from healthy hearts.

More specifically, the project was organized in the following steps:

1. Identification of altered pathways linked with mechanotransduction,
2. Characterization of morphological and functional properties in CPC in response to physical stimuli,
3. Evaluation of YAP and MRTF-A nuclear translocation in CPC in response to physical stimuli,
4. Identification of upstream regulators of YAP and MRTF-A subcellular localization employing specific pharmacologic inhibitors.

3. METHODS

3.1. Patient enrollment and ethics

Patient enrolled for this study have suffered for ischemic-induced end-stage heart failure (stage D AHA classification) and underwent cardiac transplantation at the University Hospital of Udine.

The study, in accordance with the Declaration of Helsinki, was approved by the Ethics Committee of Udine (2 August 2011, reference number 47831) and written informed consent was obtained from each patient.

3.2. Cardiac progenitor cells isolation

Human cardiac progenitor cells (CPCs) employed in this study were isolated as in (Beltrami et al., 2007) from atrial samples collected from healthy hearts and from explanted ischemic end-stage failing hearts of patients undergoing heart transplantation at the University Hospital of Udine.
Atrial fragments were first mechanically dissociated using scalpels and then enzymatically by incubation in a 0.1% Collagenase type II solution (Sigma-Aldrich) for 20 minutes at 37°C in a tube rotator. Collagenase activity was stopped by adding 0.5% Bovine Serum Albumin (Sigma Aldrich) in Basic Buffer (BB) and, once fragments have sedimented, cell suspension was centrifuged at 300 g for 5 minutes. Supernatant was discarded, pellet resuspended in 5 ml of BB and filtered through a pre-wet 40µm strainer (BD Falcon). The filtered suspension was centrifuged at 300 g for 5 minutes, supernatant was discarded, and cell pellet resuspended in Mesencult (STEMCELL Technologies), added with 1% Penicillin/Streptomycin (Gibco – Life Technologies). Isolated cells were finally seeded on dishes previously coated with 5µg/ml human fibronectin (Merck-Millipore) and cultured in a 5% CO_2 incubator. At passage 2 cells were switched to expansion medium.

3.3. Detachment and expansion of CPC

To detach the cells, the plates were washed with 5ml of HBSS and 2ml of TrypLE Express solution (Life Technologies) was added. Cells were incubated until the cells dissociate and 5ml of HBSS were used to inactivate enzymatic activity. Cell suspension is centrifugated at 300g for 5 minutes and the supernatant was discarded. Cell were resuspended in proper culture media and seeded in new fibronectin coated petri dish.

3.4. Cell migration – scratch assay

To evaluate the migration rate of CPC, a scratch assay was set up. Both healthy and ischemic cells were plated on 96well-plates coated with 1, 5 or 25μg/ml of fibronectin. When the confluence was reached, scratches were created utilizing 10μl tips. Phase contrast images were acquired immediately, at 4 and 8 hours and analyzed with FIJI software. The rate of cell migration was expressed as average of 4 different scratch point and it was calculated as distance traveled (μm), in the interval of time between 4 and 8 hours from the creation of the scratch.

3.5. Hydrogel substrate preparation and functionalization

Hydrogels were prepared mixing different proportions of acrylamide and bis-acrylamide to obtain substrates of different stiffness (table 3.1). Hydrogel substrates were prepared onto 12mm glass coverslips. The surface of clean coverslips was functionalized with 3-(Trimethoxysilyl) propyl-methacrylate (M6514, Sigma-Aldrich) diluted in one volume of absolute ethanol to let the polyacrylamide attach to the glass. After 2-4 minutes coverslips were washed twice with absolute ethanol and then with distilled water. Coverslips were let air-dry. A glass surface was treated with Dichlorodimethylsilane (440272, Sigma-Aldrich) to avoid polyacrylamide attachment and used as support to distribute 20 μl of polyacrylamide solution on which functionalized coverslips were laid on. At completed polymerization, hydrogels were washed at least for 16 hours in distilled water at 4°C before functionalization.

Hydrogel surface were functionalized with 0.1mg/ml of Sulfo-SANPAH solution (22589, Thermofisher) and exposed to a UV light source for 20 minutes. Hydrogels were washed twice with sterile PBS, covered with a fibronectin solution (1μg/ml or 25μg/ml) and incubated overnight at 4°C. Hydrogels were then washed with PBS twice before seeding the cells.

Stiffness	**40% acrylamide (ml)**	**4% bis-acrylamide (ml)**	**APS**	**TEMED**	**Distilled water (ml)**
16 kPa	2.5	0.37	1%	0.1%	7.13
231 kPa	5	3.75	1%	0.1%	2.25

Table 3.1. Chemicals for hydrogels preparation.

3.6. Immunofluorescence analysis

For immunofluorescence analysis, CPC were fixed in 4% paraformaldehyde for 15 min and then permeabilized with 0.3% Triton X–100 in PBS. Samples were then incubated with anti-YAP antibody (1:300, sc-101199, Santa Cruz Bio) and anti-MRTF-A (1:300, PA5-56557, Life-Technologies) overnight at 4°C, followed by incubation with Alexa-Fluor 488 anti-mouse and Alexa-Fluor 633 anti-rabbit secondary antibodies (1:800, Molecular Probes) at 37°C for 1.30 h. Focal adhesion were stained with anti-PAXILLIN antibody (1:100, 05-417, Millipore) overnight at 4°C, followed by Alexa-Fluor 633 anti-mouse secondary antibodies. To visualize cells, actin was stained with rhodamine phalloidin (R415 Life Technologies) for 20' at 37°C and DAPI (4',6-Diamidine-2'-phenylindole dihydrochloride) in Vectashield (Vector Laboratories) was used for nuclear staining and mounting. All the images used for analyzed the cell shaping and the ratio of YAP and MRTF-A were acquired using an epifluorescence microscope (DM6000B, Leica Microsystems) equipped with DFC365FX camera (Leica Microsystems) with a 63X immersion oil objective. Images of paxillin for focal adhesion analysis were acquired with a confocal microscope (TCS SP8 STED, Leica Microsystems) equipped with a 40X immersion water objective. At least 30 cells were measured.

3.7. Atomic force microscopy

Cells' forces were measured with an Atomic Force Microscopy (NanoWizard II, JPK instruments, Berlin, Germany) coupled with an inverted optical microscope (Axiovert 200; Zeiss). For indentation measures "tipless" triangular cantilevers, with spring constant of k=0.32 N m^{-1} (Nanoworld, Cr/Au back-side coating) were used, on which a silica 4.5μm diameter beads where attached using UV sensible light (NOA 73 Norland Optical Adhesive). Before measures, elastic constant of cantilever was calibrated with "thermal noise" method in the fluid chamber. Measures were performed in the fluid chamber at room temperature, in which hydrogel or glass supports with cells where placed in advance. For each cell, 15 curves have been taken for single point with 3 second delay each to another and with a setpoint (relative to indentation force) of 0.5nN and 5μm s^{-1} speed. At least 10 cells were measured.

3.8. Real time pcr

Rna from cell pellet was extracted with RNeasy (Qiagen) according to manufacturer's instructions. Total RNA concentration and quality were determined by measuring the absorbance at 260nm (A260) using a Nanodrop spectrophotometer (Nanodrop 1000, Thermo Scientific).

Prior to retro-transcription, eventual DNA contamination was removed by treatment with DNAse I (Invitrogen). cDNA was synthesized using Superscript III, Oligo(dT)12-18, dNTPs mix and RNaseOUT (Invitrogen) according to manufacturer's instruction.

Real-Time-qPCR analyses were performed on triplicate sampling of retrotranscribed cDNA using a LightCycler480 (Roche) and analyzed with the Roche software, version 1.5. Expression levels were normalized to GAPDH. Primer sequences used to amplify CYR61, CTGF and ANKRD1 are listed in table 3.2. Data are expressed as $2^{\wedge -(\Delta ct)}$.

GENE	**Forward primer**	**Reverse primer**
CYR61	CCTTGTGGACAGCCAGTGTA	ACTTGGGCCGGTATTTCTTC
CTGF	AGGAGTGGGTGTGTGACGA	CCAGGCAGTTGGCTCTAATC
ANKRD1	AGTAGAGGAACTGGTCACTGG	TGGGCTAGAAGTGTCTTCAGAT

Table 3.2 Primer sequences

3.9. Drug treatment

At 4th passage, cells were treated according to what reported in table 3.3. Cells were exposed to drug 16 hours after seeding. Prior to receive serum free medium, cells were exposed to 16 hours with medium with 0.1% serum to avoid cell loss. For a control, cells were treated with the vehicle alone (DMSO).

TREATMENT	**TARGET**	**[ ]**	**TIME**
CI-1040	MEK	50nM	2h
FAK inhibitor 14	FAK	10μM	2h
Latrunculin-A	ACTIN	25 μM	2h
Y-27632	RHO	12.5 μM	2h
Serum free medium	//	//	2h

Table 3.3 Resume table reporting treatments with their corresponding target, dosage and time.

3.10. Bioinformatic analysis

List of differential expressed genes obtained from (Gianfranceschi et al., 2016) were subjected to bioinformatic analysis with the Gene Ontology Consortium – Enrichment Analysis tool (http://geneontology.org/) and KEGG mapper (https://www.genome.jp/kegg/mapper.html).

3.11. Image analysis

FIJI software was used to analyze all the images for this study. "Cell shape descriptors" function of FIJI was used for morphological evaluation of cells.

Ratio of Yap and Mrtf were calculated as ratio of mean nuclear signal and mean perinuclear signal. Nuclear signal was selected with a mask on dapi staining; perinuclear signal was referred to a 3μm zone surrounding the nucleus.

3.12. Statistical analysis

Data are described as median and interquartile range.

Gaussian distribution of data was assessed employing the Kolmogorov/Smirnov test. Comparison among groups with one independent variable was performed with Kruskal/Wallis test followed by Dunn's post-hoc test. Comparison among groups with 2 independent variables was performed employing repeated measurements two-way ANOVA followed by Sidak's multiple comparison test. Correlation coefficients (R^2) were computed from linear regression curves of data.

A $p<0.05$ was considered significant.

Analysis were conducted with GraphPad Prism 6.0 for Windows.

3.13. Solution and culture media

Basic Buffer: MEM Joklik (Sigma-Aldrich 56449C), 4,7 g/l HEPES (Sigma-Aldrich), 0,3 g/l Glutamine (Sigma-Aldrich), 0,25 g/l Taurine (Sigma-Aldrich), 1% Penicillin/Streptomycin, Insulin 20 U/L (Sigma-Aldrich), pH 7,4.

Incubation buffer: (0,5% BSA in Basic Buffer), pH 7,4.

Expansion medium: 60% DMEM low glucose (Invitrogen), 40% MCDB-201 (Sigma-Aldrich), 1 mg/ml linoleic acid-BSA (Sigma-Aldrich), dexamethasone 10-9M (Sigma-Aldrich), 2-fosfate ascorbic acid 10-4 M (Sigma-Aldrich), 1X Insulin transferrin sodium-selenite (Sigma-Aldrich), 2% Fetal bovine serum (FBS; Stem Cell Technologies), 10 ng/ml human-PDGF-BB (Preprotech EC), 10ng/ml human-EGF (Preprotech, EC).

PFA 4%: 4g of paraformaldehyde in 100ml PBS, pH 7,4.

4. RESULTS

4.1. Gene expression and biological analysis

To evaluate whether cardiac pathology perturbs the mechanosensing capacity of cardiac progenitors (CPC), we re-analyzed the transcriptional profiles of CPC isolated from healthy (n=4) and ischemic (n=4) hearts that were obtained in a previous study of our group (Gianfranceschi et al., 2016). Only differentially expressed genes (DEG) that showed a significant ($p \leq 0.05$) expression difference of at least 1.7-fold between healthy and ischemic were considered. 372 genes and 423 genes were found to be up-regulated and down-regulated in cells from ischemic hearts, respectively.

To understand the biological function of the results of the transcriptomic analysis, we performed a new functional annotation analysis using two different pathways databases: Gene Ontology and KEGG.

Importantly, Gene Ontology (GO) analysis showed that, with regard to the:

a) "**Biological Process**" category, 183 and 189 ontologies resulted to be downregulated and upregulated in ischemic cells, respectively (Table S1 and S2). In both groups, the GO term "*Regulation of cell adhesion*" is represented by 38 downregulated genes and by 30 enriched genes. In the group of enriched genes, the GO term "*Actin cytoskeleton organization*" appears, where 21 genes were upregulated.
b) "**Molecular Function**" category, 7 and 19 ontologies resulted to be downregulated and upregulated in ischemic cells, respectively (Table S1 and S2). In agreement with what seen above the link with cell adhesion and cytoskeleton is confirmed by genes involved in "*Extracellular matrix structural constituent*" and "*Cytoskeletal protein binding*".
c) "**Cellular component**" category, 65 and 79 ontologies resulted to be downregulated and upregulated in ischemic cells, respectively (Table S1 and S2). A total of 52 genes displayed a different expression in the "*Focal adhesion*" group. Moreover, the "C*ytoskeleton*" entry included 65 genes upregulated in ischemic cells.

Finally, KEGG analysis enabled us to link the list of DEG to specific pathways. Interestingly, among others, the enriched pathways comprise the "*Focal adhesion*" and "*Regulation of actin cytoskeleton*" gene sets (Figure 4.1).

Altogether, bioinformatic analysis indicated that the expression of genes involved in the regulation of cell adhesion and cytoskeleton dynamics, both involved in cell mechanics, is altered in CPC isolated from ischemic hearts.

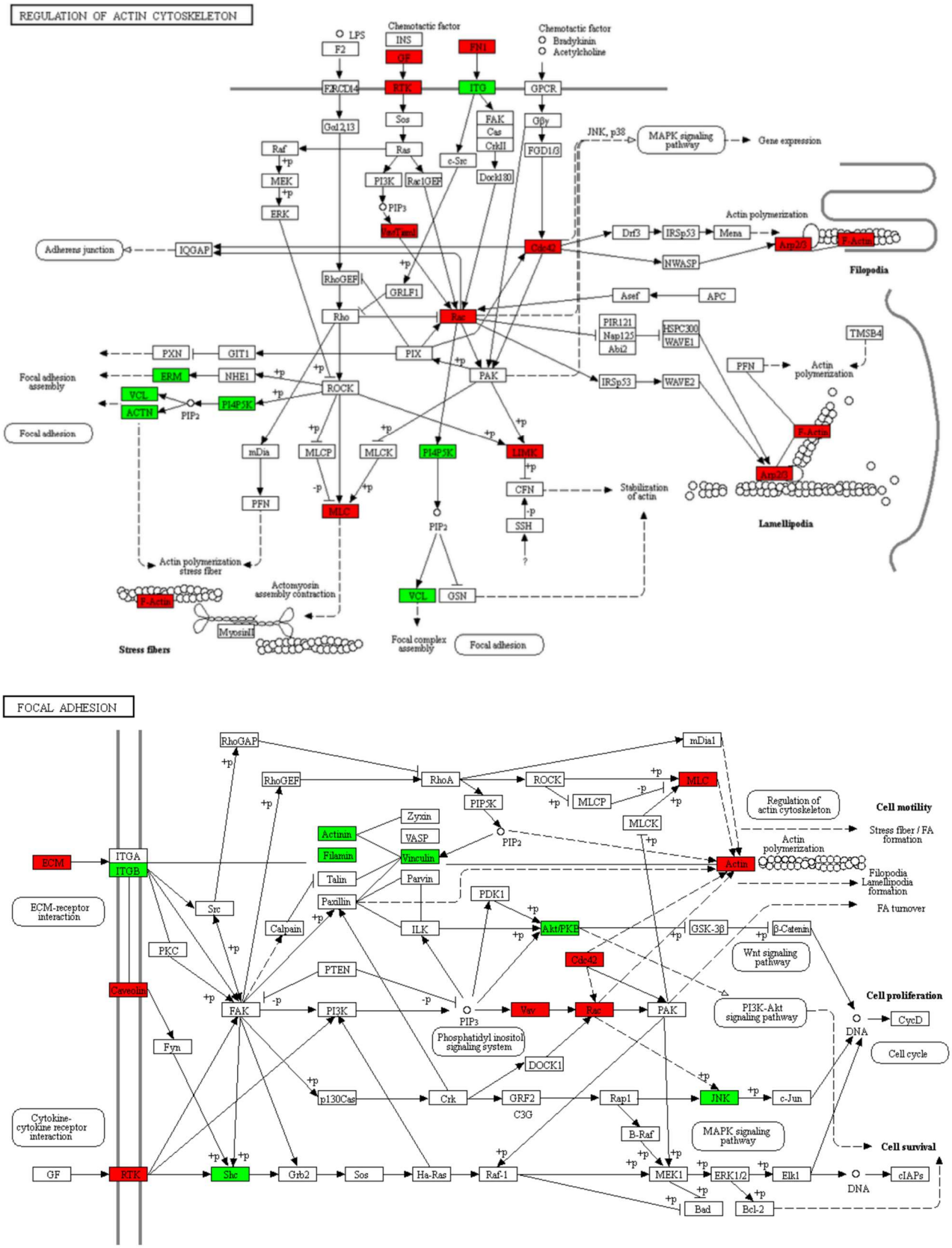

Figure 4.1 **Kegg map analysis**. Graphical representation of "Regulation of actin cytoskeleton" and "Focal adhesion" pathways. Red and green blocks underline down-regulated and up-regulated genes in ischemic CPC respectively.

4.2. *Morphological properties of cpc*

Together with cell growth, division and death, cell shape is an indicator of cell health.

Since both focal adhesions and the cytoskeleton are critical regulators of the proper physical proprieties and structure of the cells (Kuo, 2013), we started investigating whether differences in "*Focal adhesion*" and "*Regulation of actin cytoskeleton*" pathways, resulted in altered cell morphology in vitro.

To test this hypothesis, we first studied and compared the morphological features of healthy and ischemic cells (n=5 each) using the FIJI function Shape Descriptors.

To avoid the attenuation of possible differences as a consequence of the extensive *in vitro* culture and to ensure that cells had enough space to spread (i.e. to avoid cell contacts), cells were plated in sparse conditions and fixed 2 and 4 hours after plating. After seeding, the analysis was performed on cells stained with phalloidin, to highlight the F-actin cytoskeleton.

Morphometric analysis of fluorescent images (Figure 4.2) showed that cells isolated from ischemic hearts spread over a significantly higher area of the substrate and displayed a less elongated shape when compared with healthy ones at the 4 hours' time point. Concerning "*solidity*", a parameter that describes the presence of branches emanating from the cell body (e.g. filipodia and lamellipodia), the major difference was apparent at 4 hours, although the value does not reach significance ($p=0.08$).

The results of this first morphological evaluation suggest the involvement of pathways controlling cytoskeleton dynamics in ischemic cells and that these parameters can be used as an indicator of cell health.

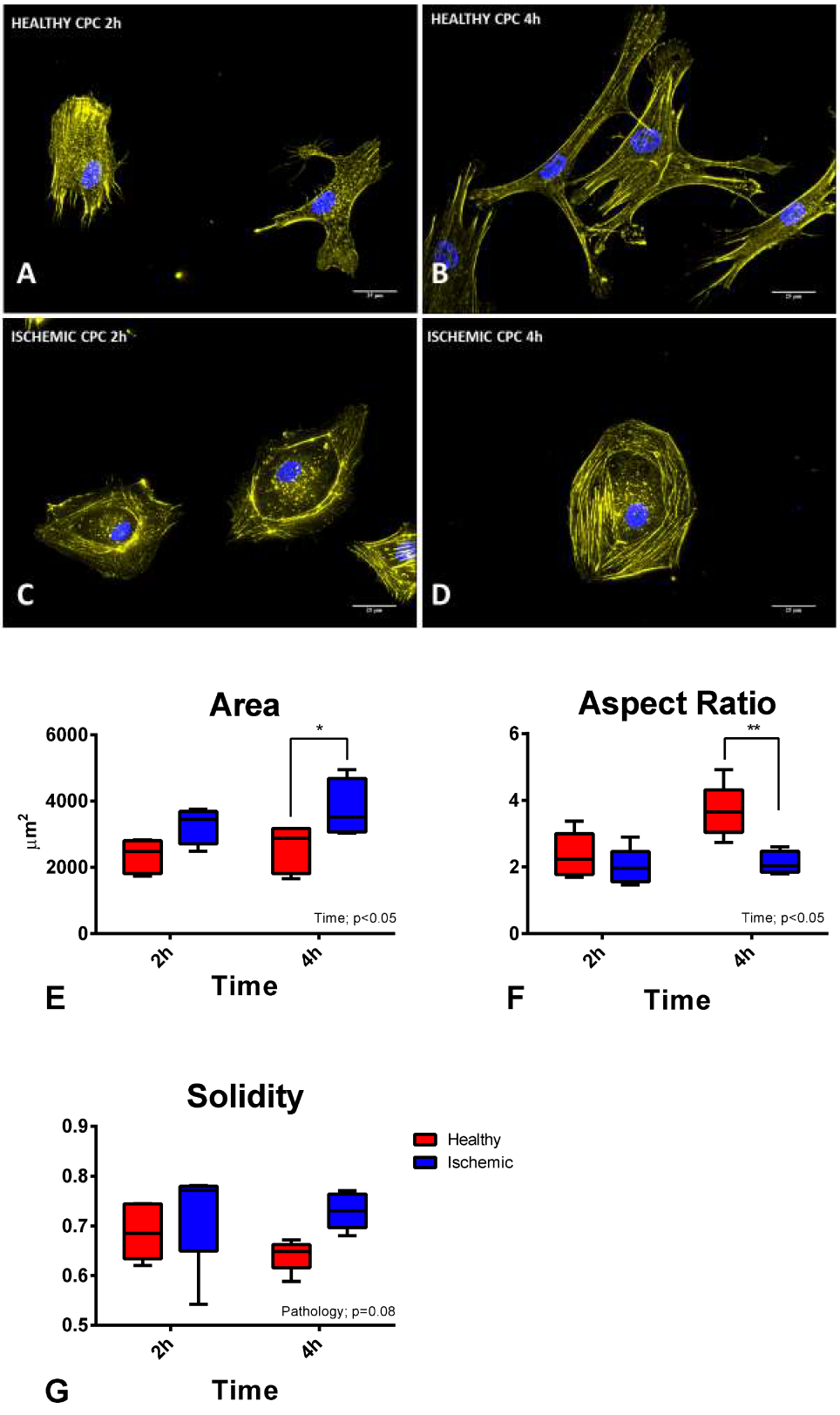

Figure 4.2 **Morphological characterization of CPC in function of time**. Representative fluorescence images of healthy CPC (**A**-**B**) and ischemic CPC (**C**-**D**) stained with actin dye phalloidin (yellow). Nuclei were stained with DAPI (blue). Box and whiskers plots compare CPC values of area (**E**), aspect ratio (**F**) and solidity (**G**) at 2 and 4 hours. N=5 each. *p<.05; **p<.01. Scale bar 25µm.

4.3. *Cytoskeletal properties of cpc*

To assess if the morphological differences described above were paralleled by a different organization of both the cytoskeleton and of its interaction with the substrate, we analyzed the F-actin network and the morphologic features of focal adhesions.

In collaboration with the undergraduate student Eliana Pomarè, we cultured CPC isolated from normal and pathologic hearts onto glass coverslips coated with 1μg/ml or 25 μg/ml of fibronectin. The morphometric analysis of the actin stress fibers (SF) was conducted on phalloidin stained cells, employing an ImageJ macro (Eltzner, Wollnik, Gottschlich, Huckemann, & Rehfeldt, 2015) that segments the distinct fibers and measures their number. As shown in figure 4.3, ischemic CPC present a cytoskeleton characterized by a larger number of SF, compared to healthy CPC.

To analyze the presence and number of focal adhesions, cells were grown on a glass substrate coated with fibronectin (both 1 and 25 μg/ml) and stained with an anti-paxillin antibody (Figure 4.4 F). Quantitatively, we observed that cells isolated from failing hearts were characterized by a significantly larger absolute number of focal adhesions/cells. However, when we compared the ratio between the area covered by focal adhesions to the cell area, the result was the opposite (Figure 4.4 G).

Altogether these data indicate that CPC isolated from normal and pathologic hearts differ in their actin cytoskeleton dynamics and in the ability to interact with the substrate via focal adhesions.

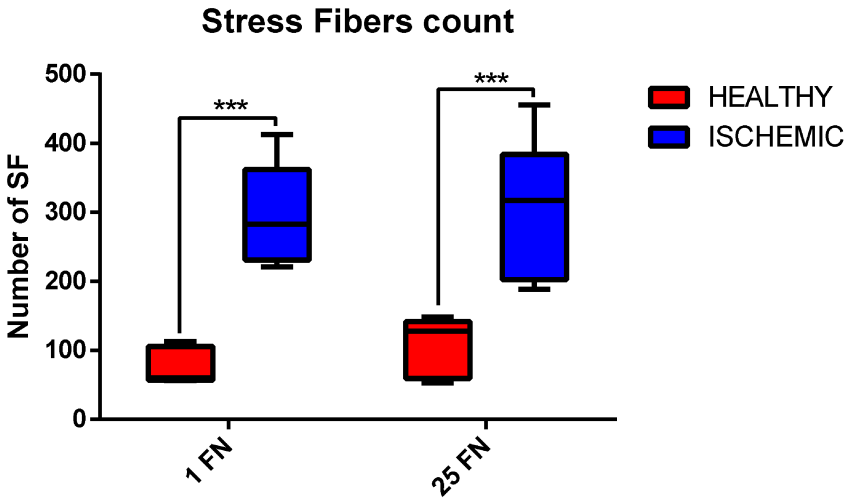

Figure 4.3 S**tress fiber count**. Comparison of stress fibers number in healthy and ischemic CPC seeded on 1μg/ml (1FN) or 25μg/ml (25FN) of fibronectin. Healthy, N=5; Ischemic, N=6. ***p=0.0001.

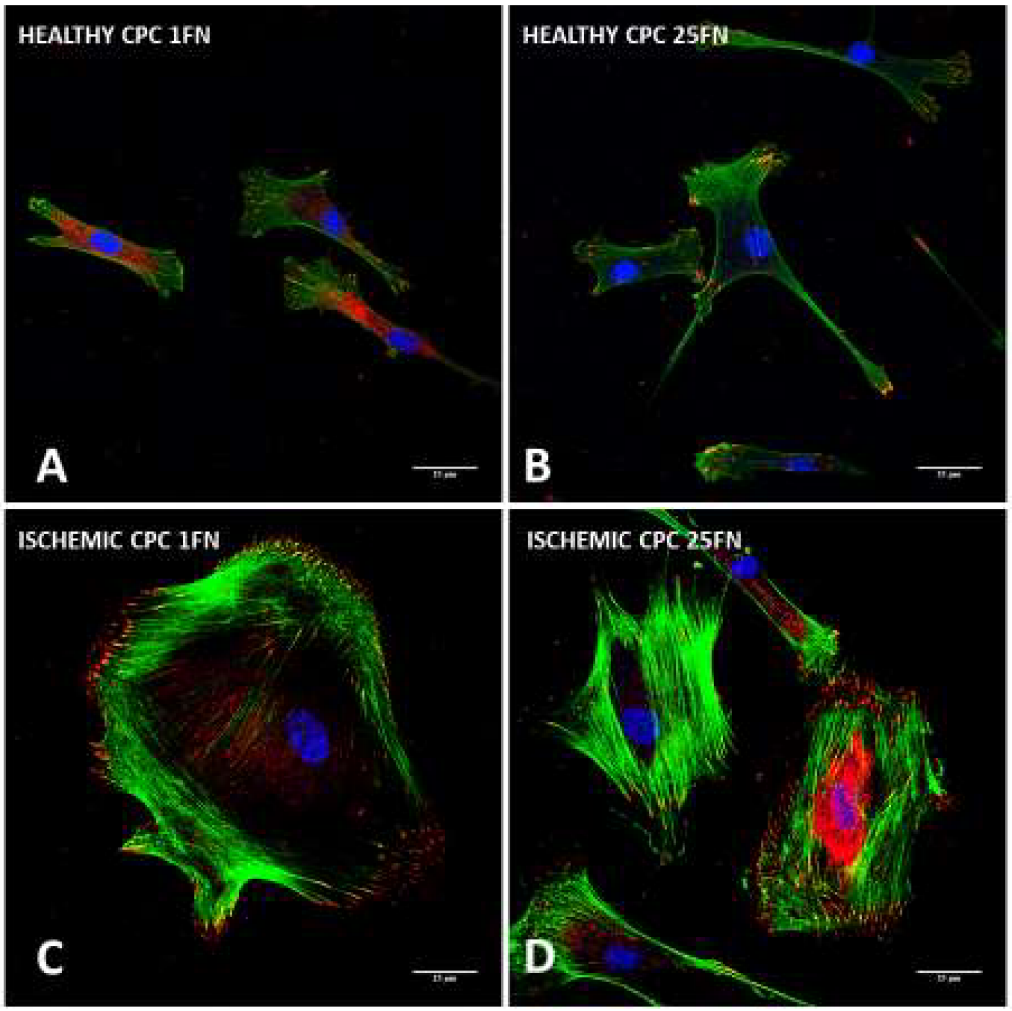

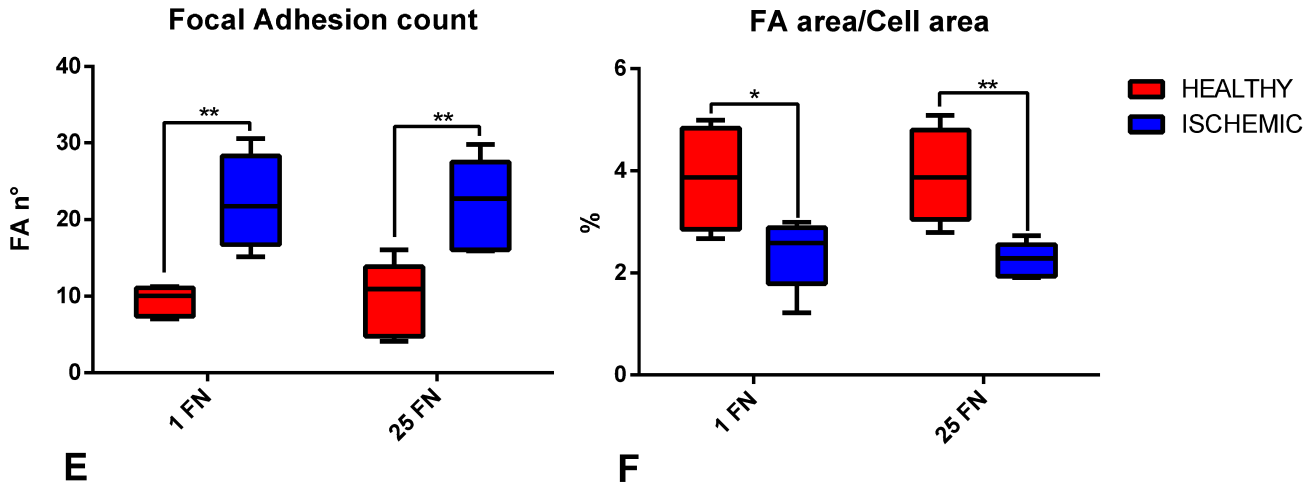

Figure 4.4 **Focal adhesion characterization.** Representative fluorescence images of healthy CPC (**A**-**B**) and ischemic CPC (**C**-**D**). Focal adhesions are stained with paxillin (red) and actin cytoskeleton is stained with phalloidin (green). Nuclei were stained with DAPI (blue). Focal adhesions are compared as absolute number (**E**) or as area occupied by focal adhesion on total cell area in % (**F**). Healthy, N=5; Ischemic, N=6. *p<.05; **p<.01. Scale bar 25μm. FN= Fibronectin 1FN=1μg/ml; 25FN 25μg/ml.

4.4. *Migratory properties of cpc*

Since the ability of cells to polarize has been associated with their migratory properties (Cramer, 2010) we directly verified this possibility by performing a scratch assay. For this purpose, cells were cultured onto 1, 5 and 25 (μg/ml) fibronectin coated plastic dishes. Once confluence was reached, a wound was created in the cell monolayer and images were taken to assess the distance covered by cells in 4 hours. As shown in figure 4.5, consistently with morphometric analyses, healthy cells can modulate their migration speed as a function of fibronectin concentration, reaching a peak velocity with 5 (μg/ml) fibronectin. Conversely, pathologic cells were insensitive to variations in the concentration of fibronectin coating. Indeed, the direct comparison of the distance covered by cells at 4 hours, on 5 (μg/ml) fibronectin concentration showed that healthy CPC display a significantly higher migration speed than CPC isolated from ischemic hearts.

Altogether these results indicate that the morphologic differences observed by comparing cells isolated from normal and pathologic hearts can also be coupled with important functional differences.

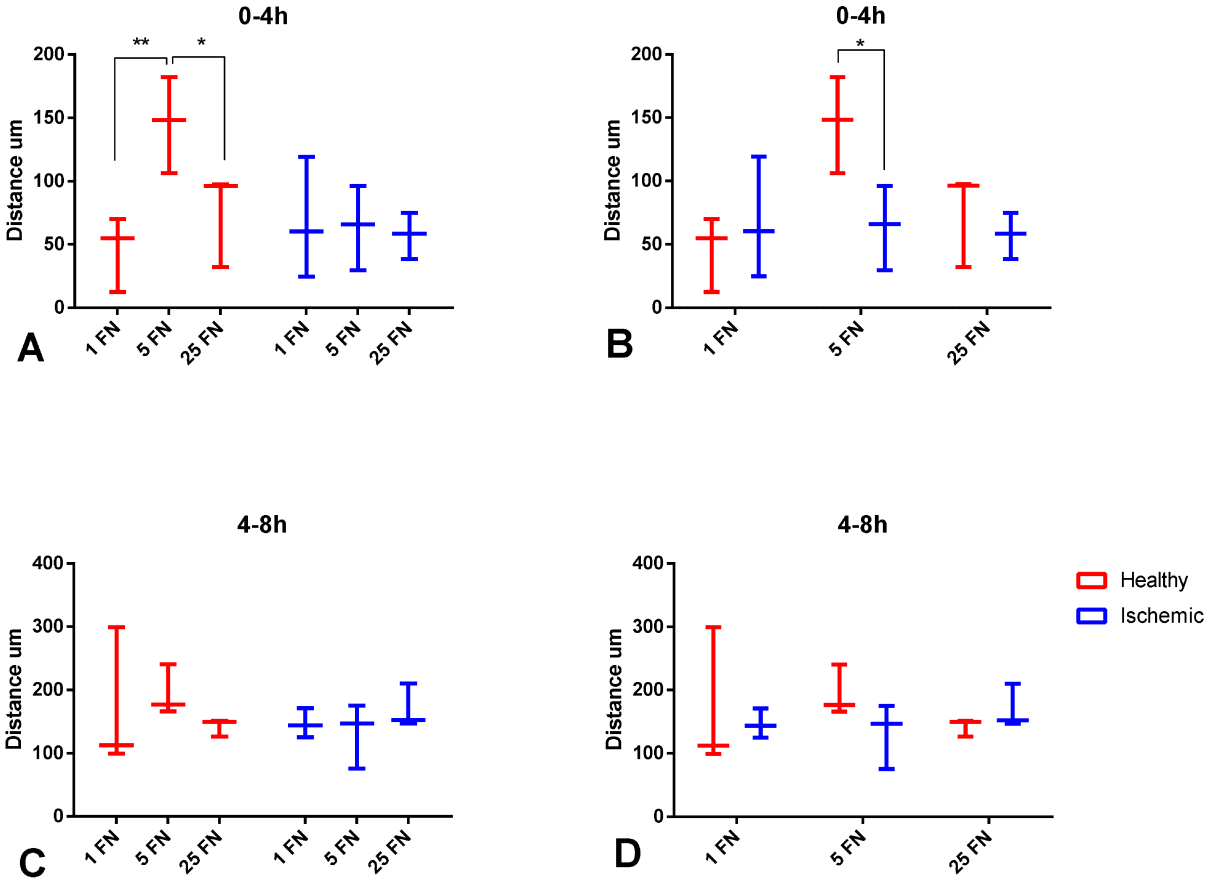

Figure 4.5 **Effects of fibronectin on cell motility.** CPC migration on different fibronectin concentration were evaluated in an 8 hours period. Images were taken at 4 and 8 hours after scratch. Migration has been calculated as distance covered by cells at 0-4 hours interval (A-B) and 4-8 hours interval (C-D). N=3 each. *p<.05; **p<.01.

4.5. *Response to modification of substrate stiffness*

Supported by the pieces of evidence obtained in the previous experiment, we decided to better investigate the mechanotransduction properties of CPC. Cytoskeletal dynamics are profoundly influenced by external physical factors and matricellular composition, so we decided to force the cells to respond to different stimuli with the aim to compare their responses. The stimuli adopted to achieve this purpose were the modification of the stiffness of the culture substrate and its fibronectin-coating concentration, since these factors mimic the alterations observed in failing hearts. For this specific purpose, cells were grown onto either polyacrylamide gels with nominal Young modulus (E) of 16kPa (in the range of muscle tissue) and 231kPa (in the range of infarcted cardiac tissue) or on glass coverslips (whose E is GPa) (Hiesinger et al., 2012; Sachot & Castano, 2014).

4.5.1. *Single substrate comparison*

At 16kPa, the softer stiffness used in this experiment, ischemic and healthy cells displayed an average spread area of 1,445μm^2 and 3,500 μm^2, respectively, with a marked difference at 25 μg/ml of fibronectin (Figure 4.6 E). The aspect ratio at 1 μg/ml fibronectin shows no significant differences, whereas at 25 μg/ml fibronectin, healthy cells are 38% longer than the pathological counterpart (3,01 ± 0,19 vs 2,17 ± 0,23) (Figure 4.6 F). No significant differences were observed in the solidity parameter (Figure 4.6 G).

At 231kPa, sharp morphological differences arise between the two population of cells. At 1 as well as 25 μg/ml fibronectin concentrations, both the area and the aspect ratio are significantly different: cells from healthy hearts are extensively spread and more polarized than the pathological counterpart (Figure 4.7 E-F). For both parameters, variations in fibronectin concentration further increases the differences. This is more apparent in dictating the cell polarization differences. At this stiffness, in fact, a higher fibronectin concentration is important for sprouting ability, that is significative different in favor of healthy cells (Figure 4.7 G).

When CPC were cultured onto glass coverslips, cells isolated from ischemic hearts showed a larger area than healthy cells (Figure 4.8 E), that, in turns, are characterized by a longer shape (Figure 4.8 F) as well as marked sprouting at higher fibronectin concentration (Figure 4.8 G).

4.5.2. *Comparison of cpc response to substrate stiffness at constant fibronectin concentrations*

We then compared the global response to stiffness of the two groups of cells as a function of fibronectin, finding diametrically opposite behaviors. As shown, in healthy cells, the spreading area does not vary in response to incremented substrate stiffness, under both fibronectin concentration conditions (Figure 4.9 A-B). As opposed, cells obtained from ischemic hearts increase their area as a function of substrate

stiffness, in particular from 16kPa to 231kPa, and the process is more apparent at lower fibronectin concentrations.

As opposed to what observed with the area parameter, cells obtained from ischemic hearts do not respond to variations in fibronectin concentration in terms of elongation and sprouting. Conversely, healthy cells are very responsive, with marked differences at 16kPa to 231kPa.

4.5.3. Comparison of response to fibronectin variations at constant stiffness

Regarding the effect of fibronectin concentration in cell behavior, we observed that cells isolated from ischemic hearts do not vary any of the measured parameter, at any stiffness (Figure 4.10). On the contrary, in healthy cells, fibronectin stimulates a response, promoting a strong elongation and branching at 231kPa.

Summarizing, healthy cells have a greater ability to polarize and to emit protrusions, compared with cells from ischemic hearts, that, in turns, show a larger spread area with the tendency to increase in response to stiffness.

Altogether, these results suggest that mechanosensing in cells isolated from ischemic cells is impaired.

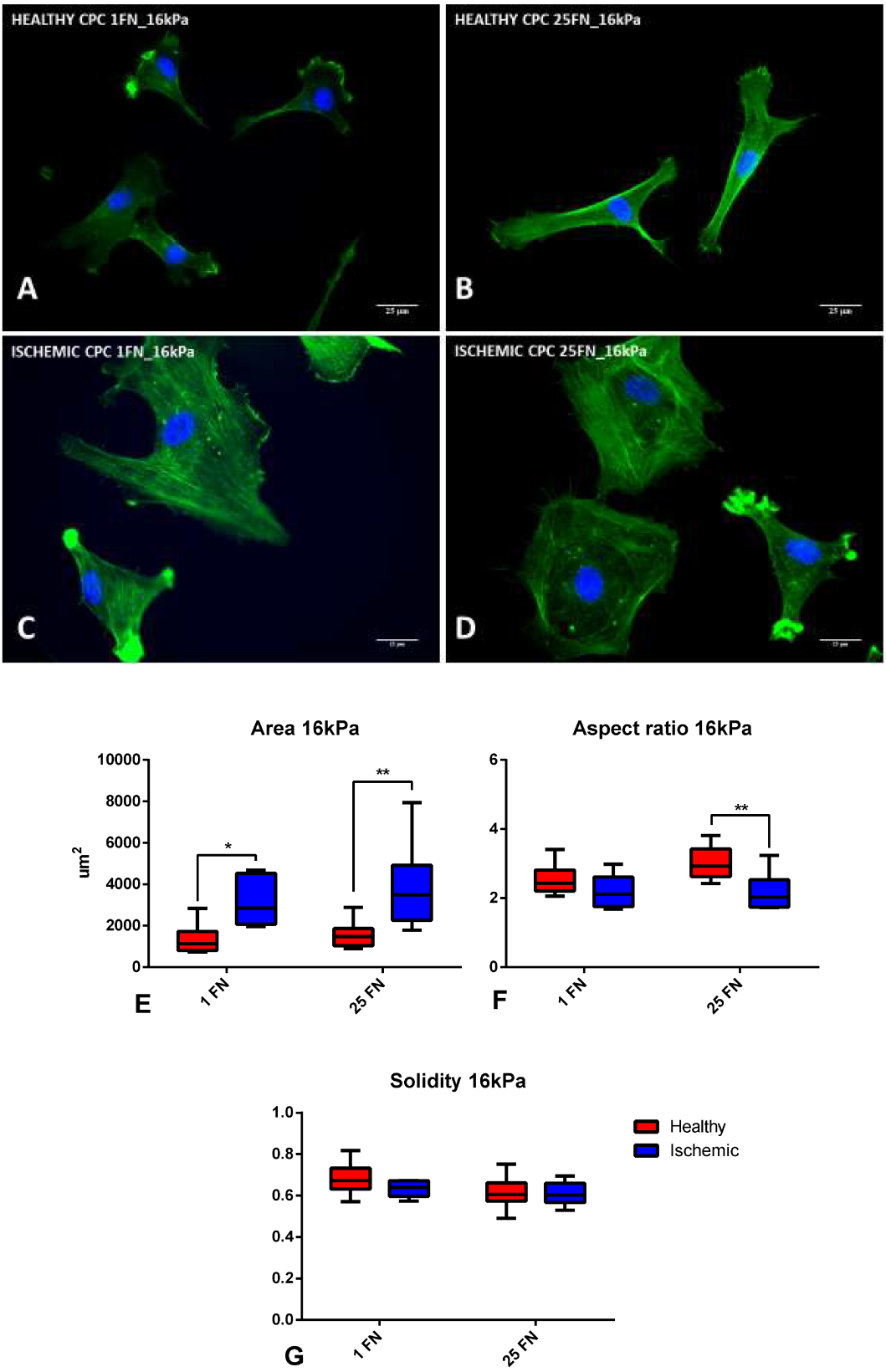

Figure 4.6 **CPC morphological characterization on 16kPa stiffness.** Representative fluorescence images of healthy CPC (**A**-**B**) and ischemic CPC (**C**-**D**) stained with actin dye phalloidin (green). Nuclei were stained with DAPI (blue). Box and whiskers plots compare CPC values of area (**E**), aspect ratio (**F**) and solidity (**G**) at different fibronectin concentration. Healthy, N=6; Ischemic, N=6. *p<.05; **p<.01. Scale bar 25µm. FN= Fibronectin 1FN=1µg/ml; 25FN 25µg/ml

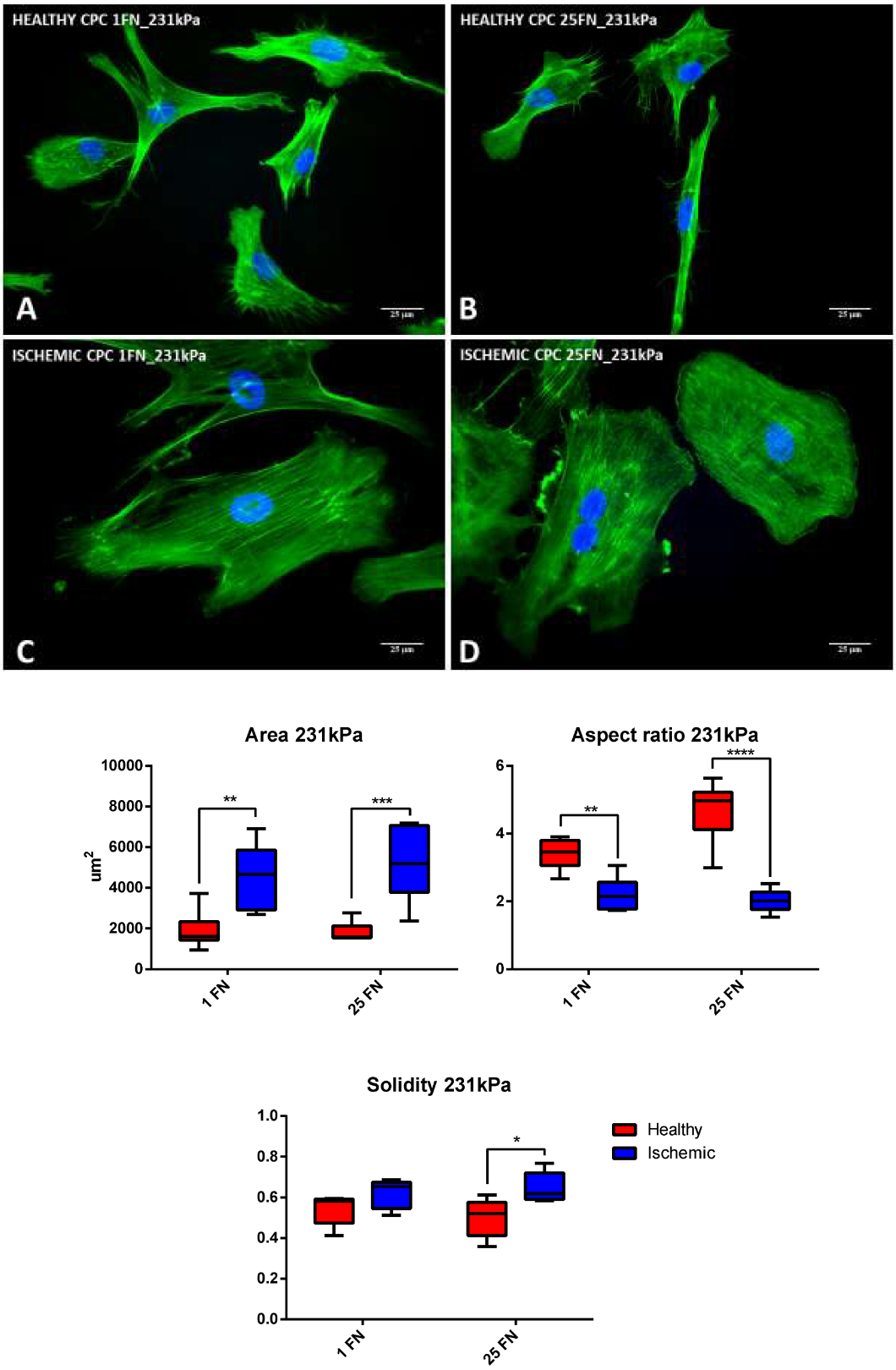

Figure 4.7 **CPC morphological characterization on 231kPa stiffness.** Representative fluorescence images of healthy CPC (**A**-**B**) and ischemic CPC (**C**-**D**) stained with actin dye phalloidin (green). Nuclei were stained with DAPI (blue). Box and whiskers plots compare CPC values of area (**E**), aspect ratio (**F**) and solidity (**G**) at different fibronectin concentration. Healthy, N=6; Ischemic, N=6. *p<.05; **p<.01; ***p<.001; ****p<.0001. Scale bar 25µm. FN= Fibronectin 1FN=1µg/ml; 25FN 25µg/ml

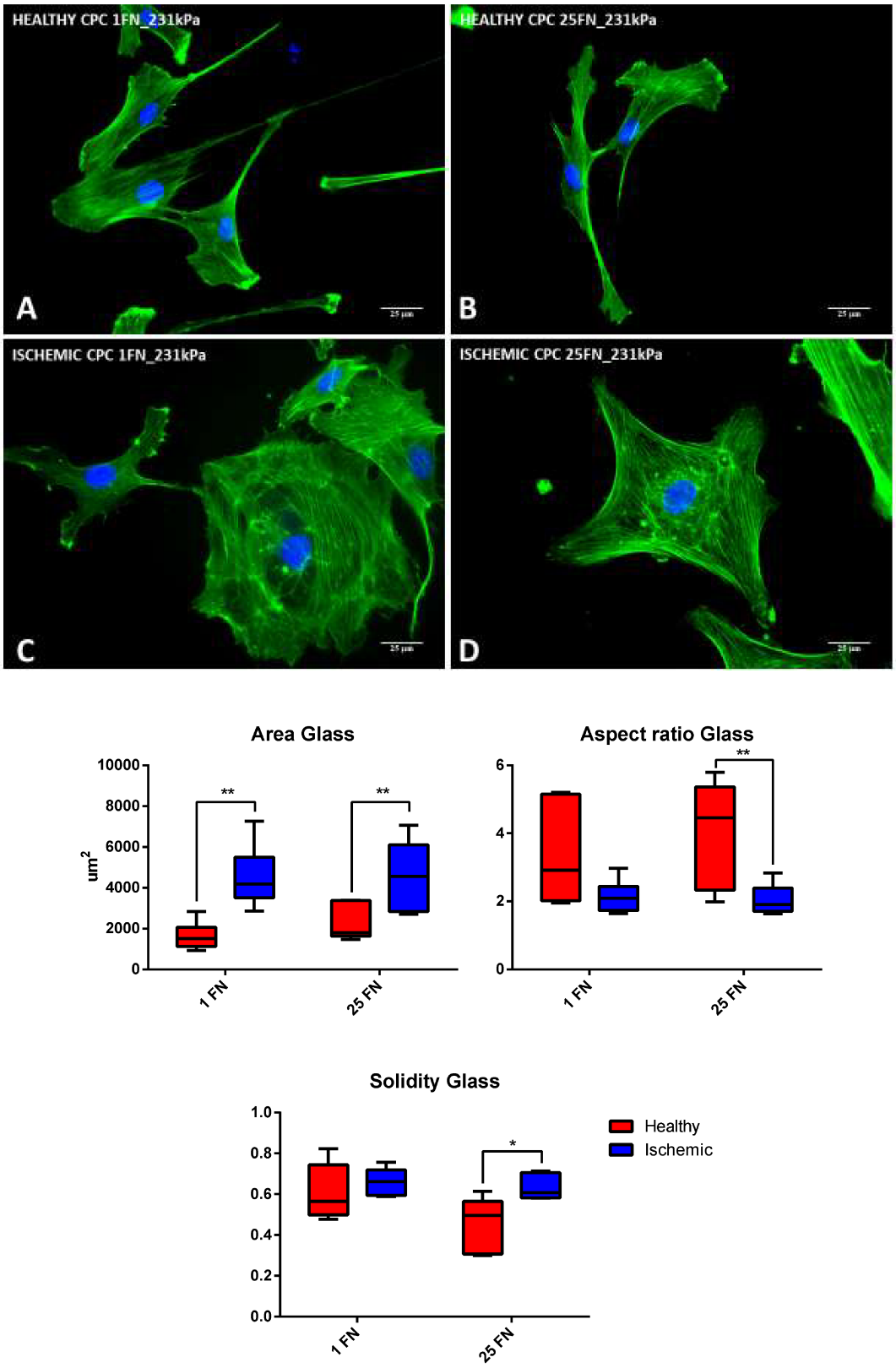

Figure 4.8 **CPC morphological characterization on Glass.** Representative fluorescence images of healthy CPC (**A**-**B**) and ischemic CPC (**C**-**D**) stained with actin dye phalloidin (green). Nuclei were stained with DAPI (blue). Box and whiskers plots compare CPC values of area (**E**), aspect ratio (**F**) and solidity (**G**) at different fibronectin concentration. Healthy, N=6; Ischemic, N=6. *p<.05; **p<.01. Scale bar 25μm. FN= Fibronectin 1FN=1μg/ml; 25FN 25μg/ml

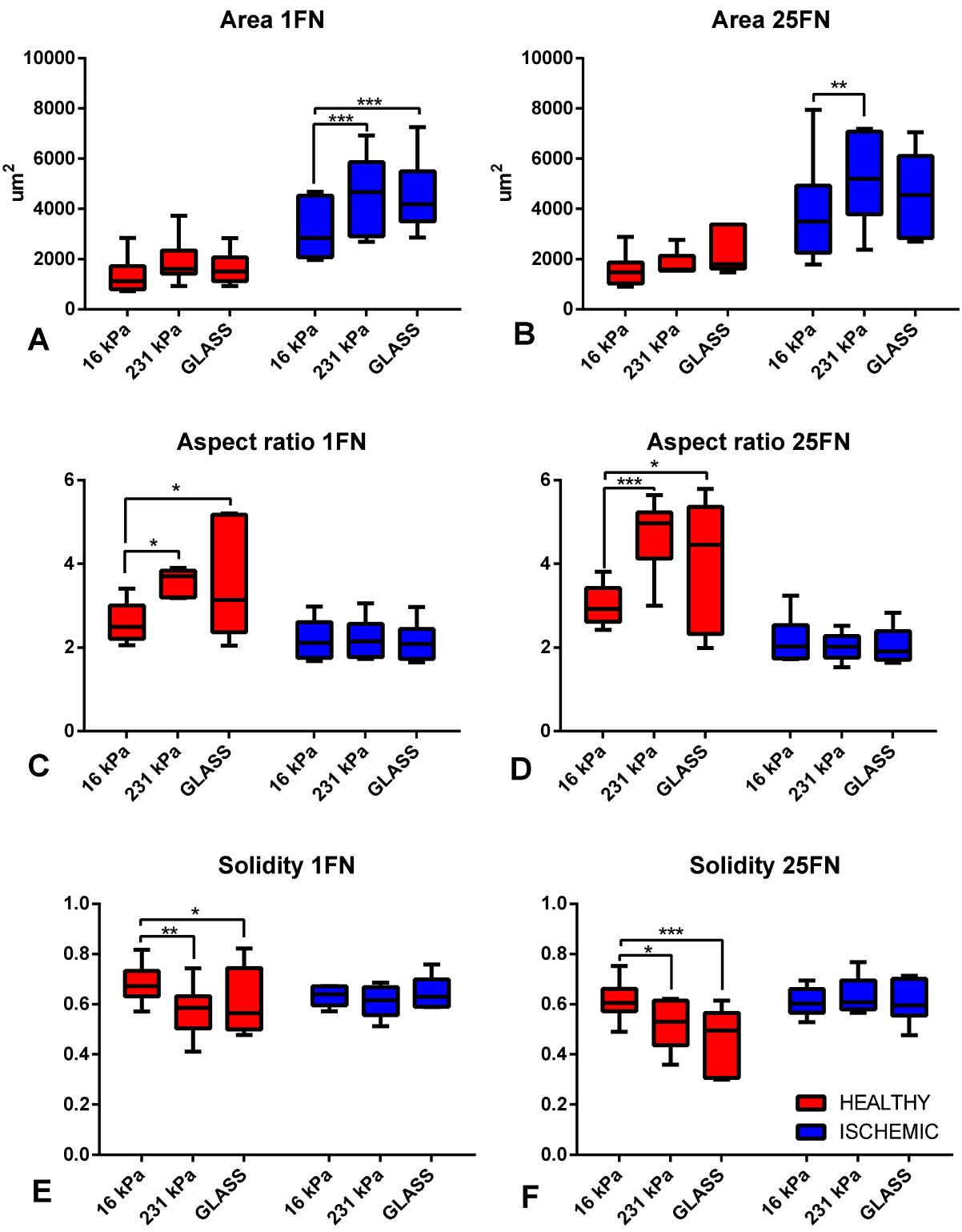

Figure 4.9 **Comparison of stiffness-induced morphological changes**. CPC morphological changes are stratified by fibronectin concentration and compared for stiffness response. Box and whiskers plots compare CPC values of area (**A-B**), aspect ratio (**C-D**) and solidity (**E-F**) at different stiffness. Healthy, N=6; Ischemic, N=6. *p<.05; **p<.01; ***p<.001. Scale bar 25μm. FN= Fibronectin 1FN=1μg/ml; 25FN 25μg/m

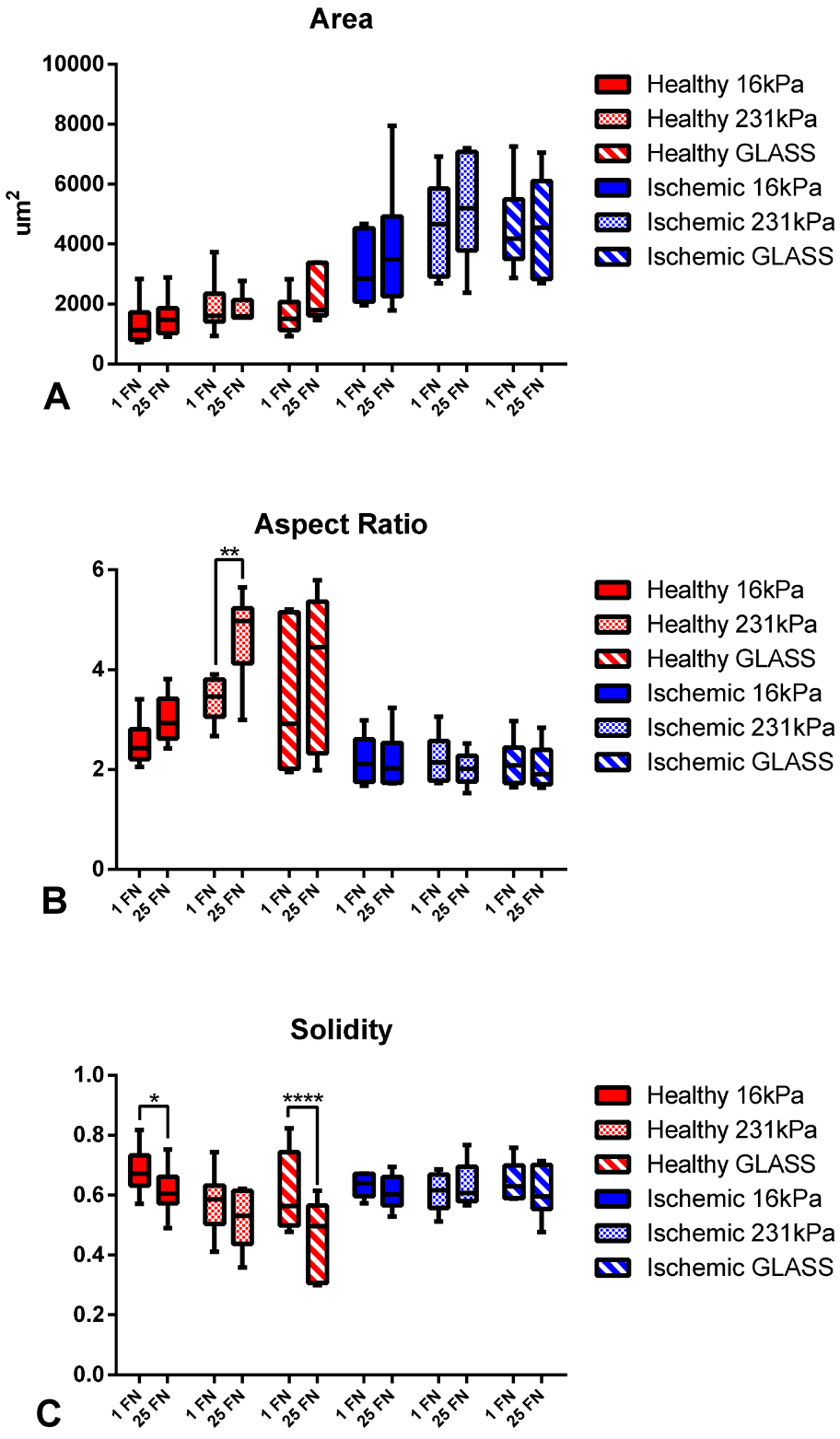

Figure 4.10 **Comparison of fibronectin-induced morphological changes**. For each morphological parameter, effects of fibronectin where compared within the same stiffness condition. Box and whiskers plots compare CPC values of area (**A**), aspect ratio (**B**) and solidity (**C**). Healthy, N=6; Ischemic, N=6. *p<.05; **p<.01; ****p<.0001. Scale bar 25µm. FN= Fibronectin 1FN=1µg/ml; 25FN 25µg/ml.

4.6. *Cpc stiffness characterization*

Given the link between stiffness and YAP/MRTF-A translocation and the pivotal role of the latter to, in turn, induce cell stiffening, we characterized CPC by their Young's modulus with Atomic Force Microscopy (AFM) in collaboration with the group of Professor Lazzarino (IOM-CNR Laboratory TASC, Trieste, Italy). When CPC Young's modulus where compared on different substrate, healthy and ischemic CPC did not differ significantly for E (Figure 4.11 H). Striking, differences in response to stiffness are evident. In fact, it is clearly observable that ischemic CPC did not modulate their stiffness in response to substrate stiffness, ability that characterized only healthy CPC (Figure 4.11 I).

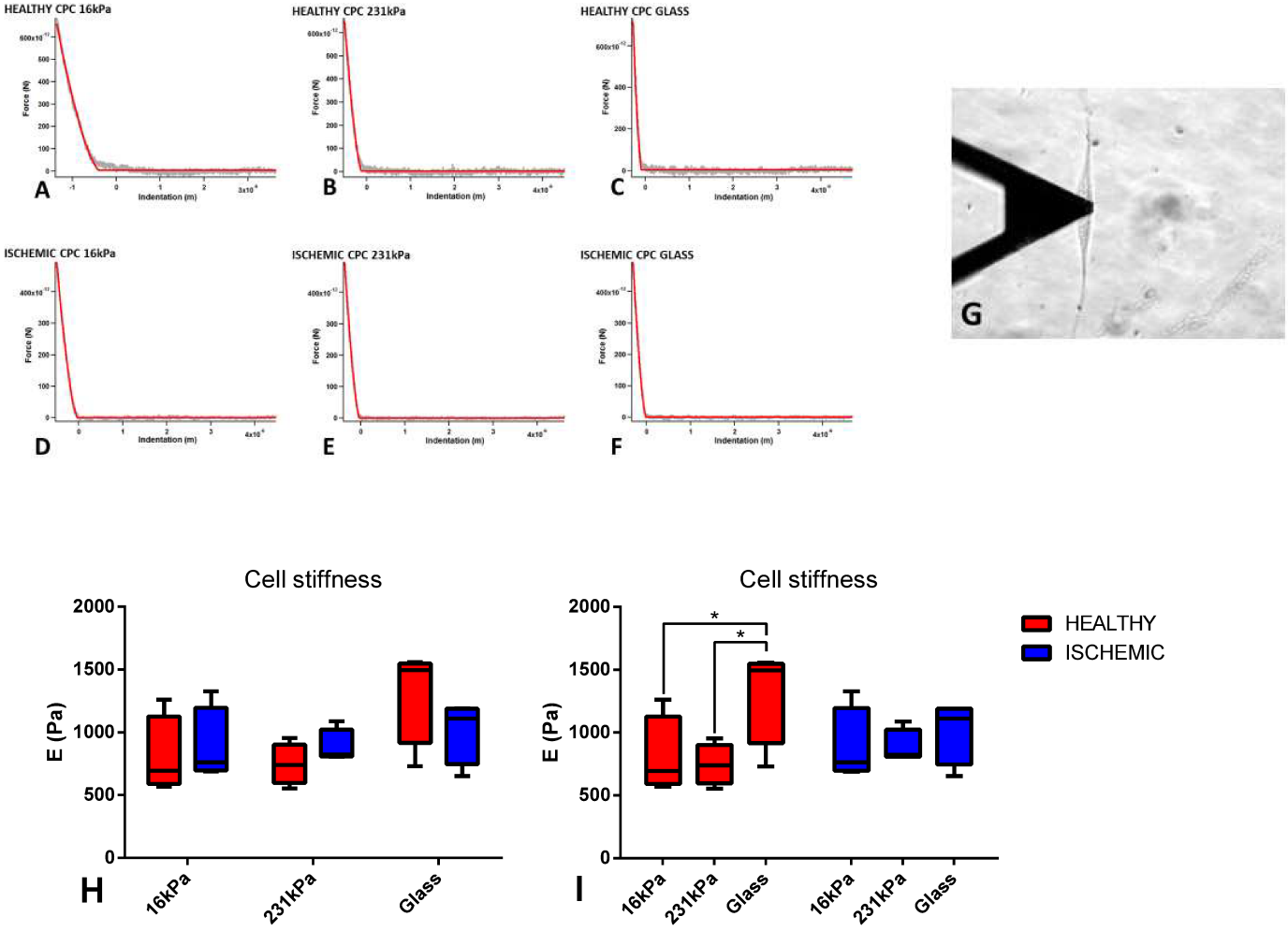

Figure 4.11 **Atomic force microscopy measures** Representative AFM indentation curves evidencing the different responses to stiffness in healthy (**A**-**B**-**C**) and ischemic CPC (**D**-**E**-**F**). Differential interference contrast image depicting the cantilever brought into contact a CPC (**G**). The stiffness responses of CPC to substrates of different rigidity, coated with 25µg/ml of fibronectin, were measured with an atomic force microscope. Responses in Young' modulus (E) were compared to evidence differences on a particular substrate (**H**) or to evidence differences of a global trend (**I**). Healthy, N=4; Ischemic, N=4. *p<.05.

4.7. Nucleocytoplasmic shuttling of YAP in response to fibronectin

Since we demonstrated that CPC obtained from healthy and pathologic hearts behave differently when exposed to mechanical stimuli, we decided to study one of the best-known transducers of these stimuli into a biochemical response (i.e. YAP). The nuclear translocation of this transcriptional co-activator, in fact, is closely linked to cytoskeleton rearrangement and tension.

For this purpose, we initially evaluated the nucleocytoplasmic shuttling of YAP as a function of fibronectin concentration. To this aim, we immunofluorescencently labeled CPC, cultured employing the above described experimental conditions, and computed the ratio between the mean fluorescence intensity of the nuclear signal and the mean intensity of a 3μm large area surrounding the nucleus (i.e. nucleus/cytoplasmic ratio or n/c). To avoid the interference due to the contact inhibition of cell growth, cells were seeded in sparse conditions and fixed 4 hours thereafter. This time point was chosen since maximal differences between the two cell types emerged from previous experiments (see paragraph 4.2, "Morphological properties of CPC"). In healthy cells, we recorded an increase in YAP nuclear localization when moving from 1 to 25μg/ml of fibronectin (Figure 4.12 H). A similar trend was not observed in cells obtained from ischemic hearts, that are insensitive to this stimulus, as suggested by their incapacity to regulate the nuclear localization of YAP (Figure 4.12 G). Moreover, this difference in sensitiveness to fibronectin is confirmed when the n/c ratios of YAP of CPC obtained from normal and pathologic hearts were compared. In fact, healthy cells not only have a functional YAP nuclear shuttling as a function of fibronectin, but also display a higher YAP n/c ratio (Figure 4.12 I).

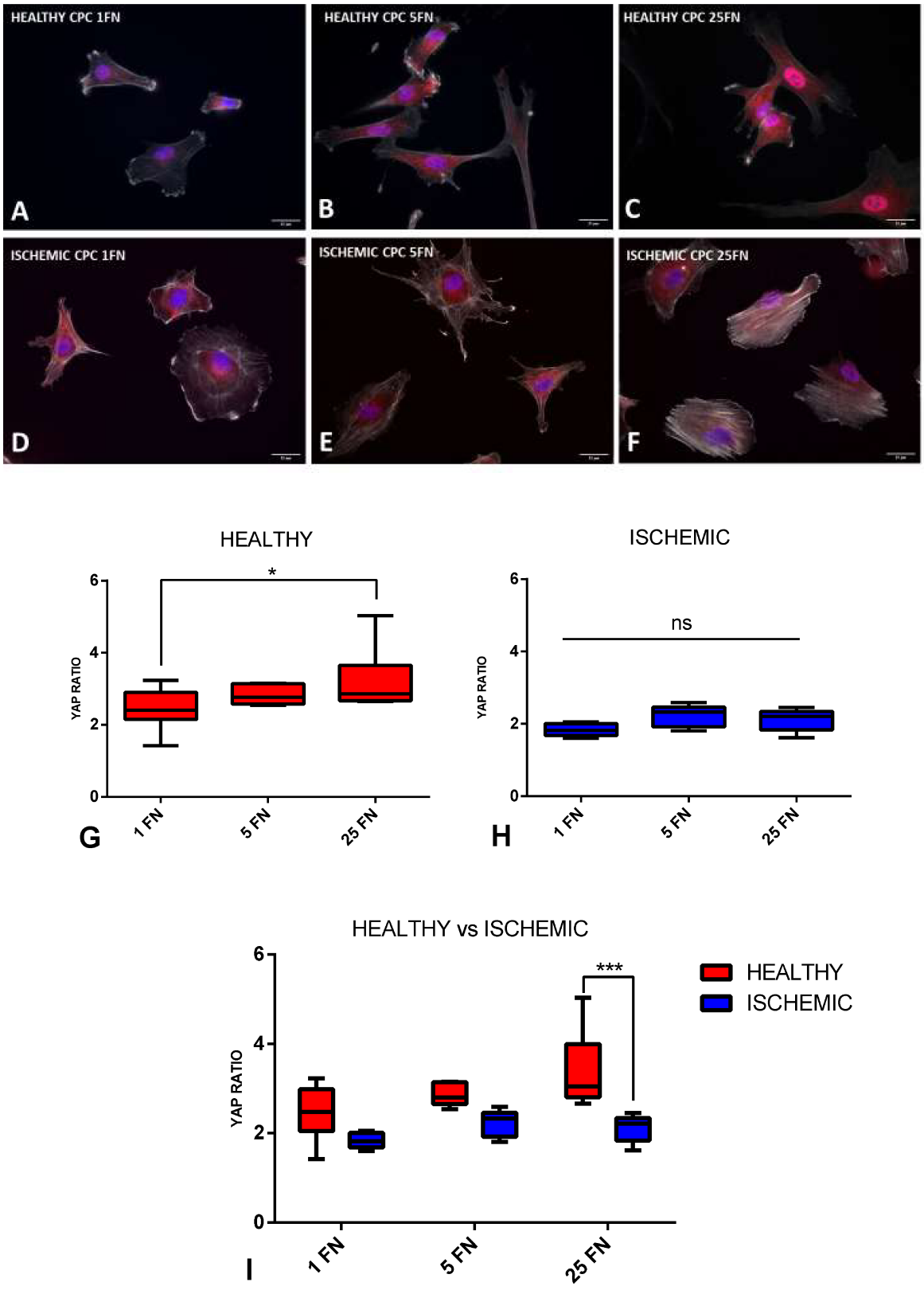

Figure 4.12 **Effects of fibronectin on YAP ratio.** Representative fluorescence images of healthy CPC (**A**-**C**) and ischemic CPC (**D**-**F**) stained with actin dye phalloidin (white) and YAP (red). Nuclei were stained with DAPI (blue). Scale bar 25μm. Box and whiskers plots are used to compare values of YAP ratio on Healthy CPC (**G**) and Ischemic CPC (**H**) alone plus Healthy vs Ischemic (**I**) at different fibronectin concentration. Healthy, N=7; Ischemic, N=8. *p<.05; ***p<.001. FN= Fibronectin 1FN=1μg/ml; 5FN=5μg/ml; 25FN 25μg/ml

4.8. *Nucleocytoplasmic shuttling of YAP in response to mechanical stimuli*

Once demonstrated that CPC isolated from healthy and ischemic hearts have a different regulation of YAP as function of fibronectin concentration, we decided to assess if those differences were also observed in response to variations of the substrate stiffness, in combination with different fibronectin concentrations.

Surprisingly, CPC isolated from either healthy or pathologic hearts did not differ in their ability to promote YAP nuclear localization at 16 and 231kPa, at both fibronectin concentrations (Figure 4.13-14). However, consistently with previous experiments, when cells were plated on glass at a concentration of 25μg/ml fibronectin, YAP n/c ratio was significantly higher in healthy cells than in CPC isolated from ischemic hearts (Figure 4.15). When results were stratified according to fibronectin concentration, we confirmed that the glass substrate is the major inducer of YAP nuclear translocation, independently of fibronectin, only in healthy cells. Indeed, this behavior is negated to cells isolated from ischemic hearts (Figure 4.16). Moreover, only healthy CPC are able to respond to fibronectin concentration despite only on Glass (Figure 4.17).

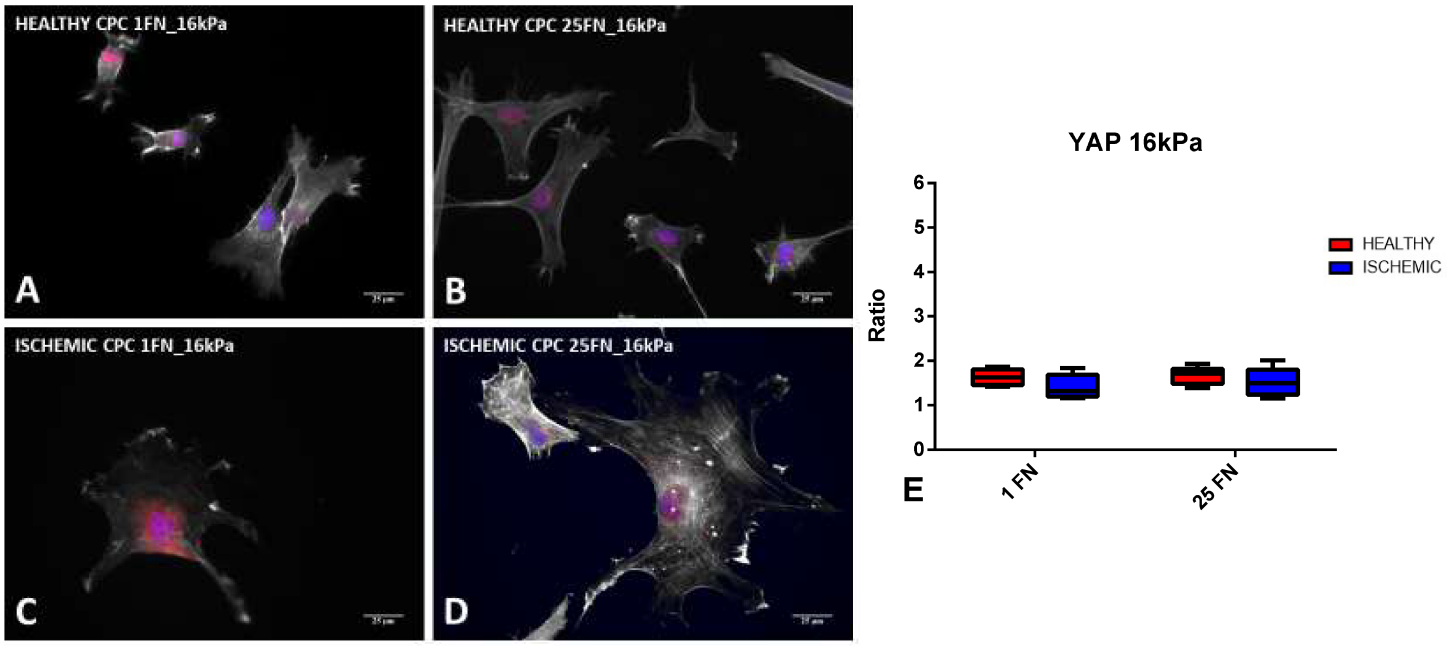

Figure 4.13 **Effects of 16kPa stiffness and fibronectin on YAP localization.** Representative fluorescence images of healthy CPC (**A**-**B**) and ischemic CPC (**C**-**D**) stained with actin dye phalloidin (white) and YAP (red). Nuclei were stained with DAPI (blue). Scale bar 25μm. Box and whiskers plots are used to compare values of YAP ratio on healthy and ischemic CPC (**E**). Healthy, N=6; Ischemic, N=6. FN= Fibronectin 1FN=1μg/ml; 25FN 25μg/ml.

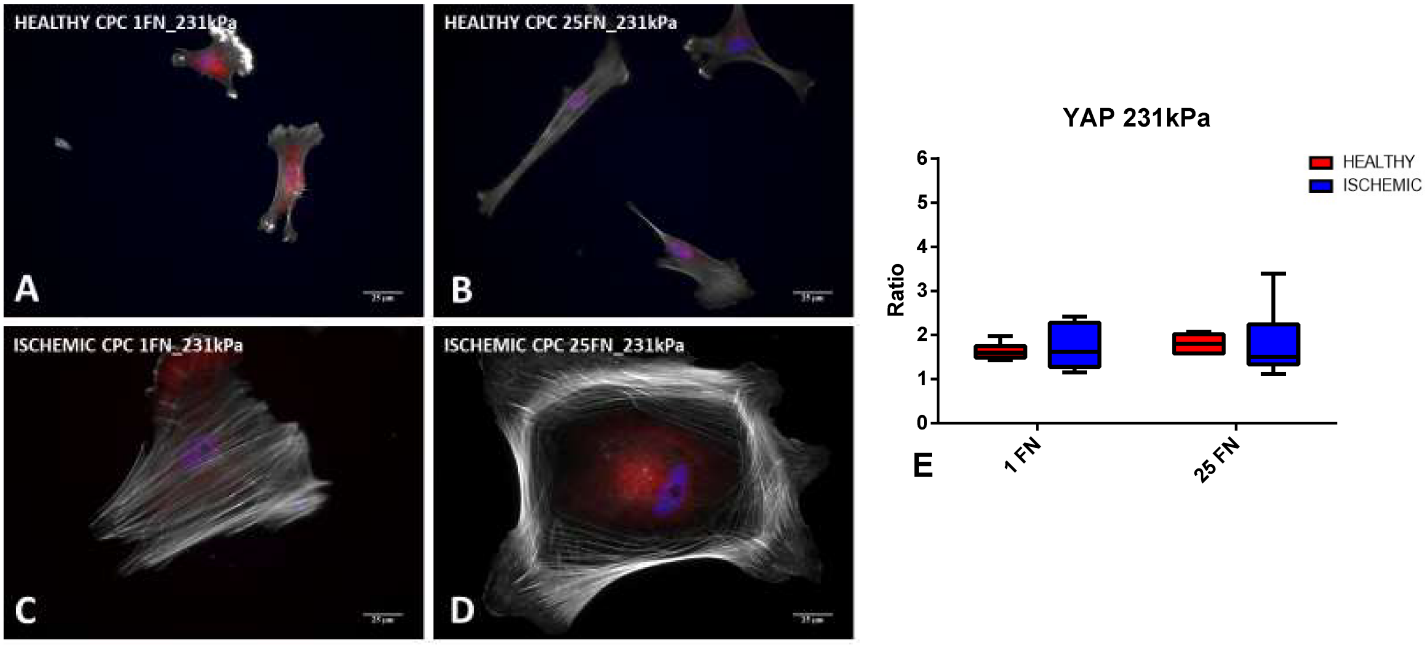

Figure 4.14 **Effects of 231kPa stiffness and fibronectin on YAP localization.** Representative fluorescence images of healthy CPC (**A**-**B**) and ischemic CPC (**C**-**D**) stained with actin dye phalloidin (white) and YAP (red). Nuclei were stained with DAPI (blue). Scale bar 25μm. Box and whiskers plots are used to compare values of YAP ratio on healthy and ischemic CPC (**E**). Healthy, N=6; Ischemic, N=6. FN= Fibronectin 1FN=1μg/ml; 25FN 25μg/ml

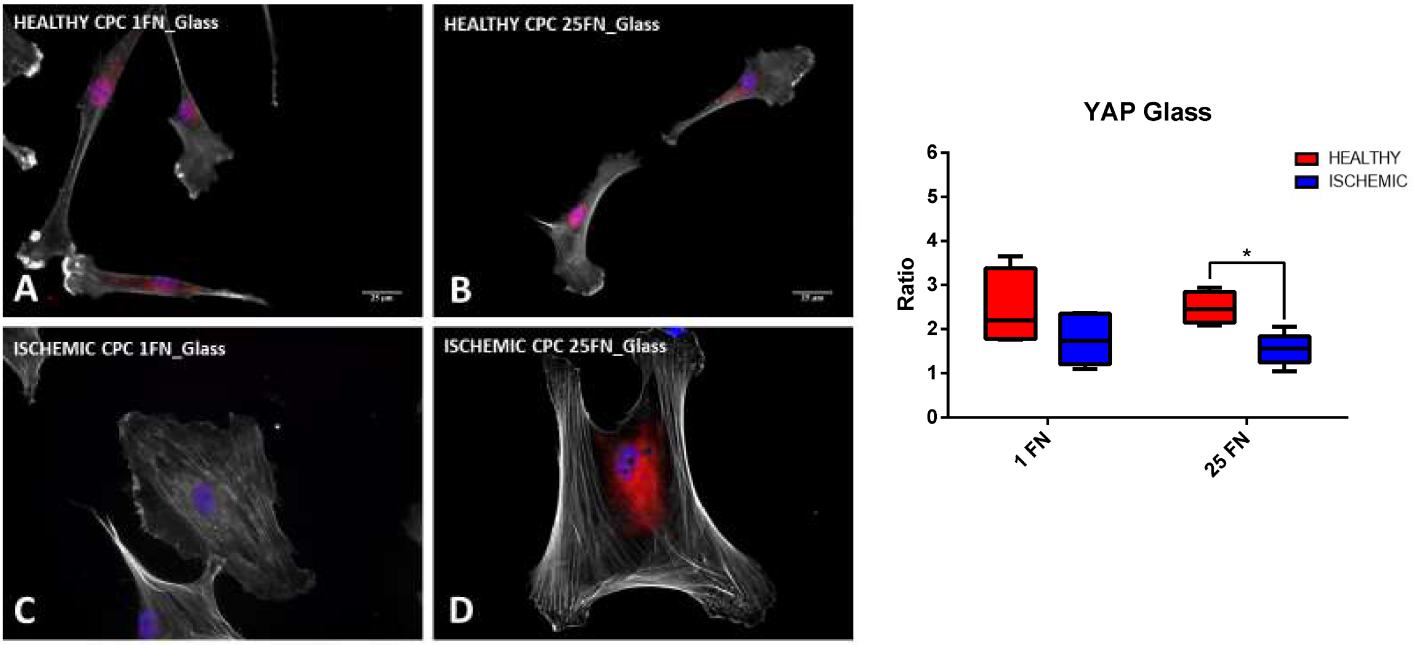

Figure 4.15 **Effects of Glass and fibronectin on YAP localization.** Representative fluorescence images of healthy CPC (**A**-**B**) and ischemic CPC (**C**-**D**) stained with actin dye phalloidin (white) and YAP (red). Nuclei were stained with DAPI (blue). Scale bar 25µm. Box and whiskers plots are used to compare values of YAP ratio on healthy and ischemic CPC (**E**). Healthy, N=6; Ischemic, N=6. *p<.05. FN= Fibronectin 1FN=1µg/ml; 25FN 25µg/ml

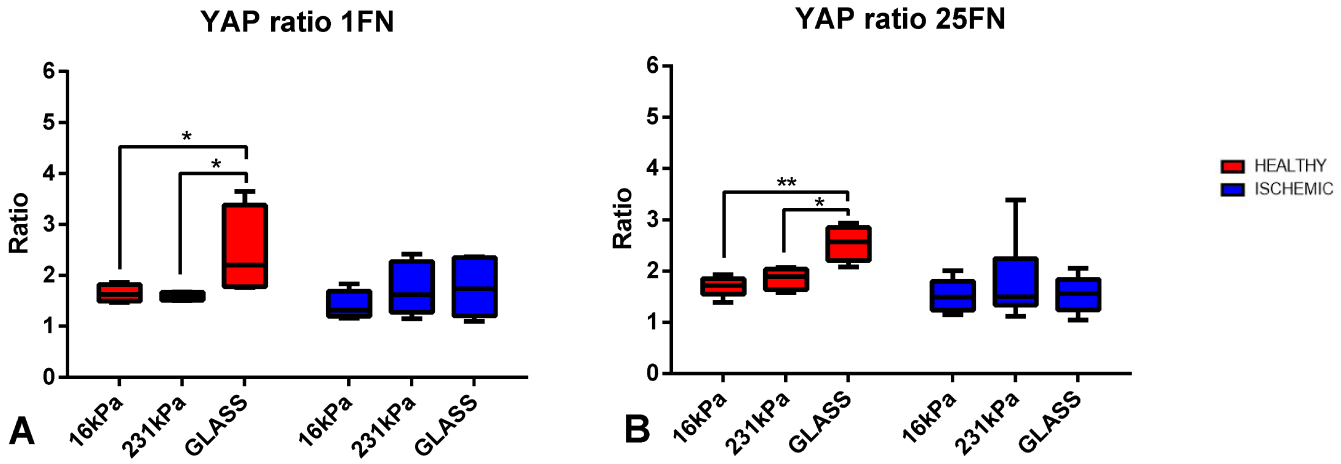

Figure 4.16 **Effects of stiffness on YAP shuttling** CPC YAP ratio values are stratified by fibronectin concentration 1µg/ml (**A**) and 25µg/ml (**B**) and responses to stiffness were compared. Healthy, N=6; Ischemic, N=6. *p<.05; **p<.01 FN= Fibronectin 1FN=1µg/ml; 25FN 25µg/ml.

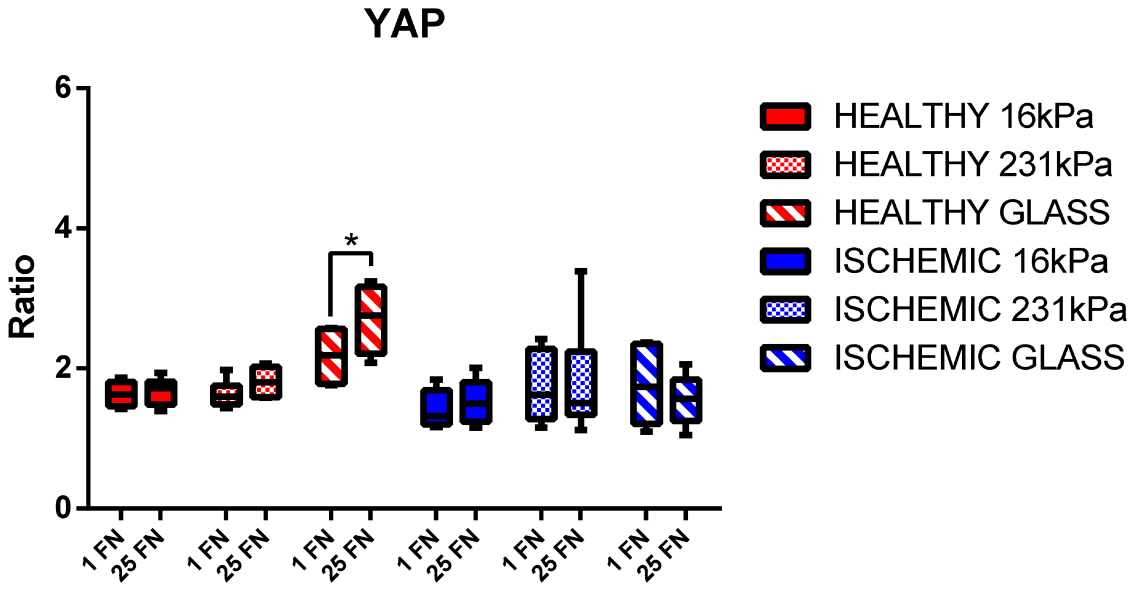

Figure 4.17 **Effects of fibronectin in YAP shuttling** CPC YAP ratio responses were compared in function of fibronectin concentration. Healthy, N=6; Ischemic, N=6. *p<.05. FN= Fibronectin 1FN=1µg/ml; 25FN 25µg/ml.

4.9. *Nucleocytoplasmic shuttling of MRTF-A in response to mechanical stimuli*

Since it has been shown that another mechanotransducer (i.e. Myocardin related transcription factor, MRTF-A), that responds to substrate stiffness or direct integrin engagement, may functionally interact with YAP by modulating cytoskeleton dynamics (Foster, Gualdrini, & Treisman, 2018), we investigated the effects of substrate stiffness and fibronectin concentration on the nucleocytoplasmic shuttling of MRTF-A, employing the same experimental conditions adopted for the YAP shuttling experiment. In this case, the results we obtained were in line with those previously observed for YAP. Specifically, CPC obtained from normal hearts showed a stronger MRTF-A nuclear positivity than those obtained from pathologic hearts, when plated on glass (Figure 4.20). This difference reached statistical significance at 1μg/ml fibronectin concentration. Moreover, we observed an increase in the nuclear shuttling of MRTF-A as a function of substrate stiffness only in CPC derived from normal hearts. This behavior was not observed in pathologic heart derived cells (Figure 4.21).

As shown in Figure 4.22, neither cells derived from normal hearts nor cells obtained from ischemic organs modulated the nuclear localization of MRTF-A as a function of fibronectin concentration in none of the tested substrates. Therefore, MRTF-A is less sensitive than YAP to variations in the concentration of extracellular fibronectin.

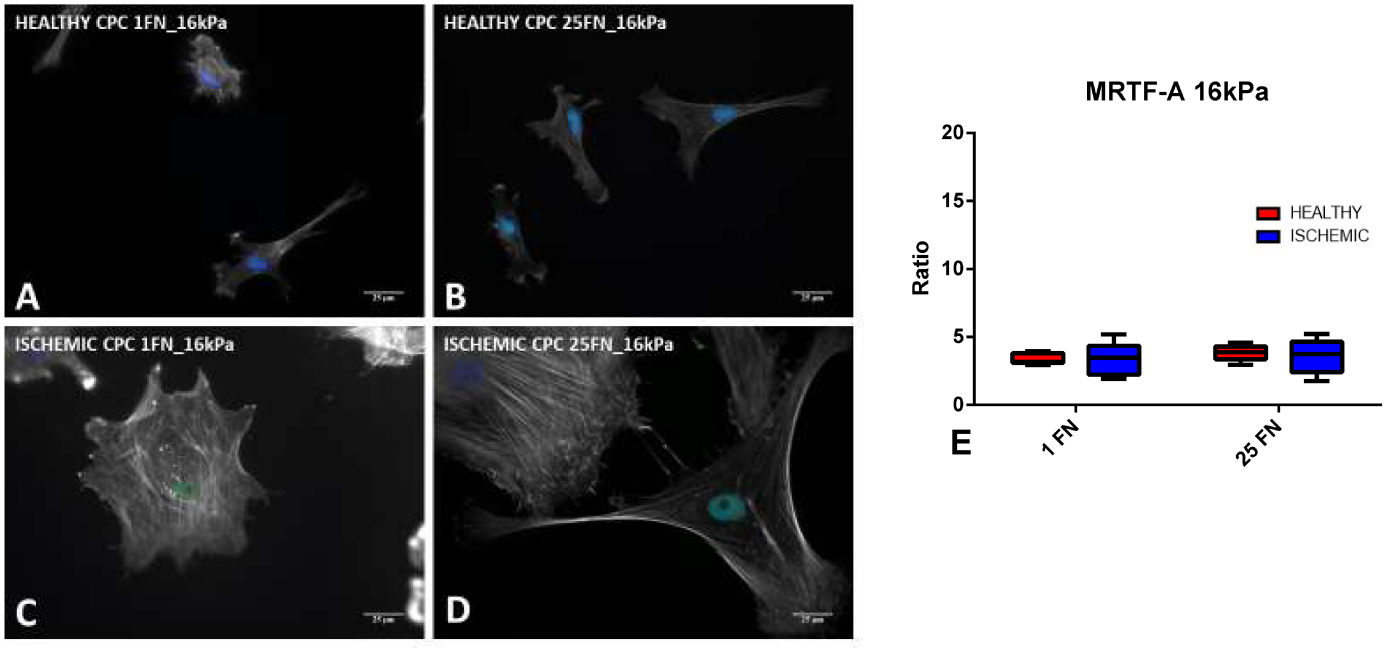

Figure 4.18 **Effects of 16kPa stiffness and fibronectin on MRTF-A localization.** Representative fluorescence images of healthy CPC (**A**-**B**) and ischemic CPC (**C**-**D**) stained with actin dye phalloidin (white) and MRTF-A (green). Nuclei were stained with DAPI (blue). Scale bar 25μm. Box and whiskers plots are used to compare values of YAP ratio on healthy and ischemic CPC (**E**). Healthy, N=6; Ischemic, N=6. FN= Fibronectin 1FN=1μg/ml; 25FN 25μg/ml.

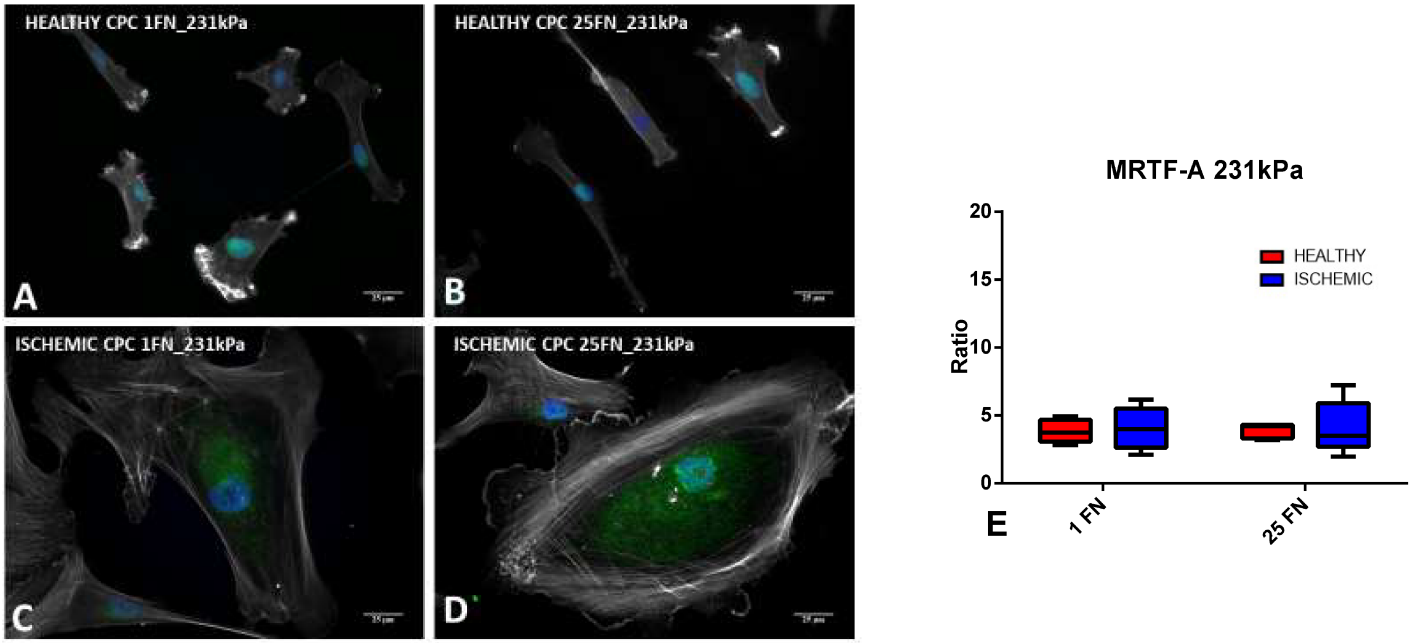

Figure 4.19 **Effects of 231kPa stiffness and fibronectin on MRTF-A localization.** Representative fluorescence images of healthy CPC (**A**-**B**) and ischemic CPC (**C**-**D**) stained with actin dye phalloidin (white) and MRTF-A (green). Nuclei were stained with DAPI (blue). Scale bar 25μm. Box and whiskers plots are used to compare values of YAP ratio on healthy and ischemic CPC (**E**). Healthy, N=6; Ischemic, N=6. FN= Fibronectin 1FN=1μg/ml; 25FN 25μg/ml

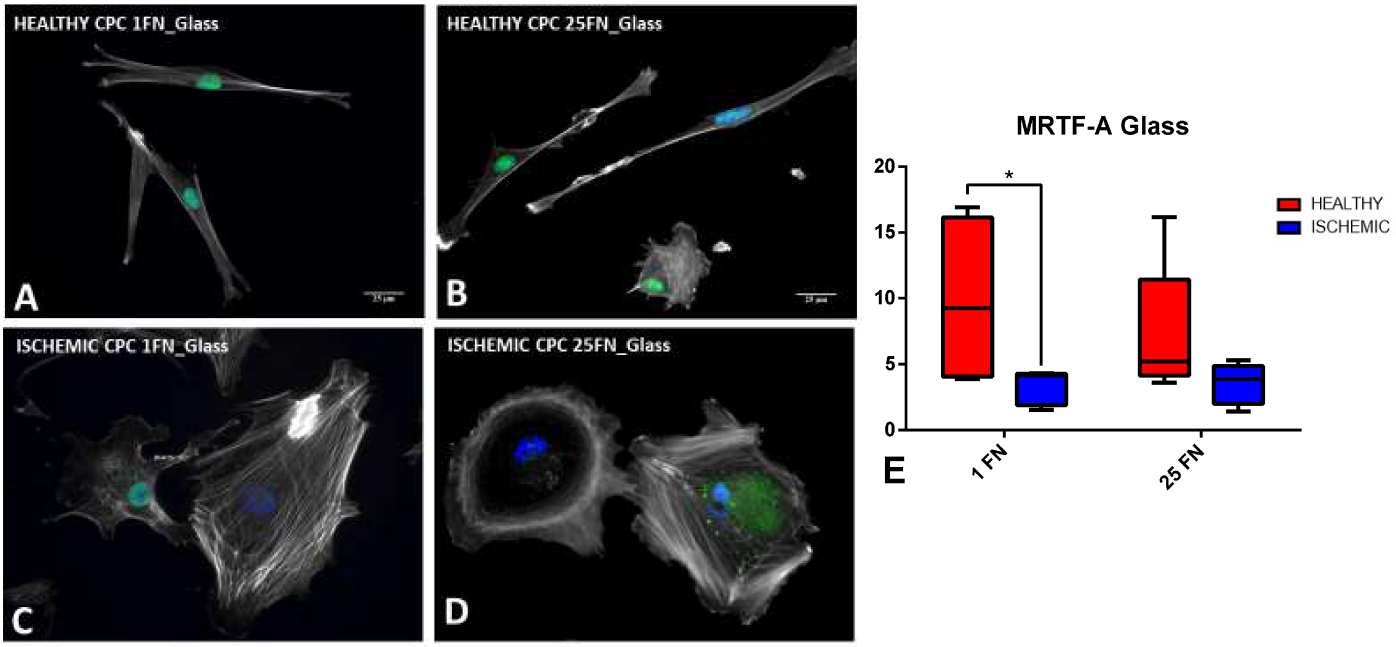

Figure 4.20 **Effects of 231kPa stiffness and fibronectin on MRTF-A localization.** Representative fluorescence images of healthy CPC (**A**-**B**) and ischemic CPC (**C**-**D**) stained with actin dye phalloidin (white) and MRTF-A (green). Nuclei were stained with DAPI (blue). Scale bar 25µm. Box and whiskers plots are used to compare values of YAP ratio on healthy and ischemic CPC (**E**). Healthy, N=6; Ischemic, N=6. p*<.05 FN= Fibronectin 1FN=1µg/ml; 25FN 25µg/ml.

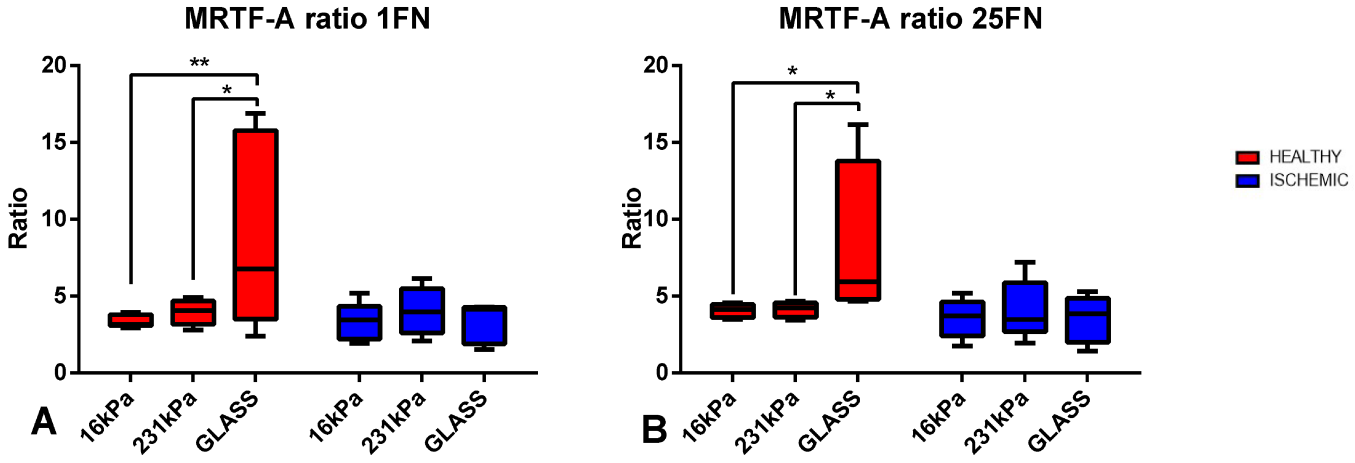

Figure 4.21 **Effects of stiffness on YAP shuttling** CPC YAP ratio values are stratified by fibronectin concentration 1µg/ml (**A**) and 25µg/ml (**B**) and responses to stiffness were compared. Healthy, N=6; Ischemic, N=6. *p<.05; **p<.01 FN= Fibronectin 1FN=1µg/ml; 25FN 25µg/ml.

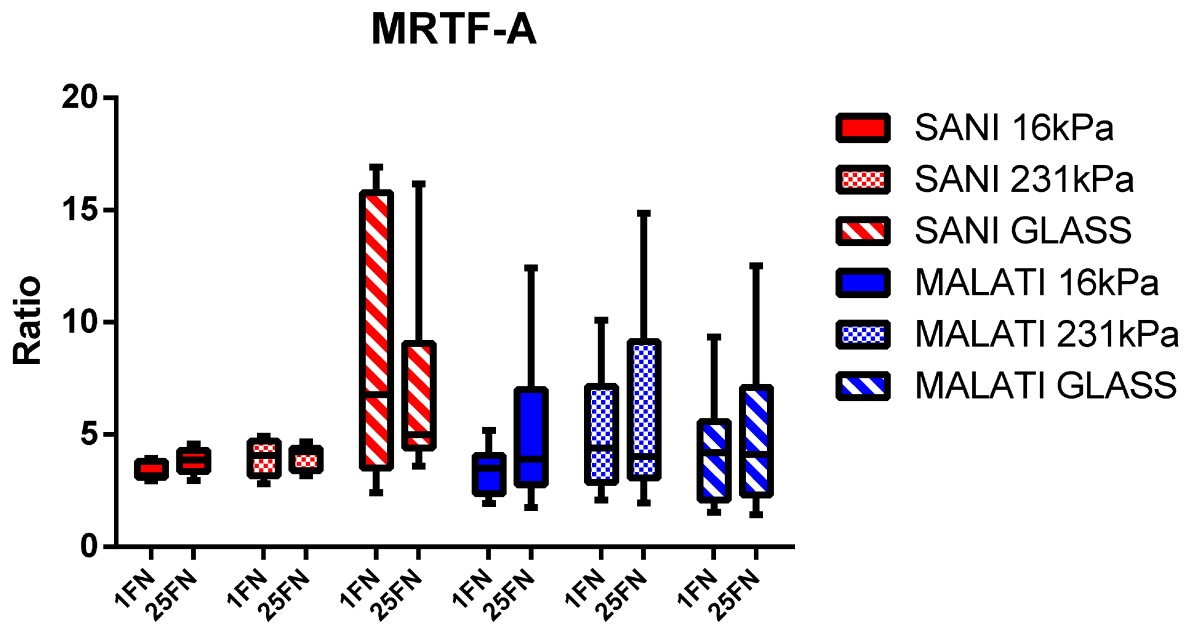

Figure 4.22 **Effects of fibronectin on MRTF-A shuttling** CPC MRTF-A ratio responses were compared in function of fibronectin concentration. Healthy, N=6; Ischemic, N=6. FN= Fibronectin 1FN=1μg/ml; 25FN 25μg/ml.

4.10. *Analysis of the correlation between the nucleocytoplasmic shuttling of MRTF-A and the YAP one.*

As aforementioned, fibronectin is less powerful than stiffness to generate YAP and MRTF-A responses. Indeed, it produces an increase in the n/c YAP ratio of healthy cell grown on glass only. However, as previously introduced, a mutual dependence of MRTF-A and YAP pathways has been shown in cancer associated fibroblasts. To assess whether some level of evidence of this interaction was also observed in our experimental setting, we correlated the expression levels of YAP with those of MRTF-A.

For this aim, we correlated the levels of expression of YAP and MRTF-A of CPC grown on substrates with different stiffness and compared the correlation coefficient values (R^2) of the two group of cells. Intriguingly, healthy cells displayed, with respect to CPC isolated from ischemic hearts, a significantly higher R^2 on glass, both at 1 and 25μg/ml of fibronectin. Moreover, when cells were grown onto 25μg/ml fibronectin a significant difference of R^2 between the two cell types was also observed, when cells were plated onto the 231kPa substrate (Figure 4.23).

Altogether, these data indicate that only healthy cells promote the nuclear translocation of both YAP and MRTF-A, despite this behavior reaches significance mainly when cells are plated on glass. Most intriguingly, the described mutual dependence of MRTF-A and YAP pathways is more apparent in cells isolated from normal hearts, while pathology seems to reduce it.

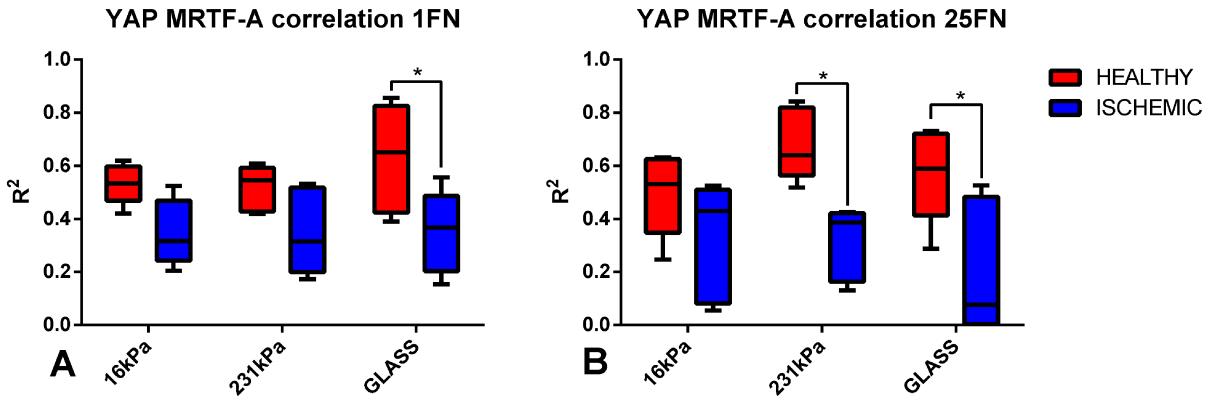

Figure 4.23 **Effects of stiffness on simultaneous YAP-MRTF shuttling** CPC's YAP and MRTF correlation values (R^2) are stratified by fibronectin concentration 1μg/ml (**A**) and 25μg/ml (**B**) and responses to stiffness were compared. Healthy, N=6; Ischemic, N=6. *p<.05. FN= Fibronectin 1FN=1μg/ml; 25FN 25μg/ml.

4.11. *Effect of microenvironmental cues on the expression of YAP and MRTF-A target genes*

To corroborate our findings on the nucleocytoplasmic shuttling of the two transcription factors with data concerning the transcriptional modulation of some of their target genes, we analyzed, by real-time PCR, the levels of transcripts whose regulation of expression is shared by both YAP/TEAD and MRTF-A/SRF transcription factors.

Specifically, focusing only at 25μg/ml, we observed that, consistently with the reported differences in the nuclear localization of YAP and MRTF-A in CPC isolated from normal and pathologic hearts, 2 of the three genes (i.e. CYR61 and ANKRD1) are more expressed in healthy CPC than in CPC obtained from pathologic hearts. Due to a high degree of variability in healthy CPC, we could not demonstrate the modulation of gene expression as a function of substrate stiffness.

Altogether these data support the notion that, in healthy CPC, both YAP/TEAD and MRTF-A/SRF regulated transcription is more active than in pathologic CPC.

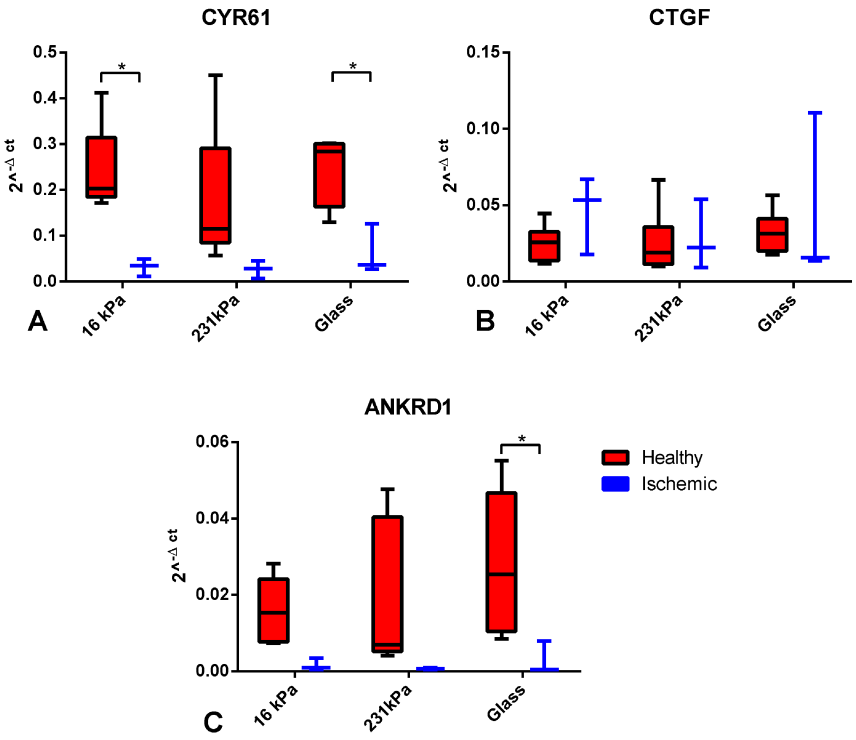

Figure 4.24 **YAP-MRTF-A regulated genes evaluation** Effectiveness function of YAP and MRTF was assessed by evaluating the transcripts of CYR61 (**A**), CTGF (**B**) and ANKRD1 (**C**), with real-time pcr. Healthy, N=4; Ischemic, N=3. *p<.05.

4.12. *Identification of the modulators of YAP and MRTF-A pathways by means of pharmacologic inhibition of upstream regulators of the pathways*

Last, we explored the effects on YAP and MRTF-A in healthy and ischemic cells, acting on pathways controlling their nuclear localization. Figure 4.25 summarizes the possible modulators of YAP and MRTF-A nuclear shuttling and the interventions that we have tested to assess their involvement in the differential regulation of these two factors in the two different cell types.

Concerning the effect of the described interventions on YAP nuclear translocation, we observed that the removal of serum from culture medium is a potent signal that causes the significant downmodulation of YAP nuclear localization. Only CPC isolated from pathologic hearts, cultured on 25μg/ml fibronectin did not respond to this stimulus. Interestingly, as opposed to serum deprivation, MEK inhibition significantly promoted the nuclear localization of YAP in both cell types, under every tested experimental condition. Latrunculin-A (Lat-A) treatment, instead, exerted an opposite effect, under every tested condition, but on CPC isolated from ischemic hearts cultured on 25μg/ml fibronectin coated substrates. Intriguingly, the ROCK inhibitor Y27632 reduced YAP nuclear localization only in healthy cells cultured in the presence of 1μg/ml fibronectin. Last, the inhibition of FAK showed no effects on YAP n/c ratio (Figure 4.26; 4.27).

Regarding the effects of these interventions on MRTF-A nuclear localization, we only observed a downregulation of the MRTF-A n/c ratio when cells grown on 1μg/ml fibronectin were treated with Lat-A. This effect was not observed in CPC isolated from pathologic hearts. Conversely, the effect of serum deprivation on MRTF-A nuclear localization was only observed in CPC isolated from failing hearts grown on 1μg/ml fibronectin coated dishes (Figure 4.28; 4.29).

Noteworthy, the analysis of the correlation between YAP and MRTF-A, demonstrated that, in serum-free condition or with FAKi, healthy cells relocate YAP and MRTF-A in a very independently mechanism (Figure 4.30).

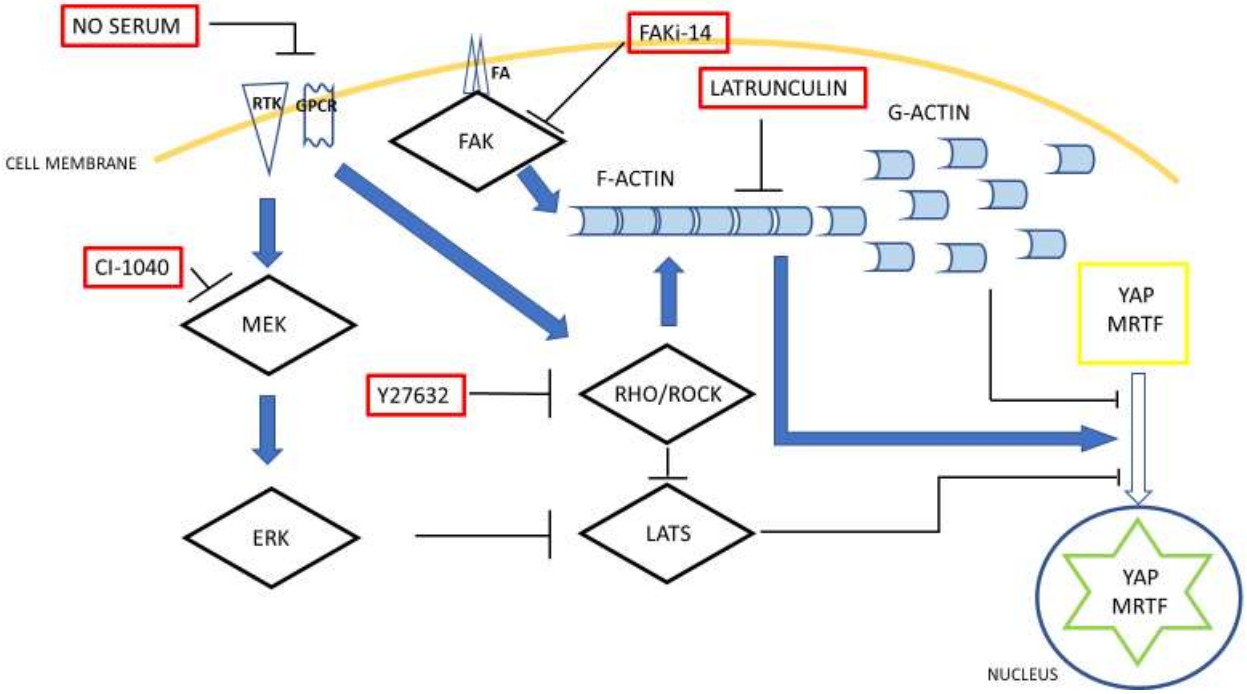

Figure 4.25 **Interventions on YAP - MRTF-A pathways**. The cartoon summarizes the key components of YAP and MRTF-A shuttling. Interventions are depicted in red boxes. Arrows indicate activation, blunt-end arrows indicate repression. FA, Focal Adhesion; GPCR, G-Protein Coupled Receptors; RTK, Receptor Tyrosine Kinase.

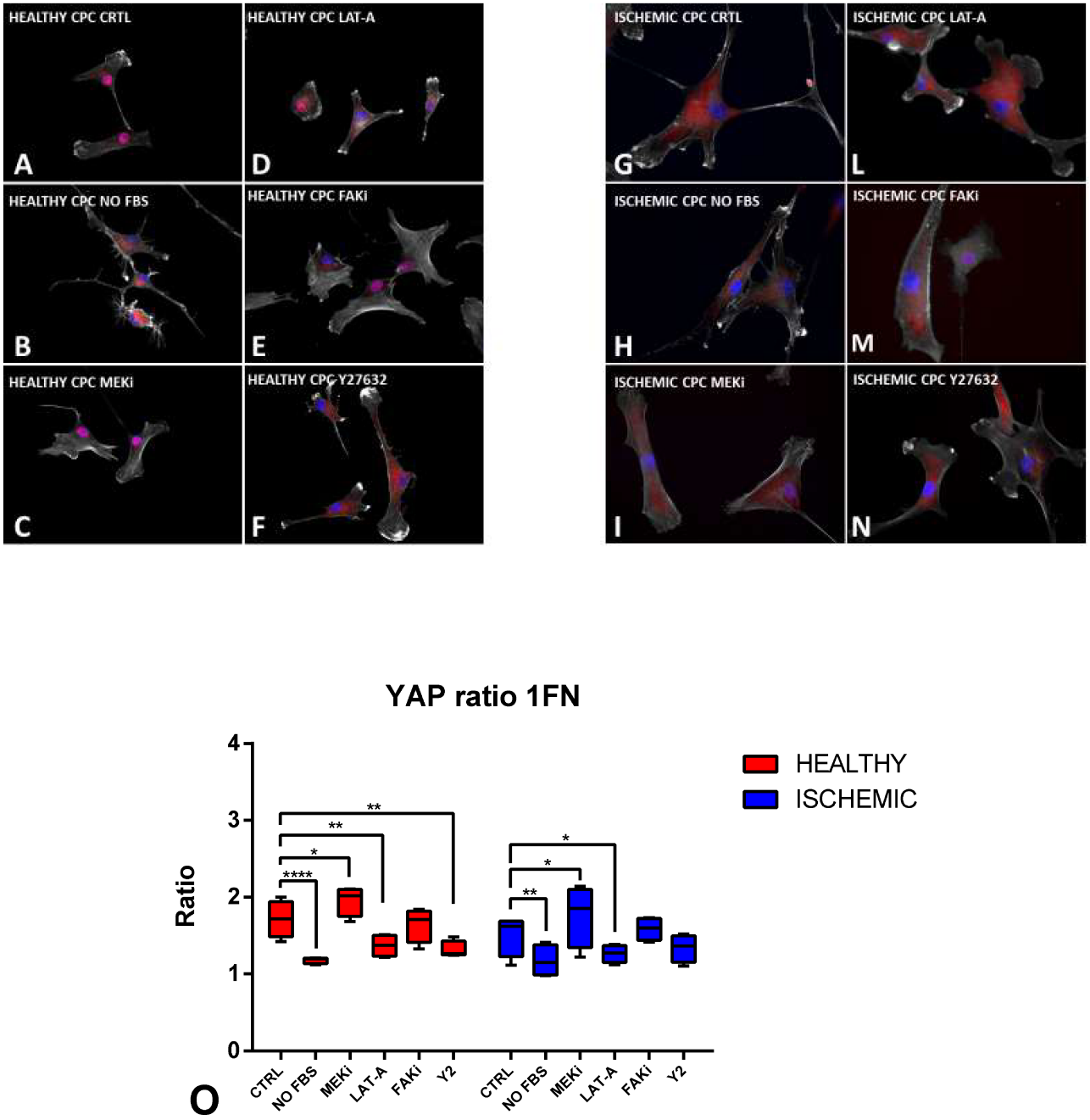

Figure 4.26 **Effect on YAP ratio after drug intervention, 1FN** Representative fluorescence images of healthy CPC (**A**-**F**) and ischemic CPC (**G**-**N**) stained with actin dye phalloidin (white) and YAP (red). Nuclei were stained with DAPI (blue). Scale bar 25µm. Box and whiskers plots are used to compare values of YAP ratio on healthy and ischemic CPC (**O**). CTRL (dmso); NO FBS (serum free media); MEKi (CI-1040); LAT-A (Latrunculin-A); FAKi (fak inhibitor 14); Y2 (Y27632). Healthy, N=4; Ischemic, N=4. p*<.05; p**<.01; p****<.0001

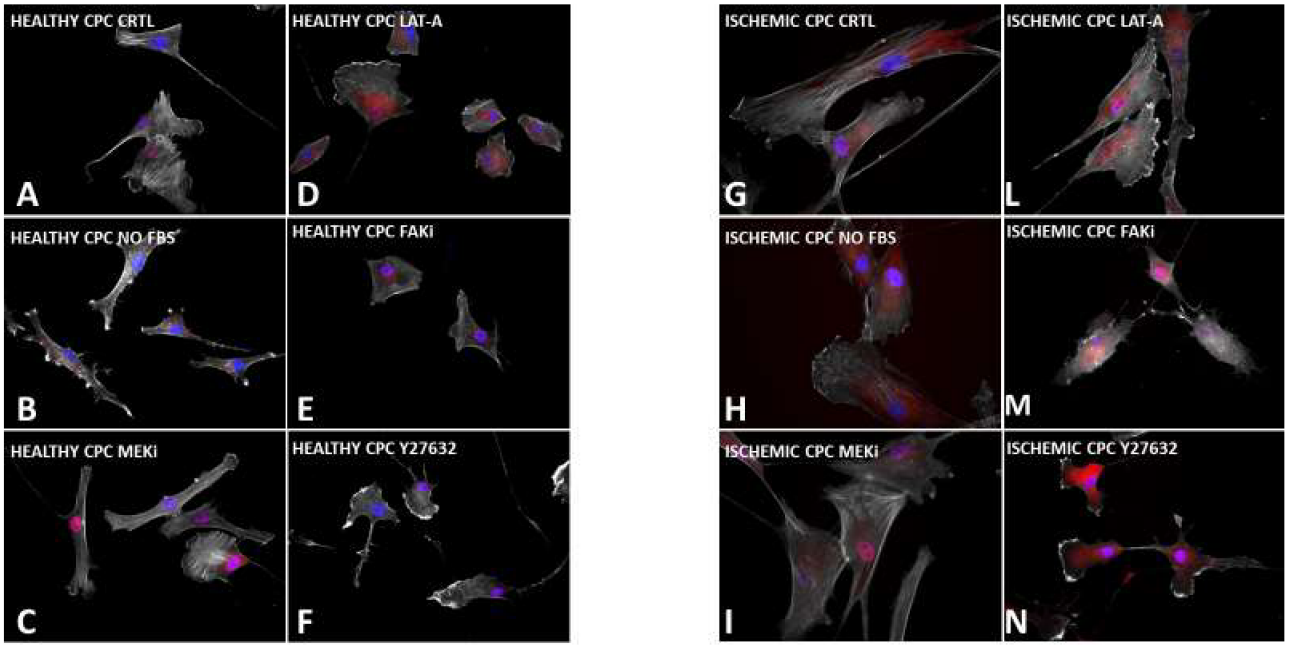

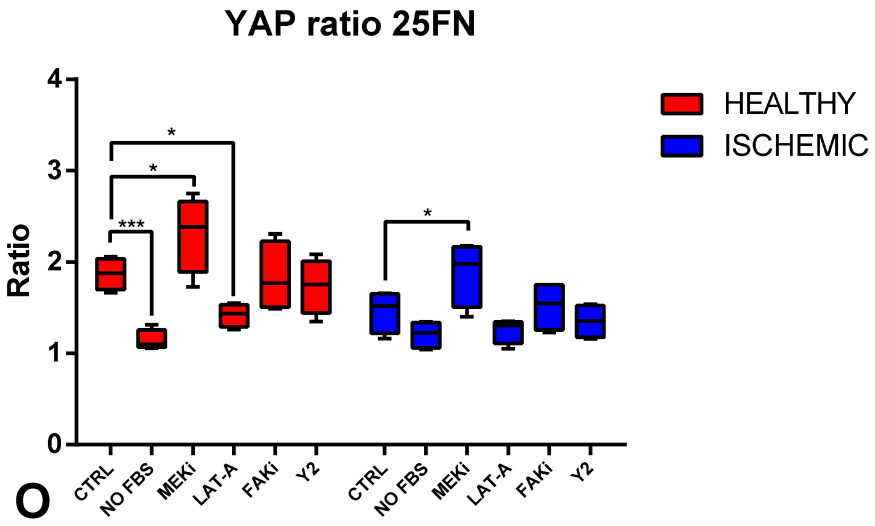

Figure 4.27 **Effect on YAP ratio after drug intervention, 25FN** Representative fluorescence images of healthy CPC (**A**-**F**) and ischemic CPC (**G**-**N**) stained with actin dye phalloidin (white) and YAP (red). Nuclei were stained with DAPI (blue). Scale bar 25µm. Box and whiskers plots are used to compare values of YAP ratio on healthy and ischemic CPC (**O**). CTRL (dmso); NO FBS (serum free media); MEKi (CI-1040); LAT-A (Latrunculin-A); FAKi (fak inhibitor 14); Y2 (Y27632). Healthy, N=4; Ischemic, N=4. p*<.05; p***<.001.

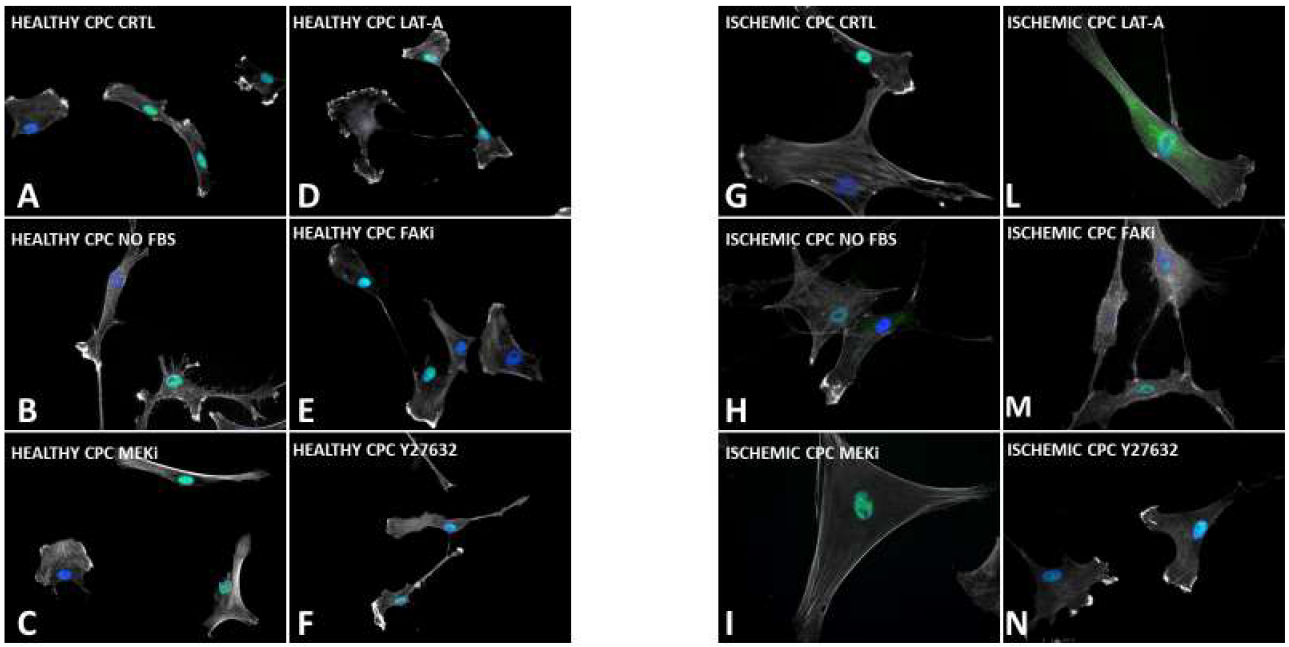

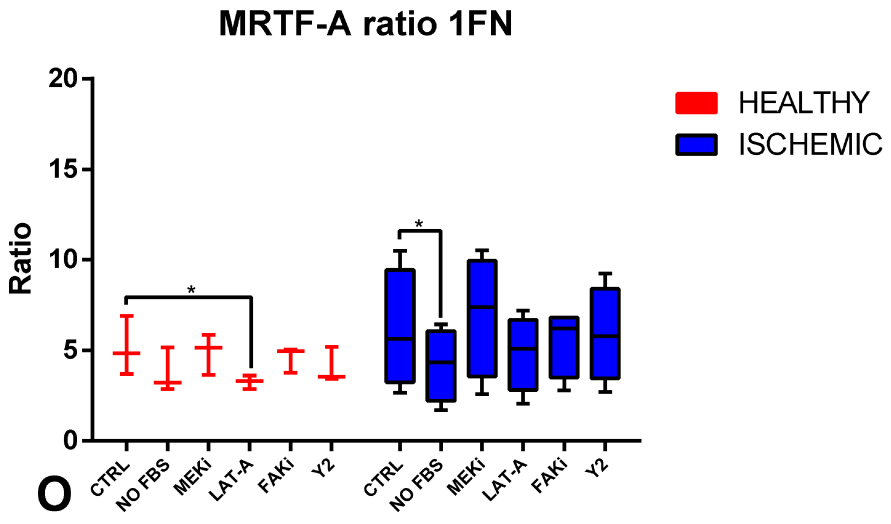

Figure 4.28 **Effect on MRTF ratio after drug intervention, 1FN** Representative fluorescence images of healthy CPC (**A**-**F**) and ischemic CPC (**G**-**N**) stained with actin dye phalloidin (white) and MRTF (green). Nuclei were stained with DAPI (blue). Scale bar 25µm. Box and whiskers plots are used to compare values of YAP ratio on healthy and ischemic CPC (**O**). CTRL (dmso); NO FBS (serum free media); MEKi (CI-1040); LAT-A (Latrunculin-A); FAKi (fak inhibitor 14); Y2 (Y27632). Healthy, N=3; Ischemic, N=4. p*<.05.

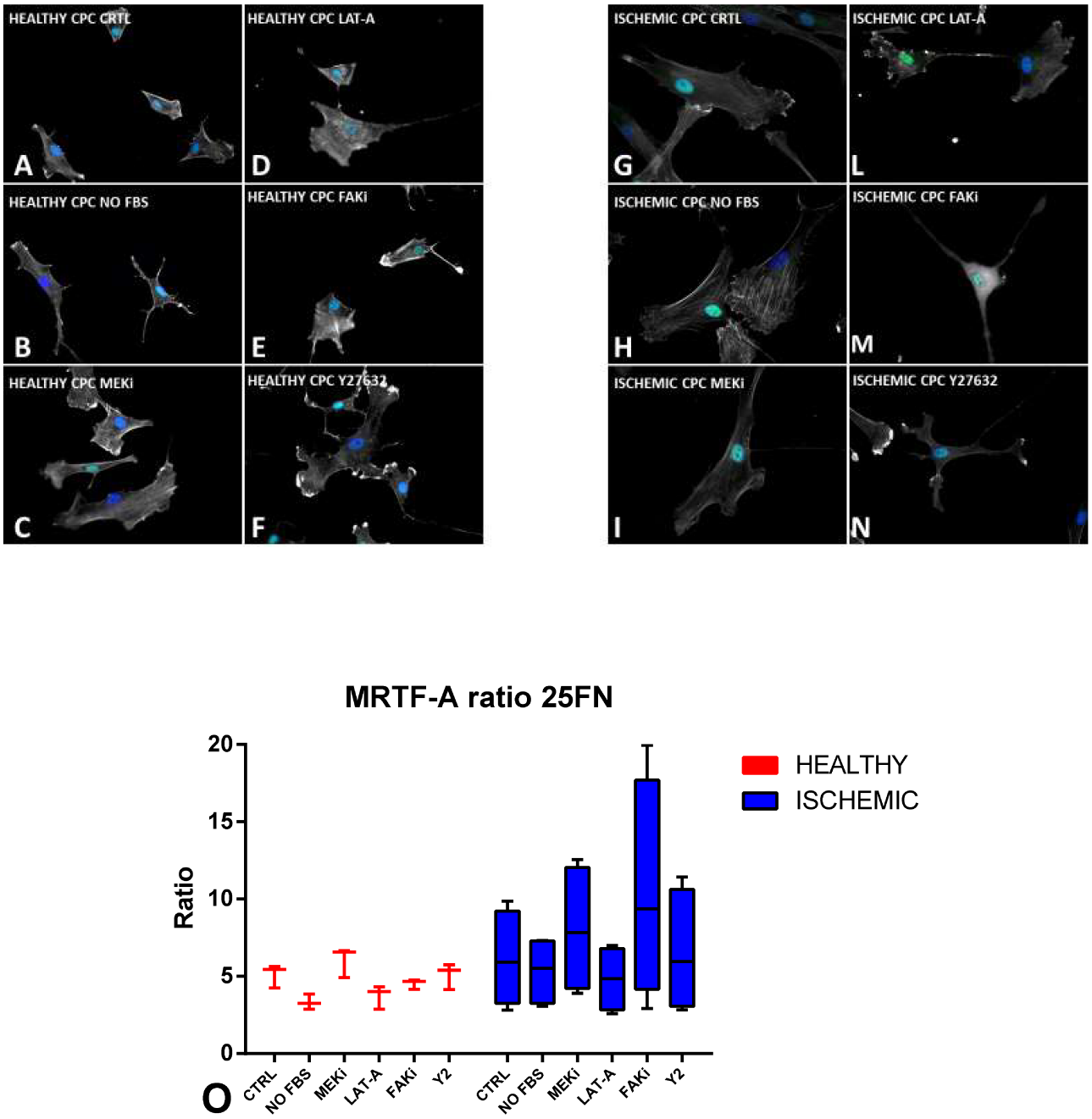

Figure 4.29 **Effect on MRTF ratio after drug intervention, 25FN** Representative fluorescence images of healthy CPC (**A**-**F**) and ischemic CPC (**G**-**N**) stained with actin dye phalloidin (white) and MRTF (green). Nuclei were stained with DAPI (blue). Scale bar 25µm. Box and whiskers plots are used to compare values of YAP ratio on healthy and ischemic CPC (**O**). CTRL (dmso); NO FBS (serum free media); MEKi (CI-1040); LAT-A (Latrunculin-A); FAKi (fak inhibitor 14); Y2 (Y27632). Healthy, N=3; Ischemic, N=4.

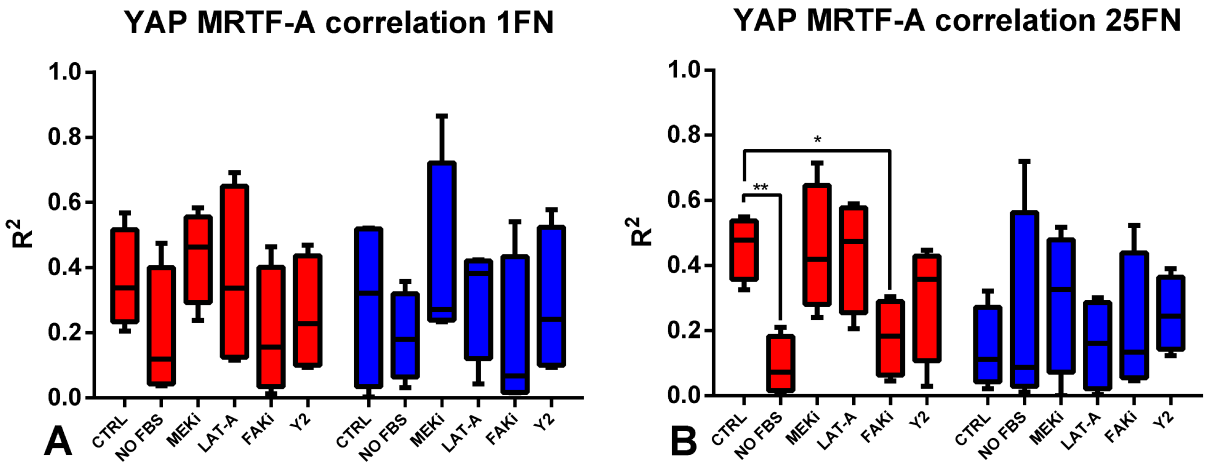

Figure 4.30 **Effects of drug intervention on simultaneous YAP-MRTF shuttling** CPC's YAP and MRTF correlation values (R^2) are stratified by fibronectin concentration 1μg/ml (**A**) and 25μg/ml (**B**) and responses to drugs were compared. Healthy, N=4; Ischemic, N=4. *p<.05; **p<.01. FN= Fibronectin 1FN=1μg/ml; 25FN 25μg/ml.

5. DISCUSSION

In the last (2016) WHO list of world's biggest killers, the doleful scepter is hold by ischemic heart disease (IHD) claiming almost 10 million lives per year. Despite improvements in the management of this disease, new therapies were not successful to restrict the mortality of IHD, that even showed an increase of deceased from the beginning of the 21th century (Bui, Anh et al., 2012). Until then, the only therapeutic option was the no-resolutive pharmacological treatment that, in the worst cases, did not avoid heart transplantation. Given these premises, a promising strategy, which is a candidate to reduce the mortality of IHD, is supposed to be cell therapy. This new therapeutic approach has been especially fueled by the discovery that heart tissue harbors an own stem cell population, stimulating the idea to regenerate the lost myocardium, taking advantage of the innate regenerative potential of stem cell. So far, several studies, including some clinical trials, have tested the feasibility to administer different sources of stem cells with the intent to modify the natural history of IHD and, possibly, to prevent cardiac transplantation (Witman & Sahara, 2018). Unfortunately, despite encouraging results, the primary end point is far from being achieved (Fisher et al., 2015).

Although several controversies, of which the scientific community is aware, concern which are the limiting factors of this therapy, there is a consensus to consider the complex modifications of the structure of the heart that characterize the progression of cardiac pathology towards heart failure, as the culprit of the suppressed potential of stem cell therapy. The ischemic heart, in fact, is characterized by a progressive shape remodeling caused by cardiomyocyte hypertrophy, matrix remodeling, and fibrosis. The resulting alteration of the extracellular matrix texture specifically describes modifications in both ECM composition and in tissue physical properties, that create an unphysiological milieu, uncompliant for stem cell function and, thus, for stem cell therapy. In this context, much attention was given to a new branch of cell biology, when pioneering studies had confirmed that cells not only rely on the classical biological stimuli (i.e. soluble factors) but also on physical cues (i.e. substrate stiffness) to regulate their proliferative, migratory and differentiation behaviors (Paluch et al., 2015). Thus, this suggests that the pathological soil established in ischemic heart is not permissive to stem cells to effectively regenerate the cardiac tissue.

Our group has already demonstrated that Cardiac Progenitor Cells (CPC) isolated from ischemic hearts differ from those isolated from healthy hearts in terms of senescence markers, telomerase activity (Cesselli et al., 2011) and autophagic flux (Gianfranceschi et al., 2016) but no data is available regarding their ability to sense physical cues. Considering that the physicochemical properties of the ECM can

affect the cell response and that the ECM of ischemic hearts is altered, we speculated that CPC isolated from failing hearts could show an impaired ability to sense the surrounding physical environment. To prove this concept, the first step of my work was to obtain pieces of evidence supporting this impairment, by analyzing the transcriptomic data generated in our previous works (Gianfranceschi et al., 2016). Bioinformatics analysis has revealed that CPC isolated from ischemic hearts account for a total of 89 differentially expressed genes belonging to the "Regulation of cell adhesion" and "Actin cytoskeletal organization" gene-sets. These data were further corroborated by the identification of the enrichment of the gene-sets "Focal adhesion" and "Regulation of actin cytoskeleton" among the differentially expressed genes. To evaluate the effective dissimilarity between CPC isolated from healthy and ischemic hearts, cytoskeleton proprieties were studied at two different time points, analyzing cell shapes. The morphological characterization has highlighted that, as a function of time, CPC isolated from ischemic hearts significantly differ from the normal counterpart in terms of: spreading area, ability to elongate (aspect ratio) and, with less evidence, in the ability to emit protrusions (solidity). As stated before, CPC isolated from ischemic hearts are senescent, a condition that is linked with cytoskeleton defects including enhanced spreading area (Nishio & Inoue, 2005). However, similar alterations in cell morphology were also observed in non-senescent fibroblasts obtained from Achilles tendon of aged mice (Arnesen & Lawson, 2006). Since cell elongation, as well as the ability of the cell to spread on the substrate, are influenced by cell adhesion (Geiger, Spatz, & Bershadsky, 2009), it is plausible that pathologic CPC are characterized by either an altered adhesion strength or an increased cell-substrate contact area. Those results were confirmed by the fact that pathologic CPC assemble a significantly higher number of focal adhesions to adhere to substrate in comparison to healthy CPC. However, when results were normalized by analyzing the fractional surface area of the cell covered by the FA, normal CPC showed a larger area covered by FA. In this regard, literature data seem to be partly contradictory. Indeed, while some Authors described, in senescent fibroblasts, increased levels of focal adhesions, and actin stress fibers, FAK and phospho-FAK (Cho et al., 2004), others showed a downregulation of specific components of the FA (i.e. paxillin and c-Src) (Nishio & Inoue, 2005). Additionally, other Authors have shown that FA proteins are aberrantly localized in the perinuclear regions, in fibroblasts obtained from aging mice (Arnesen & Lawson, 2006). However, most published works did not take into account cell hypertrophy (i.e. they did not normalize their data for the cell area or volume). As expected, instead, the migration assay showed that healthy CPC migrate faster than ischemic ones, since the number of focal adhesions has been inversely correlated to migration speed (Sieg, Hauck, & Schlaepfer, 1999). Interestingly, the migration difference is visible only at intermediate levels of adhesiveness (i.e. 5μg/mL fibronectin), which is consistent with literature data (DiMilla, Stone, Quinn, Albelda, & Lauffenburger, 1993), suggesting that healthy CPC retain a balanced focal adhesion assembly/disassembly ratio indispensable for migration (Lauffenburger & Horwitz, 1996) and, importantly, a conserved mechanosensing.

Several lines of evidence have demonstrated that surface stiffness sensing is mediated by focal adhesions (Hoffman, Grashoff, & Schwartz, 2011; Puklin-Faucher & Sheetz, 2009; Schwartz & DeSimone, 2008). In line with these findings and as expected by previous results, we demonstrated that pathologic CPC behave differently, in terms of cytoskeleton shaping, also when plated on substrates with different stiffness adsorbed with different concentration of fibronectin. In fact, on all the stiffness tested (i.e. 16kPa, 231kPa and Glass), healthy CPC display a smaller spreading area, a higher ability to polarize and to emit protrusions, when compared with pathologic CPC. Interestingly, all the differences are slightly enhanced by increasing the fibronectin concentration. Differences between healthy and ischemic CPC become strengthened when comparing their response to stiffness variation. The results demonstrate that pathologic CPC increase their spreading area as a function of substrate stiffness, showing an apparent incapacity to polarize and emit cell protrusions. On the contrary, healthy CPC spread over a smaller area, but show a superior ability to elongate and sprout. Concerning the effects of fibronectin concentration on cell behavior, we observed that only healthy CPC can sense variations in fibronectin concentrations, as demonstrated by their greater response on polarization and sprouting at 231kPa and on glass respectively. As a whole, these data demonstrate that, cells isolated from ischemic hearts have a different perception of the physical environment suggesting an improper crosstalk between mechanical cues and nucleus.

Since it has been shown that cells modulate their intracellular stiffness in accordance with the stiffness of the cell substrate, we decided to test if cardiac pathology altered this ability, investigating the mechanical properties of CPC by Atomic Force Microscopy. Focusing on the 25μg/ml fibronectin condition we noted, as expected, that healthy CPC, but not pathologic CPC, increase their internal forces as a function of substrate stiffness, even if the increment reach significance only when cells were cultured on Glass. The biochemical mechanisms responsible for the modulation of intracellular stiffness have been identified in the FAK/Cas and Rho/ROCK/myosin II pathways (Hoon, Tan, & Koh, 2016).

Moving from literature data showing that the nucleus/cytoplasmic (n/c) shuttling of YAP is a key mechanism of mechanotransduction, able to convey mechanical stimuli into proliferative or differentiation responses, we decided to investigate the subcellular localization of this co-transcriptional regulator in response to different stimuli (Low et al., 2014). We observed that YAP is translocated in the nucleus as a function of fibronectin concentration only in normal CPC, while CPC derived from ischemic hearts display a lower level of YAP n/c ratio, compared to healthy CPC. In an independent experiment, we demonstrated that, the differences in YAP n/c ratio between healthy and pathologic CPC are lost when cells are grown on a soft substrate (16 and 231 kPa). Conversely, differences similar to those observed in response to fibronectin concentration were observed, when cells were plated on a Glass substrate. Moreover, healthy CPC, but not ischemic CPC, showed to be responsive to increasing substrate

stiffness, up-modulating YAP translocation. Consistent with previous results, fibronectin concentration influenced YAP shuttling only when cells were plated on a Glass substrate and only on healthy CPC. These results corroborate those obtained from the characterization of cell morphology, further demonstrating the ability of healthy CPC to respond to substrate variation, ability lost in CPC from failing hearts. Our results are also consistent with published data, that showed an increased activity of the Hippo pathway, leading to increased YAP phosphorylation (and, therefore, its inhibition), in samples obtained from failing human hearts of both ischemic and non-ischemic origin (Leach et al., 2017).

Subsequently, we decided to focus on MRTF-A. This latter is another co-transcriptional regulator that binds to the Serum Response Factor (SRF) and responds to variations in substrate stiffness or integrin engagement. Furthermore, MRTF-A responds to Rho signals that induce a modification in the ratio between G- and F-actin. Specifically, MRTF-A can sense the intracellular levels of G-actin, shuttling between the nucleus and the cytoplasm as a consequence of its fluctuations (Foster et al., 2018). Most importantly for our work, recent studies have shown that MRTF-A and YAP/TAZ can functionally interact (Dupont et al., 2011). Precisely, since MRTF-A/SRF transcriptionally regulates many cytoskeletal genes, that are part of the YAP interactome, an indirect pathway cross-talk has been hypothesized. Furthermore, it was shown that several genes (e.g. *Ctgf*, *Cyr61*, and *Ankrd1*) contain binding sites for both TEAD and SRF, therefore a possible direct interaction between the two co-transcriptional regulators has been hypothesized (Foster et al., 2018). For these reasons, we studied the n/c shuttling of MRTF-A under the same conditions of stiffness and fibronectin in which YAP was studied. Similarly to what found with YAP, CPC obtained from ischemic and healthy hearts did not differ in MRTF-A n/c ratio when grown onto softer (16KPa and 231Kpa) substrates, whereas, when CPC were grown on Glass substrate the difference became significant. Differently from what we observed for YAP, the effects of fibronectin on MRTF-A were not significant in either group of cells.

Since, from the previous study, a partial overlapping trend of YAP and MRTF-A n/c ratio was suggested and driven by the observed functional interaction between MRTF-A and YAP, we decided to evaluate if they were coordinately regulated. Interestingly, at 1μg/ml of fibronectin, healthy CPC seeded onto Glass, showed that the synergistic translocation of YAP and MRTF-A was significantly more coordinated (in terms of R^2) in CPC obtained from normal hearts with respect to those obtained from pathologic hearts. Concerning cells grown on substrates coated with 25μg/ml fibronectin, the expression of YAP and MRTF-A was significantly more coordinated, in normal vs pathologic CPC, grown both on 231kPa gels and on glass.

YAP and MRTF-A n/c ratio data perfectly overlap with AFM data, suggesting that only in healthy cells, the link among these factors is maintained (C. X. Li et al., 2016; Morikawa et al., 2015). Lack of evidence of an increased intracellular stiffness in cells cultured on 231kPa vs 16kPa in healthy cells did not allow

us to explain why the correlation between YAP and MRTF-A in these conditions. One possibility is due to high inter sample variability and a relatively limited sample size, therefore further experiments are required to corroborate these findings.

Finally, to support nuclear translocation data, we assessed the level of the transcripts of three genes known to be regulated by both YAP and MRTF-A. Consistently with what observed in translocation experiment, two of three genes were significantly more expressed by normal vs pathologic CPC. However, due to the high variability in gene expression and relatively limited number of samples analyzed, we did not observe a modulation of gene expression as a function of either substrate stiffness or fibronectin concentration. The variability in gene expression could be ascribed to the regulation of the three genes by both YAP/TEAD and MRTF-A/SRF pathways. We are now planning to test genes regulated in a YAP/TEAD only and MRTF-A/TEAD only fashion, to dissect the contribution of the two pathways in regulating target gene expression.

Last, we explored the contribution of upstream regulators, that control the n/c shuttling of YAP and MRTF-A. To achieve this, four drugs (CI-1040, a MEK inhibitor; Latrunculin A, a F-actin inhibitor; FAKi14, a Focal adhesion kinase inhibitor; Y27632, a ROCK inhibitor) plus a serum free media condition were chosen.

Despite serum components are strong inductors of YAP nuclear localization, we demonstrated that CPC isolated from ischemic hearts are less sensitive, with respect to healthy CPC, to serum stimulation. This observation suggests that, in healthy CPC, more than in pathologic CPC, YAP control is strongly driven by lysophosphatidic acid (LPA) and sphingosine-1 phosphate (S1P), the key components of the serum that have been shown to promote Yap n/c shuttling (Yu et al., 2012). Noteworthy, LPA exerts its function via LPA1 and LPA3 receptors, activating the G-protein 12/13 and its downstream effector Rho that, in turn, modulates actin dynamics (Yu et al., 2012). Intriguingly, the downregulation of LPA1 and LPA3 exert opposing effects of on the senescence of mesenchymal stem cells, according to recent literature data (Kanehira et al., 2016). Rho activation can promote actin polymerization via both ROCK/LiM Kinase/cofilin (an actin binding protein that regulates actin depolymerization) and the formin pathways (Olson & Nordheim, 2010).Concerning ROCK activity, we have observed that its inhibitor y27632 caused the exclusion of YAP only in healthy CPC and not in pathologic CPC, suggesting that, in the latter, the Rho/ROCK pathway is less active. However, the Rho/ROCK pathway can also be activated by integrins via FAK, integrin linked kinase and Src (Schwartz & Shattil, 2000). Furthermore, it has also been shown that substrate stiffness may determine cell stiffening via the FAK/Cas pathway, promoting Rac activation and modulating peripheral actin cytoskeletal dynamics (Olson & Nordheim, 2010). Therefore, it is not surprising that at 25μg/ml of fibronectin, the effect of y27632 in healthy CPC

is masked. For the same reason, we can speculate that, the lack of serum effect on YAP in pathologic CPC grown in the presence of 25μg/ml of fibronectin could be due to integrin activation.

Concerning the mechanism linking actin polymerization status to the nuclear localization of YAP, it has been shown that different members of the MAP4K family of kinases (i.e. MAP4K1/2/3, MAP4K4/6/7 and MST1/2) respond to a variety of stimuli, including actin depolymerization, phosphorylating LATS1/2 that, in turn, phosphorylates YAP, inactivating it (Densham et al., 2009; Meng et al., 2015). Since as suggested, healthy CPC have a more active ROCK pathway, as expected, disruption of the actin network by Latrunculin-A treatment leads to a nuclear exclusion of YAP in healthy CPC. In pathologic CPC, the same effect is visible only at 1μg/ml of fibronectin whereas a slightly, but not significant effect was observed at 25μg/ml suggesting that these cells may be more resistant to Latrunculin-A treatment, possibly as a result of alternative pathways of YAP activation.

High matrix stiffness has been associated with a chronically activated FAK/Rho signaling, that, in mammary epithelial cells, is coupled with the activation of the Ras/MEK/ERK pathway (Provenzano, Inman, Eliceiri, & Keely, 2009). Importantly, a negative feedback loop is promoted by ERK on FAK phosphorylation status (Zheng et al., 2009). By testing the effect of a short FAK inhibition, we observed no inhibitory effect on YAP nuclear localization in either healthy or pathologic CPC. This result could be due to the fact that our experiment was conducted in the presence of serum, therefore the LPA stimulatory effect might have masked the FAK inhibitors effects.

Interestingly, concerning MEK, we found that its inhibition led to an increase in the nuclear localization of YAP in both healthy and ischemic CPC. Although intriguing, this piece of information is complex to discuss. With reference to our data, MEK/ERK signaling can be induced both via FAK and following LPA stimulation via Gi proteins (van Leeuwen et al., 2003). MEK and ERK may also be activated by EGF and PDGF (two growth factors present in the expansion medium of CPC) (Shaul & Seger, 2007). However, it has been recently shown that these growth factors promote YAP nuclear localization in a MEK/ERK independent fashion, via either the phosphatidyl inositol 3 kinase/PDK1 pathway or Src family kinases, respectively (R. Fan, Kim, & Gumbiner, 2013; Smoot et al., 2017). Most importantly, it has been recently been shown that MEK inhibitors and MEK1 silencing promotes the downregulation of beta-transducing repeat containing E3 ubiquitin protein ligase, a ubiquitin transferase that promotes the degradation of YAP (L. Li et al., 2013; Zhao, Li, Tumaneng, Wang, & Guan, 2010). Moreover, beyond the regulation of YAP thorough ERK, MEK can directly interact with YAP, preventing is degradation (L. Li et al., 2013). Our conflicting results suggest that MEK inhibition could have paradoxically promote ERK activation rather its inactivation thorough a negative feedback (Spirli et al., 2012).

Last, concerning MRTF-A n/c shuttling, it is regulated by the binding of this factor to G-actin via its RPEL domains. As a consequence of this interaction, the co-transcriptional regulator is retained in the

cell cytoplasm (Olson & Nordheim, 2010). Therefore, every factor that modifies the availability of G-actin in the cytoplasm (e.g. by promoting actin polymerization) modulates the n/c shuttling of MRTF-A. Therefore, serum, Rho/ROCK pathway activity, integrin signaling and FAK may indirectly modulate MRTF-A. Consistently, at 1μg/mL fibronectin concentration, actin depolymerization and serum deprivation reduced the nuclear localization of MRTF-A in healthy and pathologic CPC, respectively. Intriguingly, CPC cultured in the presence of 25μg/mL of fibronectin did not modulate MRTF-A nuclear localization in response to inhibitory treatments. In line, recent data indicate that FAK signaling, induced by mechanical stimulation, can increase the nuclear accumulation of MRTF-A in fibroblasts (Chan, Arora, Bozavikov, & McCulloch, 2009).

6. CONCLUDING REMARKS

Our work demonstrates that mechanotransduction is altered in CPC isolated from ischemic hearts and that these cells display an overall insensitivity to stiffness and to the matricellular protein fibronectin as well as a different behavior with respect to healthy CPC. These pieces of evidence are well supported by the overlapping trend of the nuclear localization of the two mechanotransduction-related co-transcription factor YAP and MRTF-A, whose nuclear translocation seems to be lost in ischemic CPC. Consistently, interfering with pathways regulating YAP and MRTF-A gave different results between healthy and ischemic CPC. Therefore, these findings suggest that investing in a deeper comprehension of CPC mechanotransduction pathways may be essential to train CPC to manage with the hostile environment of pathologic hearts, in order to avoid the seduction of the *Dark Side* of the force.

BIBLIOGRAPHY

Ahmed, M., & Ffrench-Constant, C. (2016). Extracellular Matrix Regulation of Stem Cell Behavior. *Current Stem Cell Reports*, *2*(3), 197–206. https://doi.org/10.1007/s40778-016-0056-2

Andronic, A. A., Mihaila, S., & Cinteza, M. (2016). Heart Failure with Mid-Range Ejection Fraction - a New Category of Heart Failure or Still a Gray Zone. *Maedica*, *11*(4), 320–324. Retrieved from http://www.ncbi.nlm.nih.gov/pubmed/28828050%0Ahttp://www.pubmedcentral.nih.gov/articlerender.fcgi?artid=PMC5543525

Arnesen, S. M., & Lawson, M. A. (2006). Age-related changes in focal adhesions lead to altered cell behavior in tendon fibroblasts. *Mechanisms of Ageing and Development*, *127*(9), 726–732. https://doi.org/https://doi.org/10.1016/j.mad.2006.05.003

Azevedo, P. S., Minicucci, M. F., Santos, P. P., Paiva, S. A. R., & Zornoff, L. A. M. (2013). Energy Metabolism in Cardiac Remodeling and Heart Failure. *Cardiology in Review*, *21*(3). Retrieved from https://journals.lww.com/cardiologyinreview/Fulltext/2013/05000/Energy_Metabolism_in_Cardiac_Remodeling_and_Heart.4.aspx

Barile, L., Gherghiceanu, M., Popescu, L. M., Moccetti, T., & Vassalli, G. (2013). Human cardiospheres as a source of multipotent stem and progenitor cells. *Stem Cells International*, *2013*. https://doi.org/10.1155/2013/916837

Barry, E. R., Morikawa, T., Butler, B. L., Shrestha, K., de la Rosa, R., Yan, K. S., … Camargo, F. D. (2013). Restriction of intestinal stem cell expansion and the regenerative response by YAP. *Nature*, *493*(7430), 106–110. https://doi.org/10.1038/nature11693

Beltrami, A. P., Barlucchi, L., Torella, D., Baker, M., Limana, F., Chimenti, S., … Anversa, P. (2003). Adult Cardiac Stem Cells Are Multipotent and Support Myocardial Regeneration. *Cell*, *114*(6), 763–776. https://doi.org/10.1016/S0092-8674(03)00687-1

Beltrami, A. P., Cesselli, D., Bergamin, N., Marcon, P., Rigo, S., Puppato, E., … Beltrami, C. A. (2007). Multipotent cells can be generated in vitro from several adult human organs (heart, liver, and bone marrow). *Blood*, *110*(9), 3438. Retrieved from http://www.bloodjournal.org/content/110/9/3438.abstract

Bergmann, O., Bhardwaj, R. D., Bernard, S., Zdunek, S., Barnabé-Heider, F., Walsh, S., … Frisén, J. (2009). Evidence for cardiomyocyte renewal in humans. *Science (New York, N.Y.)*, *324*(5923), 98–102. https://doi.org/10.1126/science.1164680

Boggiano, J. C., & Fehon, R. G. (2012). Growth control by committee: intercellular junctions, cell polarity, and the cytoskeleton regulate Hippo signaling. *Developmental Cell*, *22*(4), 695–702. https://doi.org/10.1016/j.devcel.2012.03.013

Bolli, R., Chugh, A. R., D'Amario, D., Loughran, J. H., Stoddard, M. F., Ikram, S., … Anversa, P. (2011). Cardiac stem cells in patients with ischaemic cardiomyopathy (SCIPIO): initial results of a randomised phase 1 trial. *Lancet (London, England)*, *378*(9806), 1847–1857. https://doi.org/10.1016/S0140-6736(11)61590-0

Bora-Singhal, N., Nguyen, J., Schaal, C., Perumal, D., Singh, S., Coppola, D., & Chellappan, S. (2015). YAP1 Regulates OCT4 Activity and SOX2 Expression to Facilitate Self-Renewal and Vascular Mimicry of Stem-Like Cells. *Stem Cells (Dayton, Ohio)*, *33*(6), 1705–1718. https://doi.org/10.1002/stem.1993

Bos, J. L., Rehmann, H., & Wittinghofer, A. (2007). GEFs and GAPs: Critical Elements in the Control of Small G Proteins. *Cell*, *129*(5), 865–877. https://doi.org/10.1016/j.cell.2007.05.018

Bui, Anh, L., Horwish, Tamara, B., & Fonarow, Gregg, C. (2012). Epidemiology and risk profile of heart failure. *Nature Publishing Group*, *8*(1), 1–25. https://doi.org/10.1038/nrcardio.2010.165.Epidemiology

Burridge, K., & Wittchen, E. S. (2013). The tension mounts: stress fibers as force-generating mechanotransducers. *The Journal of Cell Biology*, *200*(1), 9–19. https://doi.org/10.1083/jcb.201210090

Camelliti, P., Borg, T. K., & Kohl, P. (2005). Structural and functional characterisation of cardiac fibroblasts.

Cardiovascular Research, *65*(1), 40–51. https://doi.org/10.1016/j.cardiores.2004.08.020
Cao, X., Pfaff, S. L., & Gage, F. H. (2008). YAP regulates neural progenitor cell number via the TEA domain transcription factor. *Genes & Development*, *22*(23), 3320–3334. https://doi.org/10.1101/gad.1726608
Carisey, A., Tsang, R., Greiner, A. M., Nijenhuis, N., Heath, N., Nazgiewicz, A., … Ballestrem, C. (2013). Vinculin regulates the recruitment and release of core focal adhesion proteins in a force-dependent manner. *Current Biology : CB*, *23*(4), 271–281. https://doi.org/10.1016/j.cub.2013.01.009
Carraher, C. L., & Schwarzbauer, J. E. (2013). Regulation of matrix assembly through rigidity-dependent fibronectin conformational changes. *The Journal of Biological Chemistry*, *288*(21), 14805–14814. https://doi.org/10.1074/jbc.M112.435271
Castaldi, A., Chesini, G. P., Taylor, A. E., Sussman, M. A., Brown, J. H., & Purcell, N. H. (2016). Sphingosine 1-phosphate elicits RhoA-dependent proliferation and MRTF-A mediated gene induction in CPCs. *Cellular Signalling*, *28*(8), 871–879. https://doi.org/10.1016/j.cellsig.2016.04.006
Cesselli, D., Beltrami, A. P., D'Aurizio, F., Marcon, P., Bergamin, N., Toffoletto, B., … Leri, A. (2011). Effects of age and heart failure on human cardiac stem cell function. *The American Journal of Pathology*, *179*(1), 349–366. https://doi.org/10.1016/j.ajpath.2011.03.036
Chan, M. W. C., Arora, P. D., Bozavikov, P., & McCulloch, C. A. (2009). FAK, PIP5KIγ and gelsolin cooperatively mediate force-induced expression of α-smooth muscle actin. *Journal of Cell Science*, *122*(15), 2769. Retrieved from http://jcs.biologists.org/content/122/15/2769.abstract
Chiariello, M., Vaqué, J. P., Crespo, P., & Gutkind, J. S. (2010). Activation of Ras and Rho GTPases and MAP Kinases by G-Protein-Coupled Receptors BT - MAP Kinase Signaling Protocols: Second Edition. In R. Seger (Ed.) (pp. 137–150). Totowa, NJ: Humana Press. https://doi.org/10.1007/978-1-60761-795-2_8
Cho, K. A., Ryu, S. J., Oh, Y. S., Park, J. H., Lee, J. W., Kim, H.-P., … Park, S. C. (2004). Morphological Adjustment of Senescent Cells by Modulating Caveolin-1 Status. *Journal of Biological Chemistry*, *279*(40), 42270–42278. https://doi.org/10.1074/jbc.M402352200
Chugh, A. R., Beache, G. M., Loughran, J. H., Mewton, N., Elmore, J. B., Kajstura, J., … Bolli, R. (2012). Administration of cardiac stem cells in patients with ischemic cardiomyopathy: the SCIPIO trial: surgical aspects and interim analysis of myocardial function and viability by magnetic resonance. *Circulation*, *126*(11 Suppl 1), S54–S64. https://doi.org/10.1161/CIRCULATIONAHA.112.092627
Chung, H., Lee, B.-K., Uprety, N., Shen, W., Lee, J., & Kim, J. (2016). Yap1 is dispensable for self-renewal but required for proper differentiation of mouse embryonic stem (ES) cells. *EMBO Reports*, *17*(4), 519–529. https://doi.org/10.15252/embr.201540933
Cleutjens, J. P. M., Kandala, J. C., Guarda, E., Guntaka, R. V, & Weber, K. T. (1995). Regulation of collagen degradation in the rat myocardium after infarction. *Journal of Molecular and Cellular Cardiology*, *27*(6), 1281–1292. https://doi.org/10.1016/S0022-2828(05)82390-9
Cohn, J. N., Ferrari, R., & Sharpe, N. (2000). Cardiac remodeling-concepts and clinical implications: A consensus paper from an International Forum on Cardiac Remodeling. *Journal of the American College of Cardiology*, *35*(3), 569–582. https://doi.org/10.1016/S0735-1097(99)00630-0
Cramer, L. P. (2010). Forming the cell rear first: breaking cell symmetry to trigger directed cell migration. *Nature Cell Biology*, *12*, 628. Retrieved from http://dx.doi.org/10.1038/ncb0710-628
del Rio, A., Perez-Jimenez, R., Liu, R., Roca-Cusachs, P., Fernandez, J. M., & Sheetz, M. P. (2009). Stretching Single Talin Rod Molecules Activates Vinculin Binding. *Science*, *323*(5914), 638. Retrieved from http://science.sciencemag.org/content/323/5914/638.abstract
Densham, R. M., O'Neill, E., Munro, J., Konig, I., Anderson, K., Kolch, W., & Olson, M. F. (2009). MST Kinases Monitor Actin Cytoskeletal Integrity and Signal via c-Jun N-Terminal Kinase Stress-Activated Kinase To Regulate p21Waf1/Cip1 Stability. *Molecular and Cellular Biology*, *29*(24), 6380–6390. https://doi.org/10.1128/MCB.00116-09
deRan, M., Yang, J., Shen, C. H., Peters, E. C., Fitamant, J., Chan, P., … Wu, X. (2014). Energy stress regulates Hippo-YAP signaling involving AMPK-mediated regulation of angiomotin-like 1 protein. *Cell Reports*, *9*(2), 495–503. https://doi.org/10.1016/j.celrep.2014.09.036
Di Meglio, F., Castaldo, C., Nurzynska, D., Romano, V., Miraglia, R., Bancone, C., … Montagnani, S. (2010). Epithelial–mesenchymal transition of epicardial mesothelium is a source of cardiac CD117-positive stem cells in adult human heart. *Journal of Molecular and Cellular Cardiology*, *49*(5), 719–727. https://doi.org/10.1016/j.yjmcc.2010.05.013

Diez, J. (Javier), Querejeta, R. (Ramón), Lopez, B. (Begoña), Gonzalez, A. (Arantxa), Larman, M. (Mariano), & Martinez-Ubago, J. L. (José L. . (2002). Losartan-dependent regression of myocardial fibrosis is associated with reduction of left ventricular chamber stiffness in hypertensive patients. Retrieved from http://dadun.unav.edu/handle/10171/19850

DiMilla, P. A., Stone, J. A., Quinn, J. A., Albelda, S. M., & Lauffenburger, D. A. (1993). Maximal migration of human smooth muscle cells on fibronectin and type IV collagen occurs at an intermediate attachment strength. *The Journal of Cell Biology*, *122*(3), 729–737. Retrieved from https://www.ncbi.nlm.nih.gov/pubmed/8335696

Discher, D. E., Janmey, P., & Wang, Y. (2005). Tissue Cells Feel and Respond to the Stiffness of Their Substrate. *Science*, *310*(5751), 1139. Retrieved from http://science.sciencemag.org/content/310/5751/1139.abstract

Discher, D. E., Mooney, D. J., & Zandstra, P. W. (2009). Growth factors, matrices, and forces combine and control stem cells. *Science (New York, N.Y.)*, *324*(5935), 1673–1677. https://doi.org/10.1126/science.1171643

Du, K. L., Chen, M., Li, J., Lepore, J. J., Mericko, P., & Parmacek, M. S. (2004). Megakaryoblastic Leukemia Factor-1 Transduces Cytoskeletal Signals and Induces Smooth Muscle Cell Differentiation from Undifferentiated Embryonic Stem Cells. *Journal of Biological Chemistry*, *279*(17), 17578–17586. https://doi.org/10.1074/jbc.M400961200

Dupont, S., Morsut, L., Aragona, M., Enzo, E., Giulitti, S., Cordenonsi, M., … Piccolo, S. (2011). Role of YAP/TAZ in mechanotransduction. *Nature*, *474*, 179. Retrieved from http://dx.doi.org/10.1038/nature10137

Editors, T. L. (2014). Expression of concern: the SCIPIO trial. *Lancet (London, England)*, *383*(9925), 1279. https://doi.org/10.1016/S0140-6736(14)60608-5

Eltzner, B., Wollnik, C., Gottschlich, C., Huckemann, S., & Rehfeldt, F. (2015). The Filament Sensor for Near Real-Time Detection of Cytoskeletal Fiber Structures. *PLOS ONE*, *10*(5), e0126346-. Retrieved from https://doi.org/10.1371/journal.pone.0126346

Engler, A. J., Sen, S., Sweeney, H. L., & Discher, D. E. (2006). Matrix Elasticity Directs Stem Cell Lineage Specification. *Cell*, *126*(4), 677–689. https://doi.org/10.1016/j.cell.2006.06.044

Epelman, S., Liu, P. P., & Mann, D. L. (2015). HHS Public Access, *15*(2), 117–129. https://doi.org/10.1038/nri3800.Role

Esnault, C., Stewart, A., Gualdrini, F., East, P., Horswell, S., Matthews, N., & Treisman, R. (2014). Rho-actin signaling to the MRTF coactivators dominates the immediate transcriptional response to serum in fibroblasts. *Genes and Development*, *28*(9), 943–958. https://doi.org/10.1101/gad.239327.114

Fabry, B., Klemm, A. H., Kienle, S., Schäffer, T. E., & Goldmann, W. H. (2011). Focal adhesion kinase stabilizes the cytoskeleton. *Biophysical Journal*, *101*(9), 2131–2138. https://doi.org/10.1016/j.bpj.2011.09.043

Fan, D., Takawale, A., Lee, J., & Kassiri, Z. (2012). Cardiac fibroblasts, fibrosis and extracellular matrix remodeling in heart disease. *Fibrogenesis & Tissue Repair*, *5*(1), 15. https://doi.org/10.1186/1755-1536-5-15

Fan, R., Kim, N.-G., & Gumbiner, B. M. (2013). Regulation of Hippo pathway by mitogenic growth factors via phosphoinositide 3-kinase and phosphoinositide-dependent kinase-1. *Proceedings of the National Academy of Sciences of the United States of America*, *110*(7), 2569–2574. https://doi.org/10.1073/pnas.1216462110

Ferraro, F., Celso, C. Lo, & Scadden, D. (2010). Adult stem cels and their niches. *Advances in Experimental Medicine and Biology*, *695*, 155–168. https://doi.org/10.1007/978-1-4419-7037-4_11

Finch-Edmondson, M., & Sudol, M. (2016). Framework to function: Mechanosensitive regulators of gene transcription. *Cellular and Molecular Biology Letters*, *21*(1), 1–23. https://doi.org/10.1186/s11658-016-0028-7

Fisher, S. A., Doree, C., Mathur, A., & Martin-Rendon, E. (2015). Meta-Analysis of Cell Therapy Trials for Patients With Heart Failure. *Circulation Research*, *116*(8), 1361–1377. https://doi.org/10.1161/CIRCRESAHA.116.304386

Fletcher, D. A., & Mullins, R. D. (2010). Cell mechanics and the cytoskeleton. *Nature*, *463*, 485. Retrieved from http://dx.doi.org/10.1038/nature08908

Florea, V. G., & Cohn, J. N. (2014). The Autonomic Nervous System and Heart Failure. *Circulation Research*, *114*(11), 1815–1826. https://doi.org/10.1161/CIRCRESAHA.114.302589

Foster, C. T., Gualdrini, F., & Treisman, R. (2018). Mutual dependence of the MRTF – SRF and YAP – TEAD pathways in cancer-associated fibroblasts is indirect and mediated by cytoskeletal dynamics, 1–15. https://doi.org/10.1101/gad.304501.117.

Geiger, B., Spatz, J. P., & Bershadsky, A. D. (2009). Environmental sensing through focal adhesions. *Nature Reviews Molecular Cell Biology*, *10*, 21. Retrieved from http://dx.doi.org/10.1038/nrm2593

Gianfranceschi, G., Caragnano, A., Piazza, S., Manini, I., Ciani, Y., Verardo, R., … Beltrami, A. P. (2016). Critical role of lysosomes in the dysfunction of human Cardiac Stem Cells obtained from failing hearts. *International Journal of Cardiology*, *216*, 140–150. https://doi.org/10.1016/j.ijcard.2016.04.155

Gnecchi, M., Zhang, Z., Ni, A., & Dzau, V. J. (2008). Paracrine mechanisms in adult stem cell signaling and therapy. *Circulation Research*, *103*(11), 1204–1219. https://doi.org/10.1161/CIRCRESAHA.108.176826

Goldenberg, I., Grossman, E., Jacobson, K. A., Shneyvays, V., & Shainberg, A. (2001). Angiotensin II-induced apoptosis in rat cardiomyocyte culture: a possible role of AT1 and AT2 receptors. *Journal of Hypertension*, *19*(9). Retrieved from https://journals.lww.com/jhypertension/Fulltext/2001/09000/Angiotensin_II_induced_apoptosis_in_rat.22.aspx

Guilluy, C., Swaminathan, V., Garcia-Mata, R., O'Brien, E. T., Superfine, R., & Burridge, K. (2011). The Rho GEFs LARG and GEF-H1 regulate the mechanical response to force on integrins. *Nature Cell Biology*, *13*(6), 722–727. https://doi.org/10.1038/ncb2254

Halder, G., Dupont, S., & Piccolo, S. (2012). Transduction of mechanical and cytoskeletal cues by YAP and TAZ. *Nature Reviews Molecular Cell Biology*, *13*, 591. Retrieved from http://dx.doi.org/10.1038/nrm3416

Hawkins, N. M., Petrie, M. C., Jhund, P. S., Chalmers, G. W., Dunn, F. G., & McMurray, J. J. V. (2009). Heart failure and chronic obstructive pulmonary disease: Diagnostic pitfalls and epidemiology. *European Journal of Heart Failure*, *11*(2), 130–139. https://doi.org/10.1093/eurjhf/hfn013

Hayakawa, K., Tatsumi, H., & Sokabe, M. (2012). Mechano-sensing by actin filaments and focal adhesion proteins. *Communicative & Integrative Biology*, *5*(6), 572–577. https://doi.org/10.4161/cib.21891

Heidenreich, P. A., Albert, N. M., Allen, L. A., Bluemke, D. A., Butler, J., Fonarow, G. C., … Council, S. (2013). Forecasting the impact of heart failure in the United States: a policy statement from the American Heart Association. *Circulation. Heart Failure*, *6*(3), 606–619. https://doi.org/10.1161/HHF.0b013e318291329a

Hellermann, J. P., Goraya, T. Y., Jacobsen, S. J., Weston, S. A., Reeder, G. S., Gersh, B. J., … Roger, V. L. (2003). Incidence of heart failure after myocardial infarction: Is it changing over time? *American Journal of Epidemiology*, *157*(12), 1101–1107. https://doi.org/10.1093/aje/kwg078

Herum, K., Lunde, I., McCulloch, A., & Christensen, G. (2017). The Soft- and Hard-Heartedness of Cardiac Fibroblasts: Mechanotransduction Signaling Pathways in Fibrosis of the Heart. *Journal of Clinical Medicine*, *6*(6), 53. https://doi.org/10.3390/jcm6050053

Herum, K. M., Choppe, J., Kumar, A., Engler, A. J., & McCulloch, A. D. (2017). Mechanical regulation of cardiac fibroblast profibrotic phenotypes. *Molecular Biology of the Cell*, *28*(14), 1871–1882. https://doi.org/10.1091/mbc.E17-01-0014

Hiesinger, W., Brukman, M. J., McCormick, R. C., Fitzpatrick 3rd, J. R., Frederick, J. R., Yang, E. C., … Woo, Y. J. (2012). Myocardial tissue elastic properties determined by atomic force microscopy after stromal cell-derived factor 1α angiogenic therapy for acute myocardial infarction in a murine model. *The Journal of Thoracic and Cardiovascular Surgery*, *143*(4), 962–966. https://doi.org/10.1016/j.jtcvs.2011.12.028

Higuchi, S., Lin, Q., Wang, J., Lim, T. K., Joshi, S. B., Anand, G. S., … Fujita, H. (2013). Heart extracellular matrix supports cardiomyocyte differentiation of mouse embryonic stem cells. *Journal of Bioscience and Bioengineering*, *115*(3), 320–325. https://doi.org/10.1016/j.jbiosc.2012.10.004

Ho, C. Y., Jaalouk, D. E., Vartiainen, M. K., & Lammerding, J. (2013). Lamin A/C and emerin regulate MKL1–SRF activity by modulating actin dynamics. *Nature*, *497*, 507. Retrieved from http://dx.doi.org/10.1038/nature12105

Hoffman, B. D., Grashoff, C., & Schwartz, M. A. (2011). Dynamic molecular processes mediate cellular

mechanotransduction. *Nature*, *475*, 316. Retrieved from http://dx.doi.org/10.1038/nature10316
Hoon, J., Tan, M., & Koh, C.-G. (2016). The Regulation of Cellular Responses to Mechanical Cues by Rho GTPases. *Cells*, *5*(2), 17. https://doi.org/10.3390/cells5020017
Humphries, J. D., Wang, P., Streuli, C., Geiger, B., Humphries, M. J., & Ballestrem, C. (2007). Vinculin controls focal adhesion formation by direct interactions with talin and actin. *Journal of Cell Biology*, *179*(5), 1043–1057. https://doi.org/10.1083/jcb.200703036
Hynes, R. O. (2002). Integrins. *Cell*, *110*(6), 673–687. https://doi.org/10.1016/S0092-8674(02)00971-6
Ishigami, S., Ohtsuki, S., Eitoku, T., Ousaka, D., Kondo, M., Kurita, Y., … Oh, H. (2017). Intracoronary Cardiac Progenitor Cells in Single Ventricle Physiology. *Circulation Research*, *120*(7), 1162–1173. https://doi.org/10.1161/CIRCRESAHA.116.310253
Jaalouk, D. E., & Lammerding, J. (2009). Mechanotransduction gone awry. *Nature Reviews Molecular Cell Biology*, *10*(1), 63–73. https://doi.org/10.1038/nrm2597
Ji, H., Tang, H., Lin, H., Mao, J., Gao, L., Liu, J., & Wu, T. (2014). Rho/Rock cross-talks with transforming growth factor-β/Smad pathway participates in lung fibroblast-myofibroblast differentiation. *Biomedical Reports*, *2*(6), 787–792. https://doi.org/10.3892/br.2014.323
Jourdan-Lesaux, C., Zhang, J., & Lindsey, M. L. (2010). Extracellular matrix roles during cardiac repair. *Life Sciences*, *87*(13–14), 391–400. https://doi.org/10.1016/j.lfs.2010.07.010
Kanehira, M., Fujiwara, T., Nakajima, S., Okitsu, Y., Onishi, Y., Fukuhara, N., … Harigae, H. (2016). A Lysophosphatidic Acid Receptors 1 and 3 Axis Governs Cellular Senescence of Mesenchymal Stromal Cells and Promotes Growth and Vascularization of Multiple Myeloma. *STEM CELLS*, *35*(3), 739–753. https://doi.org/10.1002/stem.2499
Kobayashi, T., & Sokabe, M. (2010). Sensing substrate rigidity by mechanosensitive ion channels with stress fibers and focal adhesions. *Current Opinion in Cell Biology*, *22*(5), 669–676. https://doi.org/https://doi.org/10.1016/j.ceb.2010.08.023
Komajda, M., & Lam, C. S. P. (2014). Heart failure with preserved ejection fraction: a clinical dilemma. *European Heart Journal*, *35*(16), 1022–1032. Retrieved from http://dx.doi.org/10.1093/eurheartj/ehu067
Kuo, J.-C. (2013). Mechanotransduction at focal adhesions: integrating cytoskeletal mechanics in migrating cells. *Journal of Cellular and Molecular Medicine*, *17*(6), 704–712. https://doi.org/10.1111/jcmm.12054
Kuwahara, K., Barrientos, T., Pipes, G. C. T., Li, S., & Olson, E. N. (2005). Muscle-specific signaling mechanism that links actin dynamics to serum response factor. *Molecular and Cellular Biology*, *25*(8), 3173–3181. https://doi.org/10.1128/MCB.25.8.3173-3181.2005
Lachowski, D., Cortes, E., Robinson, B., Rice, A., Rombouts, K., & Del Río Hernández, A. E. (2018). FAK controls the mechanical activation of YAP, a transcriptional regulator required for durotaxis. *The FASEB Journal*, *32*(2), 1099–1107. https://doi.org/10.1096/fj.201700721R
Lauffenburger, D. A., & Horwitz, A. F. (1996). Cell Migration: A Physically Integrated Molecular Process. *Cell*, *84*(3), 359–369. https://doi.org/10.1016/S0092-8674(00)81280-5
Leach, J. P., Heallen, T., Zhang, M., Rahmani, M., Morikawa, Y., Hill, M. C., … Martin, J. F. (2017). Hippo pathway deficiency reverses systolic heart failure after infarction. *Nature*, *550*, 260. Retrieved from http://dx.doi.org/10.1038/nature24045
Leask, A. (2015). Getting to the Heart of the Matter. *Circulation Research*, *116*(7), 1269–1276. https://doi.org/10.1161/CIRCRESAHA.116.305381
Leri, A., Kajstura, J., & Anversa, P. (2011). Role of cardiac stem cells in cardiac pathophysiology: a paradigm shift in human myocardial biology. *Circulation Research*, *109*(8), 941–961. https://doi.org/10.1161/CIRCRESAHA.111.243154
Levy, D., Kenchaiah, S., Larson, M. G., Benjamin, E. J., Kupka, M. J., Ho, K. K. L., … Vasan, R. S. (2002). Long-Term Trends in the Incidence of and Survival with Heart Failure. *New England Journal of Medicine*, *347*(18), 1397–1402. https://doi.org/10.1056/NEJMoa020265
Lewis-McDougall, F. C., Ruchaya, P. J., Domenjo-Vila, E., Teoh, T. S., Prata, L., Cottle, B. J., … Ellison-Hughes, G. M. (2018). Aged-senescent cells contribute to impaired heart regeneration. *BioRxiv*. Retrieved from http://biorxiv.org/content/early/2018/10/01/397216.abstract
Li, C. X., Talele, N. P., Boo, S., Koehler, A., Knee-Walden, E., Balestrini, J. L., … Hinz, B. (2016). MicroRNA-21

preserves the fibrotic mechanical memory of mesenchymal stem cells. *Nature Materials*, *16*, 379. Retrieved from http://dx.doi.org/10.1038/nmat4780

Li, L., Wang, J., Zhang, Y., Zhang, Y., Ma, L., Weng, W., … Sun, F. (2013). MEK1 promotes YAP and their interaction is critical for tumorigenesis in liver cancer. *FEBS Letters*, *587*(24), 3921–3927. https://doi.org/10.1016/j.febslet.2013.10.042

Lian, I., Kim, J., Okazawa, H., Zhao, J., Zhao, B., Yu, J., … Guan, K. L. (2010). The role of YAP transcription coactivator in regulating stem cell self-renewal and differentiation. *Genes and Development*, *24*(11), 1106–1118. https://doi.org/10.1101/gad.1903310

Liang, N., Zhang, C., Dill, P., Panasyuk, G., Pion, D., Koka, V., … Pende, M. (2014). Regulation of YAP by mTOR and autophagy reveals a therapeutic target of tuberous sclerosis complex. *The Journal of Experimental Medicine*, *211*(11), 2249–2263. https://doi.org/10.1084/jem.20140341

Low, B. C., Pan, C. Q., Shivashankar, G. V, Bershadsky, A., Sudol, M., & Sheetz, M. (2014). YAP/TAZ as mechanosensors and mechanotransducers in regulating organ size and tumor growth. *FEBS Letters*, *588*(16), 2663–2670. https://doi.org/10.1016/j.febslet.2014.04.012

Makkar, R. R., Smith, R. R., Cheng, K., Malliaras, K., Thomson, L. E., Berman, D., … Marbán, E. (2012). Intracoronary cardiosphere-derived cells for heart regeneration after myocardial infarction (CADUCEUS): a prospective, randomised phase 1 trial. *Lancet (London, England)*, *379*(9819), 895–904. https://doi.org/10.1016/S0140-6736(12)60195-0

Malliaras, K., Makkar, R. R., Smith, R. R., Cheng, K., Wu, E., Bonow, R. O., … Marbán, E. (2014). Intracoronary cardiosphere-derived cells after myocardial infarction: evidence of therapeutic regeneration in the final 1-year results of the CADUCEUS trial (CArdiosphere-Derived aUtologous stem CElls to reverse ventricULar dySfunction). *Journal of the American College of Cardiology*, *63*(2), 110–122. https://doi.org/10.1016/j.jacc.2013.08.724

Mammoto, A., & Ingber, D. E. (2009). Cytoskeletal control of growth and cell fate switching. *Current Opinion in Cell Biology*, *21*(6), 864–870. https://doi.org/https://doi.org/10.1016/j.ceb.2009.08.001

Martino, F., Perestrelo, A. R., Vinarský, V., Pagliari, S., & Forte, G. (2018). Cellular Mechanotransduction: From Tension to Function. *Frontiers in Physiology*, *9*, 824. https://doi.org/10.3389/fphys.2018.00824

Matsui, Y., Morimoto, J., & Uede, T. (2010). Role of matricellular proteins in cardiac tissue remodeling after myocardial infarction. *World Journal of Biological Chemistry*, *1*(5), 69–80. https://doi.org/10.4331/wjbc.v1.i5.69

Maytin, M., & S. Colucci, W. (2002). Molecular and cellular mechanisms of myocardial remodeling. *Journal of Nuclear Cardiology*, *9*(3), 319–327. https://doi.org/10.1067/mnc.2002.123207

McCulloch Christopher A.and Coelho, N. M. (2015). Collagen Processing and its Role in Fibrosis. In J. T. Dixon Ian M.C.and Wigle (Ed.), *Cardiac Fibrosis and Heart Failure: Cause or Effect?* (pp. 261–278). Cham: Springer International Publishing. https://doi.org/10.1007/978-3-319-17437-2_14

Menasché, P., Alfieri, O., Janssens, S., McKenna, W., Reichenspurner, H., Trinquart, L., … Hagège, A. A. (2008). The Myoblast Autologous Grafting in Ischemic Cardiomyopathy (MAGIC) Trial. *Circulation*, *117*(9), 1189–1200. https://doi.org/10.1161/CIRCULATIONAHA.107.734103

Meng, Z., Moroishi, T., Mottier-Pavie, V., Plouffe, S. W., Hansen, C. G., Hong, A. W., … Guan, K.-L. (2015). MAP4K family kinases act in parallel to MST1/2 to activate LATS1/2 in the Hippo pathway. *Nature Communications*, *6*, 8357. https://doi.org/10.1038/ncomms9357

Min, L., & Mark, E. A. (2014). Ca2+ Cycling in Heart Failure. *Circ Res.*, *113*(6), 690–708. https://doi.org/10.1161/CIRCRESAHA.113.301651

Miralles, F., Posern, G., Zaromytidou, A.-I., & Treisman, R. (2003). Actin Dynamics Control SRF Activity by Regulation of Its Coactivator MAL. *Cell*, *113*(3), 329–342. https://doi.org/10.1016/S0092-8674(03)00278-2

Mo, J.-S., Park, H. W., & Guan, K.-L. (2014). The Hippo signaling pathway in stem cell biology and cancer. *EMBO Reports*, *15*(6), 642–656. https://doi.org/10.15252/embr.201438638

Morikawa, Y., Zhang, M., Heallen, T., Leach, J., Tao, G., Xiao, Y., … Martin, J. F. (2015). Actin cytoskeletal remodeling with protrusion formation is essential for heart regeneration in Hippo-deficient mice. *Science Signaling*, *8*(375), 1–14. https://doi.org/10.1126/scisignal.2005781

Mosterd, A., Hoes, A. W., De Bruyne, M. C., Deckers, J. W., Linker, D. T., Hofman, A., & Grobbee, D. E. (1999). Prevalence of heart failure and left ventricular dysfunction in the general population. The

Rotterdam Study. *European Heart Journal*, *20*(6), 447–455. https://doi.org/10.1053/euhj.1998.1239
Münzel, T., Gori, T., Keaney, J. F., Maack, C., & Daiber, A. (2015). Pathophysiological role of oxidative stress in systolic and diastolic heart failure and its therapeutic implications. *European Heart Journal*, *36*(38), 2555–2564. https://doi.org/10.1093/eurheartj/ehv305
Nardone, G., Oliver-De La Cruz, J., Vrbsky, J., Martini, C., Pribyl, J., Skládal, P., … Forte, G. (2017). YAP regulates cell mechanics by controlling focal adhesion assembly. *Nature Communications*, *8*(May). https://doi.org/10.1038/ncomms15321
Nguyen, N., & Sussman, M. A. (2015). Rejuvenating the senescent heart. *Current Opinion in Cardiology*, *30*(3), 235–239. https://doi.org/10.1097/HCO.0000000000000161
Nishio, K., & Inoue, A. (2005). Senescence-associated alterations of cytoskeleton: extraordinary production of vimentin that anchors cytoplasmic p53 in senescent human fibroblasts. *Histochemistry and Cell Biology*, *123*(3), 263–273. https://doi.org/10.1007/s00418-005-0766-5
Nobes, C. D., & Hall, A. (1995). Rho, Rac, and Cdc42 GTPases regulate the assembly of multimolecular focal complexes associated with actin stress fibers, lamellipodia, and filopodia. *Cell*, *81*(1), 53–62. https://doi.org/10.1016/0092-8674(95)90370-4
Nobes, C. D., & Hall, A. (1999). Rho GTPases control polarity, protrusion, and adhesion during cell movement. *The Journal of Cell Biology*, *144*(6), 1235–1244. Retrieved from https://www.ncbi.nlm.nih.gov/pubmed/10087266
Ohtani, T., Mohammed, S. F., Yamamoto, K., Dunlay, S. M., Weston, S. A., Sakata, Y., … Redfield, M. M. (2012). Diastolic stiffness as assessed by diastolic wall strain is associated with adverse remodelling and poor outcomes in heart failure with preserved ejection fraction. *European Heart Journal*, *33*(14), 1742–1749. https://doi.org/10.1093/eurheartj/ehs135
Olson, E. N., & Nordheim, A. (2010). Linking actin dynamics and gene transcription to drive cellular motile functions. *Nature Reviews. Molecular Cell Biology*, *11*(5), 353–365. https://doi.org/10.1038/nrm2890
Paluch, E. K., Nelson, C. M., Biais, N., Fabry, B., Moeller, J., Pruitt, B. L., … Federle, W. (2015). Mechanotransduction: use the force(s). *BMC Biology*, *13*, 47. https://doi.org/10.1186/s12915-015-0150-4
Panciera, T., Azzolin, L., Fujimura, A., Di Biagio, D., Frasson, C., Bresolin, S., … Piccolo, S. (2016). Induction of Expandable Tissue-Specific Stem/Progenitor Cells through Transient Expression of YAP/TAZ. *Cell Stem Cell*, *19*(6), 725–737. https://doi.org/10.1016/j.stem.2016.08.009
Parlakian, A., Tuil, D., Hamard, G., Tavernier, G., Hentzen, D., Concordet, J.-P., … Daegelen, D. (2004). Targeted inactivation of serum response factor in the developing heart results in myocardial defects and embryonic lethality. *Molecular and Cellular Biology*, *24*(12), 5281–5289. https://doi.org/10.1128/MCB.24.12.5281-5289.2004
Pasapera, A. M., Schneider, I. C., Rericha, E., Schlaepfer, D. D., & Waterman, C. M. (2010). Myosin II activity regulates vinculin recruitment to focal adhesions through FAK-mediated paxillin phosphorylation. *The Journal of Cell Biology*, *188*(6), 877. Retrieved from http://jcb.rupress.org/content/188/6/877.abstract
Pellegrini, L., Tan, S., & Richmond, T. J. (1995). Structure of serum response factor core bound to DNA. *Nature*, *376*, 490. Retrieved from http://dx.doi.org/10.1038/376490a0
Piccinni, C., Antonazzo, I. C., Simonetti, M., Mennuni, M. G., Parretti, D., Cricelli, C., … Lapi, F. (2017). The Burden of Chronic Heart Failure in Primary Care in Italy. *High Blood Pressure & Cardiovascular Prevention*, *24*(2), 171–178. https://doi.org/10.1007/s40292-017-0193-4
Piot, P., & Quinn, T. C. (2013). Response to the AIDS pandemic--a global health model. *The New England Journal of Medicine*, *368*(23), 2210–2218. https://doi.org/10.1056/NEJMra1201533
Pollard, T. D., & Borisy, G. G. (2003). Cellular Motility Driven by Assembly and Disassembly of Actin Filaments. *Cell*, *112*(4), 453–465. https://doi.org/10.1016/S0092-8674(03)00120-X
Ponikowski, P., Voors, A. A., Anker, S. D., Bueno, H., Cleland, J. G. F., Coats, A. J. S., … Van Der Meer, P. (2016). 2016 ESC Guidelines for the diagnosis and treatment of acute and chronic heart failure. *European Heart Journal*, *37*(27), 2129–2200m. https://doi.org/10.1093/eurheartj/ehw128
Provenzano, P. P., Inman, D. R., Eliceiri, K. W., & Keely, P. J. (2009). Matrix density-induced mechanoregulation of breast cell phenotype, signaling and gene expression through a FAK-ERK linkage. *Oncogene*, *28*(49), 4326–4343. https://doi.org/10.1038/onc.2009.299
Puklin-Faucher, E., & Sheetz, M. P. (2009). The mechanical integrin cycle. *Journal of Cell Science*, *122*(2),

179. Retrieved from http://jcs.biologists.org/content/122/2/179.abstract
Reddy, B. V. V. G., & Irvine, K. D. (2013). Regulation of Hippo signaling by EGFR-MAPK signaling through Ajuba family proteins. *Developmental Cell*, *24*(5), 459–471. https://doi.org/10.1016/j.devcel.2013.01.020
Redfield, M. M., Jacobsen, S. J., Burnett, Jr, J. C., Mahoney, D. W., Bailey, K. R., & Rodeheffer, R. J. (2003). Burden of systolic and diastolic ventricular dysfunction in the community: Appreciating the scope of the heart failure epidemic. *JAMA*, *289*(2), 194–202. Retrieved from http://dx.doi.org/10.1001/jama.289.2.194
Ridley, A. J. (2015). Rho GTPase signalling in cell migration. *Current Opinion in Cell Biology*, *36*, 103–112. https://doi.org/10.1016/j.ceb.2015.08.005
Riveline, D., Zamir, E., Balaban, N. Q., Schwarz, U. S., Ishizaki, T., Narumiya, S., … Bershadsky, A. D. (2001). Focal contacts as mechanosensors: externally applied local mechanical force induces growth of focal contacts by an mDia1-dependent and ROCK-independent mechanism. *The Journal of Cell Biology*, *153*(6), 1175–1186. Retrieved from https://www.ncbi.nlm.nih.gov/pubmed/11402062
Roger, V. L., Weston, S. A., Redfield, M. M., & al, et. (2004). Trends in heart failure incidence and survival in a community-based population. *JAMA*, *292*(3), 344–350. Retrieved from http://dx.doi.org/10.1001/jama.292.3.344
Rossman, K. L., Der, C. J., & Sondek, J. (2005). GEF means go: turning on RHO GTPases with guanine nucleotide-exchange factors. *Nature Reviews Molecular Cell Biology*, *6*, 167. Retrieved from http://dx.doi.org/10.1038/nrm1587
Sachot, N., & Castano, E. E. and O. (2014). Hybrid Organic-Inorganic Scaffolding Biomaterials for Regenerative Therapies. *Current Organic Chemistry*. https://doi.org/http://dx.doi.org/10.2174/1385272819666140806200355
Sadoshima, J., Jahn, L., Takahashi, T., Kulik, T. J., & Izumo, S. (1992). Molecular characterization of the stretch-induced adaptation of cultured cardiac cells. An in vitro model of load-induced cardiac hypertrophy. *Journal of Biological Chemistry*, *267*(15), 10551–10560. Retrieved from http://www.jbc.org/content/267/15/10551.abstract
Sanganalmath, S. K., & Bolli, R. (2013). Cell therapy for heart failure: a comprehensive overview of experimental and clinical studies, current challenges, and future directions. *Circulation Research*, *113*(6), 810–834. https://doi.org/10.1161/CIRCRESAHA.113.300219
Sawada, Y., Tamada, M., Dubin-Thaler, B. J., Cherniavskaya, O., Sakai, R., Tanaka, S., & Sheetz, M. P. (2006). Force Sensing by Mechanical Extension of the Src Family Kinase Substrate p130Cas. *Cell*, *127*(5), 1015–1026. https://doi.org/10.1016/j.cell.2006.09.044
Schaller, M. D., Hildebrand, J. D., Shannon, J. D., Fox, J. W., Vines, R. R., & Parsons, J. T. (1994). Autophosphorylation of the focal adhesion kinase, pp125FAK, directs SH2-dependent binding of pp60src. *Molecular and Cellular Biology*, *14*(3), 1680–1688. Retrieved from https://www.ncbi.nlm.nih.gov/pubmed/7509446
Schiller, M. R. (2006). Coupling receptor tyrosine kinases to Rho GTPases—GEFs what's the link. *Cellular Signalling*, *18*(11), 1834–1843. https://doi.org/https://doi.org/10.1016/j.cellsig.2006.01.022
Schneider, M. D. (2016). Heartbreak hotel: a convergence in cardiac regeneration. *Development*, *143*(9), 1435. Retrieved from http://dev.biologists.org/content/143/9/1435.abstract
Schwartz, M. A., & DeSimone, D. W. (2008). Cell adhesion receptors in mechanotransduction. *Current Opinion in Cell Biology*, *20*(5), 551–556. https://doi.org/10.1016/j.ceb.2008.05.005
Schwartz, M. A., & Shattil, S. J. (2000). Signaling networks linking integrins and Rho family GTPases. *Trends in Biochemical Sciences*, *25*(8), 388–391. https://doi.org/10.1016/S0968-0004(00)01605-4
Seetharaman, S., & Etienne-Manneville, S. (2018). Integrin diversity brings specificity in mechanotransduction. *Biology of the Cell*, *110*(3), 49–64. https://doi.org/10.1111/boc.201700060
Segers, V. F. M., & Lee, R. T. (2008). Stem-cell therapy for cardiac disease. *Nature*, *451*, 937. Retrieved from http://dx.doi.org/10.1038/nature06800
Seong, J., Tajik, A., Sun, J., Guan, J.-L., Humphries, M. J., Craig, S. E., … Wang, Y. (2013). Distinct biophysical mechanisms of focal adhesion kinase mechanoactivation by different extracellular matrix proteins. *Proceedings of the National Academy of Sciences of the United States of America*, *110*(48), 19372–19377. https://doi.org/10.1073/pnas.1307405110

Shaul, Y. D., & Seger, R. (2007). The MEK/ERK cascade: From signaling specificity to diverse functions. *Biochimica et Biophysica Acta (BBA) - Molecular Cell Research*, *1773*(8), 1213–1226. https://doi.org/https://doi.org/10.1016/j.bbamcr.2006.10.005

Shen, Y., & Schaller, M. D. (1999). Focal adhesion targeting: the critical determinant of FAK regulation and substrate phosphorylation. *Molecular Biology of the Cell*, *10*(8), 2507–2518. https://doi.org/10.1091/mbc.10.8.2507

Sieg, D. J., Hauck, C. R., & Schlaepfer, D. D. (1999). Required role of focal adhesion kinase (FAK) for integrin-stimulated cell migration. *Journal of Cell Science*, *112*(16), 2677. Retrieved from http://jcs.biologists.org/content/112/16/2677.abstract

Small, E. M., Thatcher, J. E., Sutherland, L. B., Kinoshita, H., Gerard, R. D., Richardson, J. A., … Olson, E. N. (2010). Myocardin-related transcription factor-a controls myofibroblast activation and fibrosis in response to myocardial infarction. *Circulation Research*, *107*(2), 294–304. https://doi.org/10.1161/CIRCRESAHA.110.223172

SMG Sutton, J., & Sharpe, N. (2009). Clinical Cardiology : New Frontiers Left Ventricular Remodeling After Myocardial Infarction Pathophysiology and Therapy, 2981–2988.

Smoot, R. L., Werneburg, N. W., Sugihara, T., Hernandez, M. C., Yang, L., Mehner, C., … Gores, G. J. (2017). Platelet-derived growth factor regulates YAP transcriptional activity via Src family kinase dependent tyrosine phosphorylation. *Journal of Cellular Biochemistry*, *119*(1), 824–836. https://doi.org/10.1002/jcb.26246

Sorrentino, G., Ruggeri, N., Specchia, V., Cordenonsi, M., Mano, M., Dupont, S., … Del Sal, G. (2014). Metabolic control of YAP and TAZ by the mevalonate pathway. *Nature Cell Biology*, *16*, 357. Retrieved from http://dx.doi.org/10.1038/ncb2936

Spirli, C., Morell, C. M., Locatelli, L., Okolicsanyi, S., Ferrero, C., Kim, A. K., … Strazzabosco, M. (2012). Cyclic AMP/PKA-dependent paradoxical activation of Raf/MEK/ERK signaling in polycystin-2 defective mice treated with sorafenib. *Hepatology (Baltimore, Md.)*, *56*(6), 2363–2374. https://doi.org/10.1002/hep.25872

Takahashi, K., & Yamanaka, S. (2006). Induction of Pluripotent Stem Cells from Mouse Embryonic and Adult Fibroblast Cultures by Defined Factors. *Cell*, *126*(4), 663–676. https://doi.org/10.1016/j.cell.2006.07.024

Tamada, M., Sheetz, M. P., & Sawada, Y. (2004). Activation of a Signaling Cascade by Cytoskeleton Stretch. *Developmental Cell*, *7*(5), 709–718. https://doi.org/10.1016/j.devcel.2004.08.021

Tamkun, J. W., DeSimone, D. W., Fonda, D., Patel, R. S., Buck, C., Horwitz, A. F., & Hynes, R. O. (1986). Structure of integrin, a glycoprotein involved in the transmembrane linkage between fibronectin and actin. *Cell*, *46*(2), 271–282. https://doi.org/10.1016/0092-8674(86)90744-0

Tan, G., Shim, W., Gu, Y., Qian, L., Ying Chung, Y., Yun Lim, S., … Wong, P. (2010). Differential effect of myocardial matrix and integrins on cardiac differentiation of human mesenchymal stem cells. *Differentiation*, *79*(4), 260–271. https://doi.org/https://doi.org/10.1016/j.diff.2010.02.005

Torre, L. A., Bray, F., Siegel, R. L., Ferlay, J., Lortet-Tieulent, J., & Jemal, A. (2015). Global cancer statistics, 2012. *CA: A Cancer Journal for Clinicians*, *65*(2), 87–108. https://doi.org/10.3322/caac.21262

Uchida, S., De Gaspari, P., Kostin, S., Jenniches, K., Kilic, A., Izumiya, Y., … Braun, T. (2013). Sca1-derived cells are a source of myocardial renewal in the murine adult heart. *Stem Cell Reports*, *1*(5), 397–410. https://doi.org/10.1016/j.stemcr.2013.09.004

van Leeuwen, F. N., Olivo, C., Grivell, S., Giepmans, B. N. G., Collard, J. G., & Moolenaar, W. H. (2003). Rac Activation by Lysophosphatidic Acid LPA1Receptors through the Guanine Nucleotide Exchange Factor Tiam1. *Journal of Biological Chemistry*, *278*(1), 400–406. Retrieved from http://www.jbc.org/content/278/1/400.abstract

Varelas, X., Miller, B. W., Sopko, R., Song, S., Gregorieff, A., Fellouse, F. A., … Attisano, L. (2010). The Hippo Pathway Regulates Wnt/β-Catenin Signaling. *Developmental Cell*, *18*(4), 579–591. https://doi.org/10.1016/j.devcel.2010.03.007

Vartiainen, M. K., Guettler, S., Larijani, B., & Treisman, R. (2007). Nuclear Actin Regulates Dynamic Subcellular Localization and Activity of the SRF Cofactor MAL. *Science*, *316*(5832), 1749. Retrieved from http://science.sciencemag.org/content/316/5832/1749.abstract

Wada, K.-I., Itoga, K., Okano, T., Yonemura, S., & Sasaki, H. (2011). Hippo pathway regulation by cell

morphology and stress fibers. *Development*, *138*(18), 3907. Retrieved from http://dev.biologists.org/content/138/18/3907.abstract

Wang, D.-Z., Li, S., Hockemeyer, D., Sutherland, L., Wang, Z., Schratt, G., … Olson, E. N. (2002). Potentiation of serum response factor activity by a family of myocardin-related transcription factors. *Proceedings of the National Academy of Sciences of the United States of America*, *99*(23), 14855–14860. https://doi.org/10.1073/pnas.222561499

Wang, N. (2017). Review of cellular mechanotransduction. *Journal of Physics D: Applied Physics*, *50*(23), 233002. Retrieved from http://stacks.iop.org/0022-3727/50/i=23/a=233002

Wang, N., Butler, J. P., & Ingber, D. E. (1993). Mechanotransduction across the cell surface and through the cytoskeleton. *Science*, *260*(5111), 1124. Retrieved from http://science.sciencemag.org/content/260/5111/1124.abstract

Wang, N., & Ingber, D. E. (1994). Control of cytoskeletal mechanics by extracellular matrix, cell shape, and mechanical tension. *Biophysical Journal*, *66*(6), 2181–2189. https://doi.org/10.1016/S0006-3495(94)81014-8

Watanabe, N., Madaule, P., Reid, T., Ishizaki, T., Watanabe, G., Kakizuka, A., … Narumiya, S. (1997). p140mDia, a mammalian homolog of Drosophila diaphanous, is a target protein for Rho small GTPase and is a ligand for profilin. *The EMBO Journal*, *16*(11), 3044–3056. https://doi.org/10.1093/emboj/16.11.3044

Watkins, S. J., Borthwick, G. M., Oakenfull, R., Robson, A., & Arthur, H. M. (2011). Angiotensin II-induced cardiomyocyte hypertrophy in vitro is TAK1-dependent and Smad2/3-independent. *Hypertension Research*, *35*, 393. Retrieved from http://dx.doi.org/10.1038/hr.2011.196

Weber, K. T., Pick, R., Jalil, J. E., Janicki, J. S., & Carroll, E. P. (1989). Patterns of myocardial fibrosis. *Journal of Molecular and Cellular Cardiology*, *21*, 121–131. https://doi.org/https://doi.org/10.1016/0022-2828(89)90778-5

Williams, C., Budina, E., Stoppel, W. L., Sullivan, K. E., Emani, S., Emani, S. M., & Black 3rd, L. D. (2015). Cardiac extracellular matrix-fibrin hybrid scaffolds with tunable properties for cardiovascular tissue engineering. *Acta Biomaterialia*, *14*, 84–95. https://doi.org/10.1016/j.actbio.2014.11.035

Winograd-Katz, S. E., Fässler, R., Geiger, B., & Legate, K. R. (2014). The integrin adhesome: from genes and proteins to human disease. *Nature Reviews Molecular Cell Biology*, *15*, 273. Retrieved from http://dx.doi.org/10.1038/nrm3769

Witman, N., & Sahara, M. (2018). Cardiac Progenitor Cells in Basic Biology and Regenerative Medicine. *Stem Cells International*. https://doi.org/10.1155/2018/8283648

Wozniak, M. A., & Chen, C. S. (2009). Mechanotransduction in development: a growing role for contractility. *Nature Reviews. Molecular Cell Biology*, *10*(1), 34–43. https://doi.org/10.1038/nrm2592

Wu, J. M. F., Hsueh, Y.-C., Ch'ang, H.-J., Luo, C.-Y., Wu, L.-W., Nakauchi, H., & Hsieh, P. C. H. (2015). Circulating Cells Contribute to Cardiomyocyte Regeneration After Injury. *Circulation Research*, *116*(4), 633–641. https://doi.org/10.1161/CIRCRESAHA.116.304564

Xin, M., Kim, Y., Sutherland, L. B., Murakami, M., Qi, X., McAnally, J., … Olson, E. N. (2013). Hippo pathway effector Yap promotes cardiac regeneration. *Proceedings of the National Academy of Sciences*, *110*(34), 13839–13844. https://doi.org/10.1073/pnas.1313192110

Yamashita, H., Ichikawa, T., Matsuyama, D., Kimura, Y., Ueda, K., Craig, S. W., … Kioka, N. (2014). The role of the interaction of the vinculin proline-rich linker region with vinexin α in sensing the stiffness of the extracellular matrix. *Journal of Cell Science*, *127*(9), 1875. Retrieved from http://jcs.biologists.org/content/127/9/1875.abstract

Yancy, C. W., Jessup, M., Bozkurt, B., Butler, J., Casey, D. E., Drazner, M. H., … Wilkoff, B. L. (2013). 2013 ACCF/AHA Guideline for the Management of Heart Failure. *Circulation*, *128*(16). https://doi.org/10.1161/CIR.0b013e31829e8776

Young, J. L., & Engler, A. J. (2011). Hydrogels with time-dependent material properties enhance cardiomyocyte differentiation in vitro. *Biomaterials*, *32*(4), 1002–1009. https://doi.org/10.1016/j.biomaterials.2010.10.020

Yu, F.-X., & Guan, K.-L. (2013). The Hippo pathway: regulators and regulations. *Genes & Development*, *27*(4), 355–371. https://doi.org/10.1101/gad.210773.112

Yu, F.-X., Zhao, B., Panupinthu, N., Jewell, J. L., Lian, I., Wang, L. H., … Guan, K.-L. (2012). Regulation of the

Hippo-YAP pathway by G-protein-coupled receptor signaling. *Cell*, *150*(4), 780–791. https://doi.org/10.1016/j.cell.2012.06.037

Zhang, G.-W., Gu, T.-X., Sun, X.-J., Wang, C., Qi, X., Wang, X.-B., & Li-Ling, J. (2016). Edaravone promotes activation of resident cardiac stem cells by transplanted mesenchymal stem cells in a rat myocardial infarction model. *The Journal of Thoracic and Cardiovascular Surgery*, *152*(2), 570–582. https://doi.org/https://doi.org/10.1016/j.jtcvs.2016.02.071

Zhao, B., Lei, Q.-Y., & Guan, K.-L. (2008). The Hippo-YAP pathway: new connections between regulation of organ size and cancer. *Current Opinion in Cell Biology*, *20*(6), 638–646. https://doi.org/10.1016/j.ceb.2008.10.001

Zhao, B., Li, L., Tumaneng, K., Wang, C.-Y., & Guan, K.-L. (2010). A coordinated phosphorylation by Lats and CK1 regulates YAP stability through SCF(beta-TRCP). *Genes & Development*, *24*(1), 72–85. https://doi.org/10.1101/gad.1843810

Zhao, B., Li, L., Wang, L., Wang, C.-Y., Yu, J., & Guan, K.-L. (2012). Cell detachment activates the Hippo pathway via cytoskeleton reorganization to induce anoikis. *Genes & Development*, *26*(1), 54–68. https://doi.org/10.1101/gad.173435.111

Zhao, B., Wei, X., Li, W., Udan, R. S., Yang, Q., Kim, J., … Guan, K.-L. (2007). Inactivation of YAP oncoprotein by the Hippo pathway is involved in cell contact inhibition and tissue growth control. *Genes & Development*, *21*(21), 2747–2761. https://doi.org/10.1101/gad.1602907

Zhao, B., Ye, X., Yu, J., Li, L., Li, W., Li, S., … Guan, K.-L. (2008). TEAD mediates YAP-dependent gene induction and growth control. *Genes & Development*, *22*(14), 1962–1971. https://doi.org/10.1101/gad.1664408

Zhelev, D. V, & Hochmuth, R. M. (1995). Mechanically stimulated cytoskeleton rearrangement and cortical contraction in human neutrophils. *Biophysical Journal*, *68*(5), 2004–2014. https://doi.org/10.1016/S0006-3495(95)80377-2

Zheng, Y., Xia, Y., Hawke, D., Halle, M., Tremblay, M. L., Gao, X., … Lu, Z. (2009). FAK phosphorylation by ERK primes ras-induced tyrosine dephosphorylation of FAK mediated by PIN1 and PTP-PEST. *Molecular Cell*, *35*(1), 11–25. https://doi.org/10.1016/j.molcel.2009.06.013

Zhu, C., Li, L., & Zhao, B. (2014). The regulation and function of YAP transcription co-activator. *Acta Biochimica et Biophysica Sinica*, *47*(1), 16–28. https://doi.org/10.1093/abbs/gmu110

SUPPLEMENTARY CONTENTS

Table S.1 List of ontologys enriched in genes down-regulated in ischemic CPC

GO biological process complete	#	expected	Fold	raw P value	FDR
cellular response to chemical stimulus	114	56.02	2.03	1.55E-13	2.43E-09
cellular process	373	308.64	1.21	3.33E-13	2.62E-09
response to organic substance	112	58.17	1.93	9.33E-12	4.90E-08
Unclassified	23	68.29	.34	2.95E-11	9.28E-08
biological process	408	362.71	1.12	2.95E-11	1.16E-07
response to chemical	147	87.75	1.68	5.17E-11	1.36E-07
cellular response to organic substance	92	45.59	2.02	1.64E-10	3.68E-07
cellular metabolic process	248	183.75	1.35	8.54E-10	1.68E-06
regulation of cell adhesion	38	13.42	2.83	2.42E-08	3.81E-05
cellular response to stimulus	186	130.37	1.43	2.37E-08	4.14E-05
positive regulation of biological process	174	121.09	1.44	7.50E-08	9.08E-05
organonitrogen compound metabolic process	165	113.02	1.46	7.24E-08	9.49E-05
cellular component organization or biogenesis	168	115.73	1.45	6.72E-08	9.61E-05
biological regulation	303	248.07	1.22	8.85E-08	9.95E-05
cellular component organization	163	112.14	1.45	1.25E-07	1.15E-04
negative regulation of biological process	154	104.13	1.48	1.14E-07	1.20E-04
metabolic process	258	202.47	1.27	1.24E-07	1.22E-04
positive regulation of cellular protein metabolic process	64	31.87	2.01	1.66E-07	1.45E-04
regulation of cellular protein metabolic process	90	51.60	1.74	2.10E-07	1.57E-04
positive regulation of cellular process	156	106.86	1.46	2.01E-07	1.58E-04
localization	164	113.76	1.44	1.93E-07	1.60E-04
regulation of biological process	288	234.36	1.23	2.52E-07	1.81E-04
response to stimulus	222	169.07	1.31	3.44E-07	2.35E-04
positive regulation of protein metabolic process	66	33.98	1.94	3.65E-07	2.39E-04
regulation of biological quality	122	78.47	1.55	4.21E-07	2.65E-04
positive regulation of macromolecule metabolic process	107	66.28	1.61	5.50E-07	3.21E-04
organic substance metabolic process	246	193.13	1.27	5.43E-07	3.29E-04
regulation of protein metabolic process	95	56.80	1.67	6.33E-07	3.56E-04
positive regulation of nitrogen compound metabolic process	103	63.39	1.62	6.98E-07	3.79E-04
system development	131	87.46	1.50	9.12E-07	4.63E-04
regulation of cell proliferation	63	32.59	1.93	9.08E-07	4.76E-04
positive regulation of cellular metabolic process	105	65.63	1.60	1.02E-06	5.00E-04
positive regulation of metabolic process	111	71.36	1.56	1.68E-06	8.03E-04
cellular protein metabolic process	115	74.99	1.53	1.96E-06	8.82E-04
regulation of metabolic process	185	137.34	1.35	1.94E-06	8.96E-04
response to stress	108	69.27	1.56	2.41E-06	1.05E-03
transport	132	90.10	1.46	2.91E-06	1.21E-03
response to oxygen-containing compound	58	30.23	1.92	2.85E-06	1.21E-03
regulation of cellular process	269	220.25	1.22	3.46E-06	1.30E-03
regulation of signaling	110	71.65	1.54	3.40E-06	1.30E-03
anatomical structure development	150	106.43	1.41	3.58E-06	1.31E-03
regulation of macromolecule metabolic process	173	127.26	1.36	3.36E-06	1.32E-03

establishment of localization	134	92.44	1.45	3.70E-06	1.32E-03
negative regulation of cellular process	135	93.09	1.45	3.80E-06	1.33E-03
regulation of cell migration	38	16.39	2.32	3.31E-06	1.34E-03
regulation of cell communication	109	70.97	1.54	4.18E-06	1.40E-03
response to endogenous stimulus	56	28.86	1.94	4.10E-06	1.40E-03
enzyme linked receptor protein signaling pathway	34	14.05	2.42	4.32E-06	1.42E-03
regulation of multicellular organismal process	96	60.16	1.60	4.74E-06	1.52E-03
positive regulation of cell adhesion	24	8.13	2.95	5.12E-06	1.61E-03
regulation of cellular metabolic process	171	126.48	1.35	6.85E-06	2.11E-03
developmental process	156	113.04	1.38	7.17E-06	2.17E-03
multicellular organism development	140	99.10	1.41	8.31E-06	2.42E-03
regulation of response to stimulus	125	85.62	1.46	8.17E-06	2.43E-03
primary metabolic process	233	186.27	1.25	9.29E-06	2.66E-03
cellular response to endogenous stimulus	47	23.43	2.01	9.67E-06	2.72E-03
nitrogen compound metabolic process	223	176.60	1.26	1.01E-05	2.79E-03
cellular catabolic process	63	35.19	1.79	1.23E-05	3.33E-03
regulation of cell motility	38	17.53	2.17	1.39E-05	3.72E-03
regulation of developmental process	82	50.51	1.62	1.54E-05	3.97E-03
transmembrane receptor protein tyrosine kinase signaling pathway	26	9.93	2.62	1.57E-05	3.98E-03
cellular localization	79	48.30	1.64	1.53E-05	4.02E-03
positive regulation of proteolysis	21	7.09	2.96	1.88E-05	4.70E-03
regulation of cellular component movement	40	19.19	2.08	1.96E-05	4.82E-03
regulation of protein catabolic process	22	7.72	2.85	2.11E-05	5.12E-03
positive regulation of cell migration	25	9.61	2.60	2.49E-05	5.95E-03
catabolic process	68	40.04	1.70	2.62E-05	6.15E-03
regulation of signal transduction	97	63.82	1.52	2.84E-05	6.58E-03
extracellular structure organization	21	7.35	2.86	3.14E-05	7.17E-03
regulation of nitrogen compound metabolic process	162	122.16	1.33	4.03E-05	9.06E-03
organelle organization	100	67.27	1.49	4.33E-05	9.59E-03
sensory perception of chemical stimulus	0	10.65	< 0.01	4.43E-05	9.68E-03
regulation of locomotion	39	19.09	2.04	4.97E-05	9.77E-03
cellular macromolecule metabolic process	174	133.40	1.30	4.92E-05	9.81E-03
cellular response to cytokine stimulus	39	19.07	2.05	4.92E-05	9.93E-03
negative regulation of cell proliferation	31	13.87	2.24	5.26E-05	9.97E-03
positive regulation of molecular function	61	35.54	1.72	4.63E-05	9.98E-03
positive regulation of cellular protein catabolic process	12	2.83	4.25	5.22E-05	1.00E-02
positive regulation of phosphate metabolic process	44	22.67	1.94	4.91E-05	1.00E-02
cholesterol homeostasis	9	1.54	5.86	4.73E-05	1.01E-02
sterol homeostasis	9	1.56	5.78	5.20E-05	1.01E-02
positive regulation of phosphorus metabolic process	44	22.67	1.94	4.91E-05	1.02E-02
monocarboxylic acid transport	12	2.81	4.28	4.89E-05	1.03E-02
cell surface receptor signaling pathway	77	48.34	1.59	5.87E-05	1.10E-02
protein metabolic process	126	90.41	1.39	6.17E-05	1.12E-02
regulation of cellular protein catabolic process	16	4.90	3.27	6.27E-05	1.12E-02
positive regulation of locomotion	26	10.65	2.44	6.15E-05	1.13E-02
vesicle-mediated transport	65	38.75	1.68	6.09E-05	1.13E-02
detection of chemical stimulus	0	10.22	< 0.01	6.52E-05	1.15E-02
positive regulation of protein modification process	46	24.66	1.87	6.75E-05	1.18E-02
regulation of cell death	59	34.21	1.72	7.07E-05	1.22E-02
positive regulation of cell motility	25	9.98	2.51	7.21E-05	1.23E-02

positive regulation of cell-substrate adhesion	11	2.48	4.44	7.37E-05	1.23E-02
regulation of cell-cell adhesion	21	7.82	2.68	7.31E-05	1.24E-02
tube development	35	16.69	2.10	7.83E-05	1.30E-02
regulation of phosphorus metabolic process	59	34.74	1.70	8.35E-05	1.34E-02
regulation of phosphate metabolic process	59	34.70	1.70	8.21E-05	1.35E-02
positive regulation of protein catabolic process	15	4.49	3.34	8.32E-05	1.35E-02
positive regulation of catalytic activity	51	28.57	1.78	8.73E-05	1.39E-02
regulation of primary metabolic process	164	125.48	1.31	9.03E-05	1.39E-02
positive regulation of cellular component movement	25	10.26	2.44	8.95E-05	1.39E-02
positive regulation of proteasomal ubiquitin-dependent protein catabolic process	9	1.68	5.36	8.91E-05	1.40E-02
response to external stimulus	67	40.97	1.64	9.29E-05	1.42E-02
positive regulation of proteasomal protein catabolic process	10	2.11	4.74	9.43E-05	1.43E-02
regulation of phosphorylation	54	30.77	1.76	1.01E-04	1.51E-02
regulation of T cell activation	18	6.25	2.88	1.03E-04	1.53E-02
regulation of catalytic activity	73	45.96	1.59	1.09E-04	1.60E-02
response to cytokine	40	20.79	1.92	1.10E-04	1.61E-02
negative regulation of cell death	40	20.81	1.92	1.12E-04	1.61E-02
regulation of cell-substrate adhesion	14	4.14	3.38	1.27E-04	1.81E-02
positive regulation of response to stimulus	74	47.36	1.56	1.37E-04	1.91E-02
regulation of cellular catabolic process	32	15.36	2.08	1.36E-04	1.91E-02
positive regulation of cellular catabolic process	19	6.98	2.72	1.36E-04	1.92E-02
cytokine-mediated signaling pathway	28	12.68	2.21	1.53E-04	1.98E-02
positive regulation of signal transduction	55	32.36	1.70	1.52E-04	1.99E-02
organonitrogen compound biosynthetic process	51	29.09	1.75	1.47E-04	1.99E-02
protein localization to endoplasmic reticulum	11	2.70	4.07	1.51E-04	2.00E-02
regulation of body fluid levels	24	10.02	2.40	1.49E-04	2.00E-02
regulation of substrate adhesion-dependent cell spreading	7	1.04	6.70	1.55E-04	2.01E-02
extracellular matrix organization	18	6.45	2.79	1.51E-04	2.01E-02
regulation of leukocyte cell-cell adhesion	17	5.86	2.90	1.47E-04	2.01E-02
organic substance catabolic process	58	34.45	1.68	1.58E-04	2.02E-02
detection of chemical stimulus involved in sensory perception	0	9.52	< 0.01	1.47E-04	2.02E-02
regulation of molecular function	94	64.50	1.46	1.76E-04	2.23E-02
positive regulation of substrate adhesion-dependent cell spreading	6	.74	8.14	1.80E-04	2.26E-02
regulation of proteolysis	33	16.18	2.04	1.82E-04	2.27E-02
regulation of programmed cell death	54	31.73	1.70	1.87E-04	2.31E-02
positive regulation of phosphorylation	40	21.22	1.88	1.91E-04	2.35E-02
animal organ development	92	63.15	1.46	2.05E-04	2.50E-02
regulation of catabolic process	35	17.74	1.97	2.16E-04	2.61E-02
sensory perception of smell	0	9.18	< 0.01	2.20E-04	2.65E-02
response to wounding	26	11.47	2.27	2.29E-04	2.73E-02
regulation of immune system process	53	31.36	1.69	2.51E-04	2.84E-02
response to vitamin E	4	.25	16.27	2.41E-04	2.85E-02
symbiont process	29	13.60	2.13	2.50E-04	2.85E-02
positive regulation of ubiquitin-dependent protein catabolic process	9	1.95	4.63	2.48E-04	2.85E-02
protein modification process	91	62.49	1.46	2.48E-04	2.87E-02
cellular protein modification process	91	62.49	1.46	2.48E-04	2.89E-02
biosynthetic process	131	97.56	1.34	2.46E-04	2.89E-02
multicellular organismal process	174	137.60	1.26	2.58E-04	2.90E-02
positive regulation of proteolysis involved in cellular protein catabolic process	10	2.42	4.14	2.64E-04	2.93E-02
secretion	41	22.22	1.84	2.63E-04	2.93E-02

protein modification by small protein conjugation or removal	37	19.48	1.90	2.71E-04	2.94E-02
regulation of multicellular organismal development	63	39.29	1.60	2.71E-04	2.96E-02
positive regulation of cell communication	58	35.35	1.64	2.70E-04	2.97E-02
intracellular transport	53	31.63	1.68	2.77E-04	2.99E-02
positive regulation of signaling	58	35.52	1.63	2.84E-04	3.04E-02
positive regulation of cell-cell adhesion	15	5.08	2.95	2.99E-04	3.16E-02
anatomical structure morphogenesis	66	41.93	1.57	2.98E-04	3.17E-02
cellular protein localization	52	30.64	1.70	3.08E-04	3.23E-02
detection of chemical stimulus involved in sensory perception of smell	0	8.54	< 0.01	3.14E-04	3.27E-02
cellular macromolecule localization	52	30.83	1.69	3.21E-04	3.33E-02
regulation of cytokine production	28	13.05	2.15	3.30E-04	3.39E-02
lipid homeostasis	10	2.50	4.00	3.38E-04	3.41E-02
translational initiation	11	2.99	3.68	3.41E-04	3.42E-02
negative regulation of cellular component organization	29	14.03	2.07	3.37E-04	3.42E-02
cellular response to growth factor stimulus	23	10.04	2.29	3.37E-04	3.44E-02
viral process	26	12.06	2.16	3.64E-04	3.62E-02
xenobiotic metabolic process	10	2.54	3.94	3.82E-04	3.78E-02
regulation of proteasomal protein catabolic process	12	3.58	3.35	4.15E-04	4.09E-02
cellular response to oxygen-containing compound	37	19.66	1.88	4.35E-04	4.25E-02
organic substance biosynthetic process	128	96.35	1.33	4.58E-04	4.45E-02
protein modification by small protein removal	16	5.90	2.71	4.64E-04	4.48E-02
blood coagulation	16	5.92	2.70	4.81E-04	4.50E-02
regulation of T cell cytokine production	5	.57	8.72	4.75E-04	4.50E-02
response to growth factor	24	10.67	2.25	4.71E-04	4.52E-02
cell communication	140	107.25	1.31	4.80E-04	4.53E-02
macromolecule metabolic process	194	158.00	1.23	4.87E-04	4.53E-02
response to increased oxygen levels	5	.57	8.72	4.75E-04	4.53E-02
cellular response to xenobiotic stimulus	12	3.67	3.27	5.02E-04	4.65E-02
regulation of proteolysis involved in cellular protein catabolic process	13	4.22	3.08	5.11E-04	4.70E-02
regulation of apoptotic process	52	31.42	1.65	5.18E-04	4.71E-02
macromolecule localization	73	48.46	1.51	5.21E-04	4.71E-02
coagulation	16	5.96	2.68	5.16E-04	4.72E-02
nervous system development	70	46.11	1.52	5.28E-04	4.75E-02
regulation of localization	79	53.81	1.47	5.45E-04	4.85E-02
negative regulation of response to stimulus	52	31.61	1.65	5.43E-04	4.86E-02
response to interferon-gamma	12	3.71	3.24	5.51E-04	4.87E-02
regulation of cell morphogenesis	22	9.77	2.25	5.57E-04	4.90E-02
positive regulation of protein phosphorylation	37	20.28	1.82	5.64E-04	4.93E-02
hemostasis	16	6.02	2.66	5.73E-04	4.96E-02
blood vessel development	22	9.79	2.25	5.71E-04	4.96E-02

GO molecular function complete	#	expected	Fold	raw P value	FDR
protein binding	327	240.94	1.36	1.87E-17	8.71E-14
binding	379	308.62	1.23	1.05E-15	2.45E-12
molecular function	406	359.33	1.13	2.72E-11	3.17E-08
Unclassified	25	71.67	.35	2.72E-11	4.22E-08
structural molecule activity	42	16.69	2.52	1.21E-07	1.13E-04
signaling receptor binding	61	34.31	1.78	1.58E-05	1.05E-02
catalytic activity	165	122.82	1.34	1.57E-05	1.22E-02

extracellular matrix structural constituent	12	2.85	4.21	5.57E-05	3.24E-02
ion binding	167	127.87	1.31	7.90E-05	4.09E-02

GO cellular component complete	#	expected	Fold	raw P value	FDR
cytoplasmic part	296	197.56	1.50	4.14E-21	4.20E-18
intracellular part	380	295.42	1.29	4.08E-21	8.27E-18
cytoplasm	330	235.55	1.40	1.42E-20	9.57E-18
membrane-bounded organelle	344	253.29	1.36	5.36E-20	2.72E-17
intracellular	381	301.10	1.27	1.62E-19	6.55E-17
organelle	359	275.58	1.30	1.85E-18	6.25E-16
intracellular organelle	336	258.66	1.30	6.25E-15	1.81E-12
intracellular membrane-bounded organelle	300	222.24	1.35	5.41E-14	1.37E-11
organelle part	271	194.20	1.40	2.04E-13	4.60E-11
intracellular organelle part	265	188.18	1.41	2.37E-13	4.82E-11
vesicle	141	77.51	1.82	3.42E-13	6.30E-11
cell	402	348.86	1.15	6.30E-13	1.07E-10
cytosol	171	103.91	1.65	1.80E-12	2.60E-10
cell part	401	348.31	1.15	1.73E-12	2.69E-10
Unclassified	10	47.44	.21	2.07E-11	2.62E-09
cellular component	421	383.56	1.10	2.07E-11	2.79E-09
endomembrane system	151	90.78	1.66	4.00E-11	4.77E-09
endoplasmic reticulum	82	38.67	2.12	1.83E-10	2.06E-08
extracellular space	120	67.70	1.77	2.59E-10	2.76E-08
extracellular region part	124	71.53	1.73	4.35E-10	4.41E-08
extracellular organelle	87	43.36	2.01	5.81E-10	5.36E-08
extracellular vesicle	87	43.32	2.01	5.64E-10	5.45E-08
extracellular exosome	85	42.91	1.98	2.16E-09	1.91E-07
membrane-enclosed lumen	162	107.00	1.51	7.92E-09	6.18E-07
intracellular organelle lumen	162	107.00	1.51	7.92E-09	6.42E-07
organelle lumen	162	107.00	1.51	7.92E-09	6.69E-07
extracellular region	137	88.12	1.55	5.03E-08	3.78E-06
intracellular vesicle	86	46.97	1.83	5.98E-08	4.18E-06
cytoplasmic vesicle	86	46.91	1.83	5.85E-08	4.24E-06
endoplasmic reticulum part	57	27.45	2.08	3.10E-07	2.10E-05
cell-substrate adherens junction	26	8.34	3.12	7.89E-07	5.16E-05
protein-containing complex	157	110.34	1.42	8.92E-07	5.65E-05
cell-substrate junction	26	8.42	3.09	9.38E-07	5.76E-05
focal adhesion	25	8.28	3.02	2.21E-06	1.32E-04
adherens junction	29	11.02	2.63	4.58E-06	2.66E-04
anchoring junction	29	11.35	2.56	7.80E-06	4.40E-04
cell cortex	20	6.29	3.18	1.14E-05	6.23E-04
endoplasmic reticulum membrane	43	21.75	1.98	3.52E-05	1.88E-03
endoplasmic reticulum subcompartment	43	21.86	1.97	3.75E-05	1.95E-03
collagen-containing extracellular matrix	17	5.28	3.22	4.49E-05	2.28E-03
nuclear outer membrane-endoplasmic reticulum membrane network	43	22.22	1.93	6.67E-05	3.30E-03
nucleus	189	149.48	1.26	1.01E-04	4.87E-03
nuclear lumen	117	83.82	1.40	1.36E-04	6.42E-03
organelle subcompartment	58	34.58	1.68	1.62E-04	7.45E-03
nucleoplasm	102	71.40	1.43	1.89E-04	8.52E-03

nuclear part	125	91.97	1.36	2.28E-04	1.01E-02
extracellular matrix	22	8.87	2.48	2.36E-04	1.02E-02
non-membrane-bounded organelle	118	86.09	1.37	2.59E-04	1.07E-02
intracellular non-membrane-bounded organelle	118	85.95	1.37	2.55E-04	1.08E-02
Golgi apparatus	53	31.61	1.68	2.75E-04	1.11E-02
cytoplasmic vesicle lumen	18	6.88	2.62	3.18E-04	1.26E-02
vesicle lumen	18	6.90	2.61	3.29E-04	1.28E-02
cell junction	46	26.14	1.76	3.42E-04	1.31E-02
transferase complex	33	16.63	1.98	3.64E-04	1.37E-02
nuclear stress granule	3	.10	29.29	4.17E-04	1.54E-02
endosome	35	18.31	1.91	4.29E-04	1.55E-02
pigment granule	9	2.15	4.18	4.92E-04	1.72E-02
secretory granule lumen	17	6.55	2.59	5.06E-04	1.74E-02
melanosome	9	2.15	4.18	4.92E-04	1.75E-02
vacuole	31	15.81	1.96	6.99E-04	2.36E-02
catalytic complex	48	28.92	1.66	9.18E-04	3.05E-02
endosome lumen	5	.70	7.18	1.04E-03	3.42E-02
vacuolar lumen	11	3.48	3.16	1.12E-03	3.43E-02
ubiquitin ligase complex	15	5.80	2.59	1.09E-03	3.44E-02
secretory granule	32	17.10	1.87	1.11E-03	3.46E-02
cytoplasmic region	22	10.08	2.18	1.08E-03	3.48E-02
fibrinogen complex	3	.18	16.27	1.54E-03	4.67E-02

Table S.2 List of ontologys enriched in genes up-regulated in ischemic CPC

GO biological process complete	#	expected	Fold	raw P value	FDR
cellular component organization or biogenesis	166	102.30	1.62	3.93E-12	3.09E-08
cellular component organization	163	99.13	1.64	2.37E-12	3.73E-08
cellular process	329	272.83	1.21	1.56E-11	8.20E-08
negative regulation of biological process	149	92.05	1.62	1.71E-10	6.72E-07
biological process	361	320.63	1.13	3.42E-10	8.98E-07
Unclassified	20	60.37	.33	3.42E-10	1.08E-06
regulation of cell proliferation	65	28.81	2.26	1.36E-09	3.06E-06
response to stress	106	61.24	1.73	9.84E-09	1.55E-05
multicellular organism development	138	87.60	1.58	9.17E-09	1.60E-05
system development	126	77.32	1.63	8.69E-09	1.71E-05
anatomical structure development	144	94.08	1.53	2.13E-08	3.05E-05
localization	151	100.56	1.50	3.02E-08	3.96E-05
positive regulation of apoptotic process	33	11.05	2.99	5.74E-08	6.02E-05
negative regulation of macromolecule metabolic process	84	45.88	1.83	5.55E-08	6.24E-05
negative regulation of cell proliferation	35	12.26	2.86	6.44E-08	6.33E-05
positive regulation of programmed cell death	33	11.15	2.96	7.13E-08	6.60E-05
regulation of smooth muscle cell proliferation	15	2.37	6.32	5.49E-08	6.64E-05
organelle organization	101	59.46	1.70	7.76E-08	6.78E-05
negative regulation of cellular process	128	82.29	1.56	8.52E-08	7.05E-05
developmental process	148	99.93	1.48	1.09E-07	8.58E-05
positive regulation of cell death	34	12.10	2.81	1.42E-07	1.07E-04
platelet degranulation	14	2.32	6.04	2.55E-07	1.83E-04
negative regulation of metabolic process	87	50.25	1.73	3.98E-07	2.72E-04

establishment of localization	125	81.72	1.53	4.22E-07	2.77E-04
mRNA metabolic process	33	12.15	2.72	4.58E-07	2.88E-04
animal organ development	93	55.82	1.67	6.29E-07	3.67E-04
positive regulation of cell adhesion	24	7.19	3.34	6.22E-07	3.77E-04
positive regulation of smooth muscle cell proliferation	11	1.52	7.23	1.00E-06	5.62E-04
secretion	44	19.65	2.24	1.15E-06	6.23E-04
biological adhesion	39	16.51	2.36	1.67E-06	8.77E-04
transport	120	79.65	1.51	1.73E-06	8.79E-04
cell adhesion	38	16.40	2.32	3.08E-06	1.52E-03
RNA splicing, via transesterification reactions	19	5.29	3.59	3.44E-06	1.64E-03
exocytosis	34	14.07	2.42	4.04E-06	1.82E-03
positive regulation of cell proliferation	38	16.69	2.28	4.16E-06	1.82E-03
multicellular organismal process	165	121.64	1.36	4.02E-06	1.86E-03
response to lipid	36	15.30	2.35	5.08E-06	2.16E-03
secretion by cell	39	17.56	2.22	6.63E-06	2.75E-03
positive regulation of protein modification process	45	21.80	2.06	6.96E-06	2.81E-03
regulation of cell adhesion	30	11.86	2.53	9.77E-06	3.50E-03
regulation of molecular function	90	57.02	1.58	9.68E-06	3.54E-03
positive regulation of cell migration	24	8.49	2.83	9.46E-06	3.54E-03
positive regulation of phosphate metabolic process	42	20.04	2.10	9.37E-06	3.60E-03
positive regulation of phosphorus metabolic process	42	20.04	2.10	9.37E-06	3.69E-03
RNA splicing, via transesterification reactions with bulged adenosine as nucleophile	18	5.23	3.44	1.09E-05	3.74E-03
mRNA splicing, via spliceosome	18	5.23	3.44	1.09E-05	3.82E-03
positive regulation of cellular process	133	94.46	1.41	1.22E-05	4.07E-03
negative regulation of nitrogen compound metabolic process	70	41.28	1.70	1.44E-05	4.72E-03
RNA splicing	21	7.01	3.00	1.50E-05	4.74E-03
female pregnancy	14	3.37	4.16	1.48E-05	4.76E-03
negative regulation of gene expression	56	30.44	1.84	1.58E-05	4.86E-03
positive regulation of cell motility	24	8.82	2.72	1.71E-05	5.16E-03
embryo implantation	7	.72	9.66	1.82E-05	5.19E-03
regulation of apoptotic process	52	27.78	1.87	1.76E-05	5.22E-03
regulation of catalytic activity	69	40.63	1.70	1.79E-05	5.23E-03
response to wounding	26	10.14	2.56	2.04E-05	5.73E-03
regulation of cell death	55	30.24	1.82	2.34E-05	6.47E-03
positive regulation of phosphorylation	39	18.76	2.08	2.48E-05	6.73E-03
angiogenesis	18	5.61	3.21	2.65E-05	6.83E-03
positive regulation of protein phosphorylation	38	17.93	2.12	2.65E-05	6.94E-03
positive regulation of cellular component movement	24	9.07	2.65	2.64E-05	7.04E-03
regulation of programmed cell death	52	28.05	1.85	2.86E-05	7.14E-03
wound healing	23	8.51	2.70	2.84E-05	7.20E-03
response to stimulus	190	149.45	1.27	3.48E-05	8.55E-03
positive regulation of protein metabolic process	54	30.04	1.80	3.55E-05	8.58E-03
regulation of cell motility	34	15.50	2.19	3.87E-05	9.23E-03
positive regulation of protein kinase activity	24	9.32	2.57	4.01E-05	9.42E-03
regulated exocytosis	29	12.51	2.32	4.23E-05	9.51E-03
regulation of cell migration	32	14.49	2.21	4.33E-05	9.60E-03
biological regulation	259	219.29	1.18	4.22E-05	9.64E-03
response to organic substance	81	51.42	1.58	4.18E-05	9.68E-03
response to hypoxia	17	5.34	3.18	4.83E-05	1.00E-02
taxis	24	9.43	2.54	4.78E-05	1.00E-02

protein metabolic process	114	79.92	1.43	4.72E-05	1.00E-02
immune system process	76	47.66	1.59	4.68E-05	1.01E-02
positive regulation of locomotion	24	9.42	2.55	4.64E-05	1.01E-02
regulation of apoptotic signaling pathway	20	7.06	2.83	5.10E-05	1.04E-02
response to heat	10	1.97	5.07	5.36E-05	1.05E-02
negative regulation of cellular metabolic process	72	44.33	1.62	5.25E-05	1.06E-02
response to oxygen levels	18	5.94	3.03	5.31E-05	1.06E-02
ribonucleoprotein complex subunit organization	15	4.35	3.45	5.66E-05	1.07E-02
nitrogen compound transport	56	31.96	1.75	5.64E-05	1.08E-02
cellular response to stress	52	28.84	1.80	5.61E-05	1.09E-02
basic amino acid transmembrane transport	4	.16	24.55	6.20E-05	1.16E-02
cell activation	38	18.74	2.03	6.76E-05	1.25E-02
regulation of protein phosphorylation	47	25.31	1.86	7.19E-05	1.27E-02
response to decreased oxygen levels	17	5.52	3.08	7.13E-05	1.27E-02
positive regulation of catalytic activity	47	25.26	1.86	7.07E-05	1.28E-02
response to external stimulus	61	36.21	1.68	7.04E-05	1.29E-02
multi-multicellular organism process	14	3.95	3.55	7.58E-05	1.31E-02
regulation of biological quality	101	69.37	1.46	7.54E-05	1.32E-02
positive regulation of cell-cell adhesion	15	4.49	3.34	8.02E-05	1.36E-02
organonitrogen compound metabolic process	135	99.91	1.35	8.20E-05	1.36E-02
regulation of intracellular signal transduction	57	33.26	1.71	7.96E-05	1.36E-02
protein folding	14	3.98	3.51	8.31E-05	1.36E-02
regulation of locomotion	35	16.88	2.07	8.18E-05	1.37E-02
regulation of cellular component movement	35	16.97	2.06	8.64E-05	1.37E-02
organonitrogen compound biosynthetic process	47	25.71	1.83	8.51E-05	1.38E-02
cellular metabolic process	201	162.43	1.24	8.62E-05	1.38E-02
response to organic cyclic compound	33	15.73	2.10	8.87E-05	1.40E-02
regulation of protein metabolic process	78	50.21	1.55	9.37E-05	1.46E-02
regulation of protein kinase activity	30	13.76	2.18	9.47E-05	1.46E-02
cellular protein metabolic process	97	66.29	1.46	9.85E-05	1.48E-02
vesicle-mediated transport	58	34.26	1.69	9.79E-05	1.48E-02
regulation of protein catabolic process	19	6.83	2.78	9.73E-05	1.49E-02
cellular component assembly	71	44.49	1.60	1.07E-04	1.58E-02
regulation of developmental process	71	44.65	1.59	1.10E-04	1.60E-02
positive regulation of cellular protein metabolic process	50	28.17	1.77	1.09E-04	1.61E-02
response to temperature stimulus	12	3.13	3.83	1.25E-04	1.80E-02
regulation of phosphorus metabolic process	53	30.71	1.73	1.37E-04	1.93E-02
cellular component biogenesis	75	48.31	1.55	1.36E-04	1.93E-02
regulation of phosphate metabolic process	53	30.67	1.73	1.36E-04	1.94E-02
detection of stimulus involved in sensory perception	0	9.38	< 0.01	1.42E-04	1.98E-02
cellular response to organic substance	65	40.31	1.61	1.50E-04	2.03E-02
positive regulation of kinase activity	24	10.05	2.39	1.48E-04	2.04E-02
regulation of cellular component organization	70	44.42	1.58	1.49E-04	2.04E-02
mRNA processing	21	8.31	2.53	1.54E-04	2.08E-02
positive regulation of leukocyte chemotaxis	8	1.43	5.59	1.60E-04	2.11E-02
amino acid transmembrane transport	8	1.43	5.59	1.60E-04	2.13E-02
symbiont process	27	12.02	2.25	1.70E-04	2.22E-02
chemotaxis	23	9.40	2.45	1.72E-04	2.23E-02
response to abiotic stimulus	38	19.79	1.92	1.76E-04	2.27E-02

regulation of kinase activity	31	14.96	2.07	1.80E-04	2.29E-02
positive regulation of cellular metabolic process	86	58.01	1.48	1.79E-04	2.30E-02
positive regulation of biological process	141	107.05	1.32	1.84E-04	2.32E-02
regulation of phosphorylation	48	27.20	1.76	1.89E-04	2.36E-02
peptide metabolic process	23	9.56	2.41	1.96E-04	2.41E-02
basic amino acid transport	4	.24	16.99	1.95E-04	2.42E-02
protein targeting to ER	9	1.92	4.69	2.17E-04	2.63E-02
organic substance transport	62	38.42	1.61	2.16E-04	2.63E-02
nervous system development	65	40.76	1.59	2.24E-04	2.69E-02
cellular localization	67	42.70	1.57	2.27E-04	2.71E-02
protein localization to endoplasmic reticulum	10	2.39	4.18	2.33E-04	2.76E-02
primary metabolic process	201	164.66	1.22	2.52E-04	2.94E-02
regulation of MAPK cascade	29	13.67	2.12	2.51E-04	2.94E-02
vasculature development	22	9.07	2.43	2.63E-04	3.05E-02
regulation of transforming growth factor beta production	5	.51	9.86	2.73E-04	3.14E-02
establishment of protein localization to endoplasmic reticulum	9	1.99	4.52	2.81E-04	3.15E-02
metabolic process	215	178.98	1.20	2.80E-04	3.17E-02
peptide biosynthetic process	19	7.46	2.55	2.87E-04	3.18E-02
nitrogen compound metabolic process	192	156.12	1.23	2.79E-04	3.18E-02
regulation of peptide transport	27	12.62	2.14	2.86E-04	3.19E-02
cellular response to chemical stimulus	75	49.52	1.51	2.96E-04	3.25E-02
apoptotic process	32	16.13	1.98	3.10E-04	3.37E-02
cardiovascular system development	22	9.27	2.37	3.13E-04	3.37E-02
regulation of hydrolase activity	41	22.69	1.81	3.09E-04	3.38E-02
regulation of cellular protein metabolic process	70	45.61	1.53	3.33E-04	3.56E-02
negative regulation of protein metabolic process	36	18.99	1.90	3.38E-04	3.59E-02
actin cytoskeleton organization	21	8.56	2.45	3.55E-04	3.68E-02
regulation of signal transduction	83	56.42	1.47	3.54E-04	3.69E-02
nuclear-transcribed mRNA catabolic process	12	3.53	3.40	3.52E-04	3.70E-02
response to ketone	12	3.53	3.40	3.52E-04	3.72E-02
translation	18	6.99	2.58	3.63E-04	3.74E-02
ribonucleoprotein complex assembly	13	4.09	3.18	3.75E-04	3.83E-02
blood vessel development	21	8.65	2.43	3.77E-04	3.83E-02
positive regulation of transferase activity	25	11.35	2.20	3.81E-04	3.84E-02
response to oxygen-containing compound	46	26.73	1.72	3.91E-04	3.89E-02
amide biosynthetic process	22	9.49	2.32	3.91E-04	3.91E-02
regulation of protein modification process	53	32.21	1.65	4.08E-04	3.96E-02
regulation of biological process	242	207.18	1.17	4.03E-04	3.97E-02
regulation of transferase activity	33	16.95	1.95	4.01E-04	3.97E-02
response to chemical	107	77.57	1.38	4.07E-04	3.98E-02
positive regulation of leukocyte differentiation	10	2.59	3.86	4.25E-04	4.07E-02
regulation of localization	72	47.57	1.51	4.23E-04	4.08E-02
regulation of body fluid levels	21	8.85	2.37	4.44E-04	4.23E-02
positive regulation of T cell activation	12	3.64	3.30	4.56E-04	4.25E-02
organic acid transmembrane transport	9	2.14	4.21	4.54E-04	4.25E-02
positive regulation of nitrogen compound metabolic process	82	56.04	1.46	4.50E-04	4.27E-02
carboxylic acid transmembrane transport	9	2.14	4.21	4.54E-04	4.28E-02
positive regulation of transforming growth factor beta production	4	.31	12.99	4.64E-04	4.29E-02
leukocyte migration	17	6.54	2.60	4.73E-04	4.35E-02
SRP-dependent cotranslational protein targeting to membrane	8	1.70	4.70	4.76E-04	4.36E-02

nuclear-transcribed mRNA catabolic process, nonsense-mediated decay	9	2.15	4.18	4.81E-04	4.38E-02
positive regulation of molecular function	52	31.42	1.66	4.85E-04	4.38E-02
blood vessel morphogenesis	18	7.19	2.50	4.99E-04	4.38E-02
regulation of mitochondrion organization	11	3.15	3.49	4.98E-04	4.40E-02
detection of chemical stimulus involved in sensory perception	0	8.42	< 0.01	4.92E-04	4.40E-02
protein-containing complex subunit organization	54	33.23	1.63	4.89E-04	4.40E-02
interspecies interaction between organisms	27	12.84	2.10	4.96E-04	4.41E-02
cell-cell signaling	35	18.74	1.87	5.07E-04	4.43E-02
regulation of signaling	90	63.34	1.42	5.13E-04	4.46E-02
response to glucocorticoid	10	2.66	3.76	5.20E-04	4.50E-02
cell migration	32	16.57	1.93	5.63E-04	4.79E-02
RNA processing	30	15.23	1.97	5.61E-04	4.79E-02
response to steroid hormone	16	6.03	2.65	5.60E-04	4.82E-02

GO molecular function complete	#	expected	Fold	raw P value	FDR
protein binding	289	212.99	1.36	1.51E-15	7.03E-12
RNA binding	67	30.08	2.23	1.55E-09	1.81E-06
molecular function	358	317.64	1.13	1.22E-09	1.89E-06
binding	323	272.81	1.18	2.43E-09	2.26E-06
Unclassified	23	63.36	.36	1.22E-09	2.83E-06
identical protein binding	59	32.08	1.84	7.30E-06	5.66E-03
growth factor binding	12	2.50	4.80	1.61E-05	1.07E-02
cell adhesion molecule binding	23	8.73	2.64	4.11E-05	2.13E-02
enzyme binding	68	40.85	1.66	3.97E-05	2.31E-02
carbohydrate derivative binding	67	40.43	1.66	5.28E-05	2.46E-02
hydrolase activity, acting on acid anhydrides	34	16.59	2.05	1.23E-04	2.73E-02
hydrolase activity, acting on acid anhydrides, in phosphorus-containing anhydrides	34	16.59	2.05	1.23E-04	2.87E-02
glycosaminoglycan binding	14	4.00	3.50	8.70E-05	2.89E-02
pyrophosphatase activity	34	16.53	2.06	1.19E-04	2.92E-02
basic amino acid transmembrane transporter activity	4	.20	20.08	1.15E-04	2.98E-02
amino acid transmembrane transporter activity	8	1.34	5.97	1.05E-04	3.06E-02
anion binding	78	50.46	1.55	9.95E-05	3.09E-02
cytoskeletal protein binding	35	16.97	2.06	8.64E-05	3.09E-02
protein phosphatase activator activity	4	.20	20.08	1.15E-04	3.15E-02
nucleoside-triphosphatase activity	33	15.66	2.11	8.31E-05	3.23E-02
protein-containing complex binding	38	19.08	1.99	8.17E-05	3.46E-02

GO cellular component complete	#	expected	Fold	raw P value	FDR
intracellular organelle part	252	166.35	1.51	2.56E-18	5.19E-15
organelle	320	243.61	1.31	1.15E-17	7.77E-15
organelle part	256	171.67	1.49	8.34E-18	8.46E-15
membrane-bounded organelle	302	223.91	1.35	5.30E-17	2.69E-14
intracellular organelle	305	228.65	1.33	1.48E-16	6.01E-14
intracellular part	330	261.15	1.26	5.55E-16	1.61E-13
cytoplasm	286	208.23	1.37	4.85E-16	1.64E-13
cytoplasmic part	252	174.64	1.44	3.33E-15	8.45E-13
intracellular	331	266.17	1.24	1.58E-14	3.56E-12

intracellular membrane-bounded organelle	266	196.46	1.35	8.18E-13	1.66E-10
Unclassified	6	41.93	.14	2.62E-12	4.43E-10
cellular component	375	339.07	1.11	2.62E-12	4.83E-10
cell	356	308.39	1.15	7.65E-12	1.19E-09
extracellular space	113	59.84	1.89	1.48E-11	2.00E-09
extracellular region part	117	63.23	1.85	1.67E-11	2.11E-09
cell part	355	307.90	1.15	1.48E-11	2.14E-09
extracellular exosome	80	37.93	2.11	2.94E-10	3.32E-08
vesicle	120	68.52	1.75	2.84E-10	3.39E-08
extracellular organelle	80	38.33	2.09	3.92E-10	3.98E-08
extracellular vesicle	80	38.30	2.09	3.80E-10	4.06E-08
membrane-enclosed lumen	150	94.59	1.59	5.79E-10	5.11E-08
intracellular organelle lumen	150	94.59	1.59	5.79E-10	5.34E-08
organelle lumen	150	94.59	1.59	5.79E-10	5.59E-08
endomembrane system	132	80.25	1.64	1.38E-09	1.16E-07
cytosol	145	91.86	1.58	2.53E-09	2.06E-07
extracellular region	126	77.89	1.62	1.40E-08	1.10E-06
focal adhesion	27	7.32	3.69	1.77E-08	1.33E-06
cell-substrate adherens junction	27	7.37	3.66	2.04E-08	1.48E-06
cell-substrate junction	27	7.44	3.63	2.47E-08	1.73E-06
intracellular vesicle	79	41.52	1.90	3.40E-08	2.23E-06
cytoplasmic vesicle	79	41.46	1.91	3.31E-08	2.24E-06
protein-containing complex	146	97.54	1.50	6.40E-08	4.06E-06
intracellular non-membrane-bounded organelle	121	75.98	1.59	6.95E-08	4.27E-06
non-membrane-bounded organelle	121	76.10	1.59	7.24E-08	4.32E-06
pigment granule	13	1.90	6.84	1.87E-07	1.06E-05
melanosome	13	1.90	6.84	1.87E-07	1.09E-05
adherens junction	29	9.74	2.98	4.04E-07	2.21E-05
anchoring junction	29	10.03	2.89	7.13E-07	3.81E-05
cytoplasmic vesicle part	52	26.71	1.95	7.06E-06	3.67E-04
membrane	220	175.85	1.25	7.72E-06	3.91E-04
myelin sheath	13	2.95	4.40	1.69E-05	8.36E-04
secretory granule	34	15.12	2.25	1.79E-05	8.64E-04
cytoplasmic vesicle lumen	19	6.08	3.12	2.24E-05	1.06E-03
vesicle lumen	19	6.10	3.11	2.33E-05	1.07E-03
cell surface	35	15.99	2.19	2.85E-05	1.28E-03
whole membrane	54	29.60	1.82	2.95E-05	1.30E-03
cell junction	45	23.10	1.95	3.33E-05	1.44E-03
collagen-containing extracellular matrix	16	4.67	3.43	3.52E-05	1.49E-03
secretory vesicle	37	17.87	2.07	4.65E-05	1.92E-03
endocytic vesicle	17	5.38	3.16	5.23E-05	2.12E-03
vacuole	31	13.98	2.22	5.52E-05	2.20E-03
cytoskeleton	65	39.26	1.66	6.27E-05	2.45E-03
extracellular matrix	21	7.84	2.68	7.11E-05	2.72E-03
nuclear lumen	106	74.09	1.43	8.80E-05	3.30E-03
ribonucleoprotein complex	33	15.81	2.09	9.49E-05	3.50E-03
nuclear part	114	81.30	1.40	1.15E-04	4.18E-03
secretory granule lumen	17	5.79	2.93	1.24E-04	4.41E-03
organelle membrane	81	53.16	1.52	1.37E-04	4.79E-03
ficolin-1-rich granule lumen	10	2.25	4.45	1.45E-04	4.99E-03

chromosome	36	18.31	1.97	1.62E-04	5.48E-03
spliceosomal complex	12	3.30	3.64	1.94E-04	6.46E-03
nucleus	167	132.14	1.26	2.69E-04	8.80E-03
cytosolic large ribosomal subunit	7	1.20	5.86	3.17E-04	1.02E-02
vacuolar part	23	10.09	2.28	3.42E-04	1.08E-02
bounding membrane of organelle	60	37.44	1.60	3.57E-04	1.12E-02
lytic vacuole	26	12.15	2.14	3.78E-04	1.13E-02
actin filament bundle	7	1.23	5.69	3.74E-04	1.13E-02
lysosome	26	12.13	2.14	3.71E-04	1.14E-02
nucleoplasm	90	63.12	1.43	4.99E-04	1.47E-02
cytosolic ribosome	9	2.19	4.11	5.39E-04	1.56E-02
vacuolar membrane	18	7.28	2.47	5.74E-04	1.62E-02
cytoskeletal part	50	30.29	1.65	5.73E-04	1.64E-02
microtubule cytoskeleton	38	21.57	1.76	1.11E-03	3.05E-02
endoplasmic reticulum	54	34.19	1.58	1.10E-03	3.05E-02
cytosolic part	13	4.65	2.79	1.16E-03	3.15E-02
chromosomal part	30	16.08	1.87	1.29E-03	3.44E-02
ribosomal subunit	11	3.60	3.05	1.41E-03	3.71E-02
endoplasmic reticulum lumen	14	5.43	2.58	1.58E-03	4.12E-02
VCP-NSFL1C complex	2	.04	55.23	1.85E-03	4.69E-02
platelet alpha granule	7	1.65	4.25	1.84E-03	4.73E-02
nuclear body	26	13.53	1.92	1.97E-03	4.94E-02